ATTACHMENT 4

Holtec International Report No. HI-2104790, Revision 1,
"Nuclear Group Computer Code Benchmark Calculations"

HOLTEC
INTERNATIONAL

Holtec Center, 555 Lincoln Drive West, Marlton, NJ 08053
Telephone (856) 797- 0900
Fax (856) 797 - 0909

Nuclear Group Computer Code Benchmark Calculations

FOR

GENERIC: NON-PROPRIETARY VERSION

Holtec Report No: HI-2104790

Holtec Project No: GENERIC

Sponsoring Holtec Division: HTS

Report Class : SAFETY RELATED

Summary of Revisions

Revision 0

Original Issue

Revision 1

Additional criticality experiments were added to Appendix B. The index numbers of criticality experiments in Appendix C were updated to be consistent with a new revision of Appendix B. The benchmark of MCNP5-1.51 with ENDF/B-VII was added in Appendix D.

Table of Contents

1.0 Introduction

This report documents the criticality experiment benchmark validation calculations for the following computer codes and libraries combinations and establishes the criticality code bias and bias uncertainty for these codes:

MCNP5-1.51 with ENDF/B-V (Appendix C)
MCNP5-1.51 with ENDF/B-VII (Appendix D)

For that purpose, results from the codes are compared to the critical experiments referred to as the Haut Taux de Combustion (HTC) experiments and to the selected critical, presented in Appendix B, with geometric and material characteristics similar to that of spent fuel storage and transport casks. The simulated fuel rods used in these experiments contained uranium or mixture of uranium and plutonium oxides. In the HTC experiments the plutonium-to-uranium ratio and the isotopic compositions of both the uranium and plutonium were designed to be similar to what would be found in a typical pressurized-water reactor (PWR) fuel assembly that initially had an enrichment of 4.5 wt % ^{235}U and was burned to 37,500 MWd/MTU.

The purpose of the calculation is to determine the code bias and bias uncertainty consistent with standards such as ANSI/ANS-8.1 [1] and ANSI/ANS-8.17 [2]. Criticality safety standards ANSI/ANS-8.1 and ANSI/ANS-8.17 apply to criticality methods validation and to criticality evaluations, respectively. ANSI/ANS-8.1 requires that a validation be performed on the method used to calculate criticality safety margins and that the validation must be documented in a written report describing the method, computer program and cross section libraries used, the experimental data, the areas of applicability and the bias and margins of safety. ANSI/ANS-8.17 prescribes the criteria to establish sub-criticality safety margins.

2.0 Methodology

Validation of the computer code and continuous energy data library to perform criticality safety calculation has been performed following reference [5] methodology. The validation allows the understanding of the accuracy of the calculational methodology to predict subcriticality. Validation includes identification of the difference between calculated and experimental neutron effective multiplication factor (k_{eff}), called the bias. A set of appropriate critical experiments are selected so bias trends can be drawn through statistical analyses. The range of the benchmark parameters used to validate the calculational methodology primarily defines the area of applicability (AOA), which establishes the limits of the systems that can be analyzed using the validated criticality safety methodology.

Determination of Bias and Bias Uncertainty

Following reference [5] guide, the statistical analysis to determine the mean multiplication factor ($\overline{k_{eff}}$) and the bias uncertainty (S_p) approach involves determining the weighted mean that incorporates the uncertainty from both, measurements and calculation method as follows:

$$\sigma_i = \sqrt{\sigma_{calc-i}^2 + \sigma_{exp}^2} \quad (2\text{-}1)$$

where σ_i is the uncertainty for the ith k_{eff}, σ_{exp} is the measurement uncertainty and $\sigma_{calc\text{-}i}$ is the calculation uncertainty. Then, the weighted mean multiplication factor $\overline{k_{eff}}$ and the bias uncertainty (S_p) are given by:

$$\overline{k_{eff}} = \frac{\sum \frac{1}{\sigma_i^2}(k_{eff-i})}{\sum \frac{1}{\sigma_i^2}} \quad (2\text{-}2)$$

$$S_p = \sqrt{s^2 + \bar{\sigma}^2} \quad (2\text{-}3)$$

where s^2 is the variance about the mean and $\bar{\sigma}^2$ is the average total uncertainty, given by:

$$s^2 = \frac{\left(\frac{1}{n-1}\right)\sum \frac{1}{\sigma_i^2}\left(k_{eff-i} - \overline{k_{eff}}\right)^2}{\frac{1}{n}\sum \frac{1}{\sigma_i^2}} \quad (2\text{-}4)$$

$$\bar{\sigma}^2 = \frac{n}{\sum \frac{1}{\sigma_i^2}} \quad (2\text{-}5)$$

where n is the number of critical experiments used in the validation and $k_{eff\text{-}i}$ is the ith value of the multiplication factor.

Bias is determined by the relation:

$$Bias = \overline{k_{eff}} - 1 \quad \text{if } \overline{k_{eff}} \text{ is less than 1, otherwise } Bias = 0 \quad (2\text{-}6)$$

Because a positive bias may be nonconservative, a bias is set to zero if the calculated average k_{eff} is greater than one.

Statistical Methods

Single Sided Tolerance Limit Method

If the benchmark calculated neutron multiplication factor does not exhibit trends with the parameters, the lower tolerance limit or single sided tolerance limit method can be used. A weighted lower limit tolerance (K_L) is a single lower limit above which a defined fraction of the population of k_{eff} is expected to lie, with a prescribed confidence and within the area of the applicability. The term "weighted" refers to a specific statistical technique where the

uncertainties in the data are used to weight the data point. Data with high uncertainties will have less "weight" than data with small uncertainties.

A lower tolerance limit can be used when there are no trends apparent in the critical experiment results and the critical experiment results have a normal distribution. The method is applicable only within the limits of the validation data without extrapolating the AOA. The single sided lower tolerance limit is defined by the equation:

$$K_L = \overline{k_{eff}} - U \times S_p \tag{2-7}$$

$$If\ \overline{k_{eff}} \geq 1,\ then\ K_L = 1 - U \times S_p \tag{2-8}$$

where S_p is the square root of the pooled variance used as the mean bias uncertainty when applying the single sided tolerance limit for a normally distributed data and U is the single sided lower tolerance factor, determined from the following equations [6]. Note that for groups with larger than 50 samples, the single sided lower tolerance factor for 50 samples was conservatively used.

$$\boldsymbol{U = \frac{z_{1-p} + \sqrt{z_{1-p}^2 - ab}}{a}} \tag{2-9}$$

$$\boldsymbol{a = 1 - \frac{z_{1-\gamma}^2}{2(N-1)}} \tag{2-10}$$

$$\boldsymbol{b = z_{1-p}^2 - \frac{z_{1-\gamma}^2}{N}} \tag{2-11}$$

where z_{1-p} is the critical value from the normal distribution that is exceeded with probability $1-p$ and $z_{1-\gamma}$ is the critical value from the normal distribution that is exceeded with probability $1-\gamma$.

Confidence Band with Administrative Margin Method

If the benchmarks calculated neutron multiplication factor exhibit a trend with a given parameter, the method based on a confidence band with administrative margin can be used. This method applies a statistical calculation of the bias and its uncertainty plus an administrative margin to a linear fit of the critical experiment benchmark data.

The confidence band W is defined for a confidence level of $(1-\gamma)$ using the relationship:

$$W = \max\{w(x_{min}), w(x_{max})\} \tag{2-12}$$

where

$$w(x) = t_{1-\gamma} \times S_p \sqrt{1 + \frac{1}{n} + \frac{(x - \bar{x})^2}{\sum_{i=1,n}(x - \bar{x})^2}} \qquad (2\text{-}13)$$

and

n is the number of critical experiments used in establishing $k_{cal}(x)$,

$t_{1-\gamma}$ is the Student-t distribution statistic for $1-\gamma$ and $n-2$ degrees of freedom,

$\bar{x}$ is the mean value of the parameter x in the set of calculations,

x_{min}, x_{max} are the minimum and maximum values of the independent parameter x,

S_p is the pooled standard deviation for the set of criticality calculations given by:

$$S_p = \sqrt{s^2_{k(x)} + s^2_w} \qquad (2\text{-}14)$$

where $S^2_{k(x)}$ is the variance of the regression fit and is given by:

$$s^2_{k(x)} = \frac{1}{(n-2)}\left[\sum_{i=1,n}(k_{eff-i} - \bar{k})^2 - \frac{\{\sum_{i=1,n}(x_i - \bar{x})(k_{eff-i} - \bar{k})\}^2}{\sum_{i=1,n}(x_i - \bar{x})^2}\right] \qquad (2\text{-}15)$$

$\bar{k}$ is the mean value of the calculated k_{eff} and s_w^2 is the within-variance of the data:

$$S^2_w = \frac{1}{n}\sum_{i=1,n}\sigma_i^2 \qquad (2\text{-}16)$$

where $\sigma_i = \sqrt{\sigma^2_{calc-i} + \sigma^2_{exp}}$ is the uncertainty for the ith k_{eff}, σ_{exp} is the measurement uncertainty and σ_{calc-i} is the calculated uncertainty.

Non-parametric Statistical Treatment Method

Data that do not follow a normal distribution can be analyzed by non-parametric techniques. The analysis results in a determination of the degree of confidence that a fraction of the true population of data lies above the smallest observed value. The more data is available in the sample, the higher the degree of confidence.

The following equation determines the percent confidence that a fraction of the population is above the lowest observed value:

$$\beta = 1 - \sum_{j=0}^{m-1} \frac{n!}{j!\,(n-j)!}(1-q)^j q^{n-j} \qquad (2\text{-}17)$$

where

q is the desired population fraction (normally 0.95),

n is the number of data in one data sample,

m is the rank order indexing from the smallest sample to the largest (m=1 for the smallest sample; m=2 for the second smallest sample, etc.). Non-parametric techniques do not require reliance upon distributions, but are rather an analysis of ranks. Therefore, the samples are ranked from the smallest to the largest.

For a desired population fraction of 95% and a rank of order of 1 (the smallest data sample), the equation reduces to:

$$\beta = 1 - q^n = 1 - 0.95^n \qquad (2\text{-}18)$$

This information is then used to determine the Non-parametric Margin from Table 2.2 in Reference [5].

For non-parametric data analysis, K_L is determined by:

K_L = Smallest k_{eff} value – Uncertainty for Smallest k_{eff} – Non-parametric Margin (NPM) *(2-19)*

Single-Sided Tolerance Band Method

When a relationship between a calculated k_{eff} and an independent variable can be determined, a single-sided lower tolerance band may be used. This is a conservative method that provides a fitted curve above which the true population of k_{eff} is expected to lie. The tolerance band equation is actually a calibration curve relation.

The equation for the single-sided lower tolerance band is

$$K_L = K_{fit}(x) - S_{P_{fit}} \left\{ \sqrt{2F_a^{(2,n-2)} \left[\frac{1}{n} + \frac{(x-\bar{x})^2}{\sum (x_i - \bar{x})^2} \right]} + z_{2P-1} \sqrt{\frac{(n-2)}{\chi^2_{1-\gamma,n-2}}} \right\} \qquad (2\text{-}20)$$

where:

$K_{fit}(x)$ is the function derived from the trend analysis,

p is the desired confidence (0.95),

$F_a^{(fit,n-2)}$ is the F distribution percentile with degree of fit, n-2 degrees of freedom. The degree of fit is 2 for a linear fit,

n is the number of critical experiment k_{eff} values,

x is the independent fit variable,

x_i is the independent parameter in the data set corresponding to the "ith" k_{eff} value,

$\bar{x}$ is the weighted mean of the independent variables,

z_{2P-1} is the symmetric percentile of the Gaussian or normal distribution that contains the P fraction,

$$\gamma = (1 - p) / 2, \tag{2-21}$$

$\chi^2_{1-\gamma,n-2}$ is the upper Chi-square percentile,

$$S_{P_{fit}} = \sqrt{s_{fit}^2 + \bar{\sigma}^2} \tag{2-22}$$

$$s_{fit}^2 = \frac{\frac{1}{n-2}\Sigma\left\{\frac{1}{\sigma_i^2}\left[k_{eff_i} - K_{fit}(x_i)\right]^2\right\}}{\frac{1}{n}\Sigma\frac{1}{\sigma_i^2}} \tag{2-23}$$

Area of Applicability

The area(s) of applicability refers to the key physical parameter(s) that define a particular fissile configuration. This configuration can either be an actual system or a process. The determination of the AOA of the validation is determined following NUREG/CR-6698 steps [5]. The approach used in developing the AOA consists of the following steps:

i. Identification of the key parameters associated with the system to be evaluated.
ii. Establishment a "screening" AOA for critical experiments.
iii. Identification of criticality experiments that are within the "screening" AOA.
iv. Determination of the detailed AOA based on the selected criticality benchmark experiments.
v. Demonstration that the system to be evaluated in within the AOA provided by the critical experiments.

Steps i. and ii. are presented in subsections 2.3.1 and 2.3.2, respectively. Step iii. is presented in Appendix B. Steps iv. and v. are presented in Appendix C and D.

Key Parameters Identification

This validation will cover a number of designs but all the designs will consider the same key parameters in defining the applicability area. These parameters fall into three categories: materials, geometry and neutron energy spectra.

Regarding material, the fuel is a uranium or mixture of uranium and plutonium oxides pellets clad in a zirconium alloy. The moderator and reflector is water which in some cases has dissolved boron or gadolinium solutions. Absorber plates made of borated steel, Boral®, Zircaloy Boroflex or cadmium and absorber rods made of steel, aluminum, Gd_2O_3, Pyrex®, Vicor® or borated aluminum will be included in this validation. Some experiments were performed with steel or lead reflector screens.

Regarding geometry, the fuel in the HTC experiments is in square lattices with pin diameter – 9.5 mm and pitch in the range found on Table B-1 through Table B-6. The geometry parameters of other selected critical experiments are varied in a wide range and they can be found in references [B.6] through [B.12]. The fuel assemblies may be separated by water, water and an absorber plate or water and absorber rods. The system may be water reflected or steel/lead reflected.

Regarding the neutron energy spectra, they are thermal with EALF values in the range of 0.07 and 1.55 eV.

Table 2-1 presents the key physical parameters for AOA selected.

Screening Area of Applicability

For the key parameters selected in section 2.3.1, Table 2-1 summarizes the range of parameters for which the validation applies. These data are the base for the selection of the critical experiments, which span the range of parameters.

3.0 Assumptions

No substantial simplifying assumptions were made in the modeling of the critical experiments used for benchmarking: all experiments were modeled as full three-dimensional geometries, fuel rod arrays were modeled as lattices, all fuel rod details were modeled, and the water between the rods was modeled as specified in the experiment description. However, structures further away from the experiment, such as building walls and foundations, were not included in the models.

4.0 Computer Files

All computer files to support this analysis are provided on the Holtec server in \Projects\0\Reports\HI-2104790 and its subdirectories.

5.0 Summary

The criticality experiment benchmark validation calculations for the computer codes and libraries shown in Section 1.0 were performed for the validation of the Holtec International

criticality safety methodology. The results of calculations and the criticality code bias and bias uncertainty for these codes are presented in appropriate appendices. The similarity between the chosen experiments and the actual systems has been based on a set of screening criteria as is stated in the NUREG/CR-6698 [5].

The summary of biases and bias uncertainties for the validated computer codes is shown in Table 5.1.

6.0 References

[1] ANSI/ANS 8.1-1983, American National Standard For Nuclear Criticality Safety In Operations With Fissionable Materials Outside Reactors, American Nuclear Society, La Grange Park, Illinois.

[2] ANSI/ANS-8.17, "American National Standard for Criticality Safety Criteria for the Handling, Storage, and Transportation of LWR Fuel Outside Reactors," American Nuclear Society, La Grange Park, Illinois.

[3] Criticality Benchmark Guide for Light Water Reactor Fuel in Transportation and Storage Packages, NUREG/CR-6361 (ORNL/TM-13211), U.S. Nuclear Regulatory Commission, March 1997.

[4] J.R. Taylor, An Introduction to Error Analysis (University Science Books, Mill Valley, California, 1982).

[5] Guide for Validation of Nuclear Criticality Safety Calculational Methodology, NUREG/CR-6698, U.S. Nuclear Regulatory Commission, January 2001.

[6] M.G. Natrella, Experimental Statistics, National Bureau of Standards, Handbook 91, August 1963.

Table 2-1 Key Criticality System Parameters and Range of those Parameters in Expected Designs

Parameter	Critical Experiment Requirement	Range of Key Parameters
Fissionable Material	^{235}U, ^{239}Pu, ^{241}Pu	^{235}U, ^{239}Pu, ^{241}Pu
Isotopic Composition		
$^{235}U/U_t$	< 5.0wt%	0.16wt% to 5.74wt%
Pu/(U+Pu)	< 20wt%	1.104wt% to 20wt%
Physical Form	UO_2, MOX	UO_2, MOX
Moderator Material (coolant)	H	H
Physical Form	H_20	H_20
Density	Normal pressure & temperature condition	around 1.0 g/cm^3
Reflector Material	H	H
Physical Form	H_20	H_20
Density	Normal pressure & temperature condition	around 1.0 g/cm^3
Interstitial Reflector Material		
Plate	Steel or Lead	Steel or Lead
Absorber Material		
Soluble	None, Boron or Gadolinium	None, Boron (0 to 2550 ppm) or Gadolinium (0 to 197 ppm)
Rods	Boron	Pyrex®, Vicor®, Steel or B-Al
Separating Material		
Plate	Water, B-SS, Boral or Cadmium	Water, B-SS, Boral, Boroflex, Zircaloy or Cadmium
Geometry		
Fuel	Square/Triangle lattice of fuel pins	Square/Triangle lattice of fuel pins
Neutron Energy	Thermal spectrum	Thermal spectrum

Table 5-1 Summary of Biases and Bias Uncertainties for the Validated Computer Codes

Computer Code	Total Bias	Bias Uncertainty
MCNP5-1.51 with ENDF/B-V (Appendix C)	[redacted]	[redacted]
MCNP5-1.51 with ENDF/B-VII (Appendix D)	[redacted]	[redacted]

Appendix A

Holtec Approved Computer Program List

(total number of pages: 5 including this page)

Appendix Proprietary

Appendix B

Description of the Critical Experiments

(total number of pages: 16 including this page)

B.1. Introduction and Purpose

The purpose of this Appendix is to document the description of the full set of critical experiments selected for the benchmark validation of computer codes.

B.2. Physical Description of HTC Critical Experiments

In the 1980s, a series of critical experiments referred to as the Haut Taux de Combustion (HTC) experiments was conducted by the Institut de Radioprotection et de Sûreté Nucléaire (IRSN) at the experimental criticality facility in Valduc, France, between 1988 and 1990. The fuel rods were fabricated specifically for this set of experiments. The fuel consisted of 1-cm-long pellets contained within Zircaloy-4 cladding. The plutonium-to-uranium ratio and the isotopic compositions of both the uranium and plutonium used in the simulated fuel rods were designed to be similar to what would be found in a typical pressurized-water reactor fuel assembly that initially had an enrichment of 4.5 wt % ^{235}U and was burned to 37,500 MWd/MTU. The fuel material also includes ^{241}Am, which is present due to the decay of ^{241}Pu. The fuel rods were held in place by an upper and a lower grid and were contained in one or four assemblies placed into a rectangular tank. The critical approach was accomplished by varying the water or solution level in the tank containing the fuel pin arrays. The critical condition was extrapolated from a subcritical configuration with a multiplication factor within 0.1% of 1.000.

This section provides a summary description of the materials and physical layouts of the 156 critical configurations. Detailed descriptions of the critical experiments are presented in references [B.1] through [B.4]. The HTC experiments include configurations designed to simulate fuel handling activities, pool storage, and transport in casks constructed of thick lead or steel and were categorized into four phases.

B.2.1. Phase 1: Water-Moderated and Reflected Arrays

The first phase included 18 configurations, each involving a single square-pitched array of rods with rod pitch varying from 1.3 to 2.3 cm.

The tank was incrementally filled with water at room temperature, water being injected at the bottom of the tank. A measurement needle provided water height. Therefore, the water was used as core moderator and as reflector beneath the fuel and around the array on four sides. The critical approach parameter was the water level.

Eighteen experiments have been performed with various arrays and all are considered acceptable for use as benchmark experiments:

- 5 square or almost square array - square pitch 1.3, 1.5, 1.7, 1.9, 2.3 cm – 15 experiments,
- 1 rectangular centered array – square pitch 1.7 cm – 2 experiments,
- 1 rectangular no-centered array – square pitch 1.7 cm – 1 experiment.

The experiments key physical parameters are summarized in Table B-1.

B.2.2. Phase 2: Reflected Simple Arrays Moderated by Poisoned Water with Gadolinium or Boron

The second phase included 41 configurations that were similar to the first phase except that the water used as moderator and reflector included either boron or gadolinium in solution at various concentrations.

The tank was incrementally filled with poisoned solution at room temperature, this solution being pumped in the bottom of the tank. A measurement needle provided solution height. The critical approach parameter was the water level.

Forty one experiments are evaluated and all are considered acceptable for use as benchmark experiments. Twenty of them are performed with gadolinium solutions, and the others with boron solutions.

The experiments key physical parameters are summarized in Table B-2 through Table B-3.

B.2.3. Phase 3: Pool Storage

The third phase simulated fuel assembly storage rack conditions and included 26 configurations with 1.6 cm square rods pitch arranged into four assemblies in a 2 × 2 array. These assemblies with, in some cases, canisters, were placed on a pedestal centered inside a parallelepiped tank which was itself located on the floor in the middle (approximately) of a large room. The spacing between assemblies was varied, and some of the assemblies had B-SS, Boral®, or cadmium plates attached to the sides of the four assemblies.

The tank was incrementally filled with water at room temperature, water being pumped in at the bottom of the tank. A measurement needle provided water height. Therefore, the water was used as core moderator and as reflector beneath the fuel and around the array on four sides. The critical approach parameter was the water level.

Twenty six experiments are evaluated and all are considered acceptable for use as benchmark experiments. Eleven of them were performed with neutron absorbing canisters around the four arrays, and the others without any.

The experiments key physical parameters are summarized in Table B-4.

B.2.4. Phase 4: Shipping Cask

The fourth phase simulated cask conditions and included 71 configurations similar to the Phase 3 configurations except thick steel or lead shields were placed around the outside of the 2 × 2 array of fuel assemblies. These assemblies with, in some cases, canisters, were placed on a pedestal centered inside a parallelepiped tank which was itself located on the floor in the middle (approximately) of a large room. Space between assemblies and between assemblies and screen varied from one case to another.

The tank was incrementally filled with water at room temperature, water being pumped in at the bottom of the tank. A measurement needle provided water height. Therefore, the water was used as core moderator and as reflector beneath the fuel and around the array on four sides behind the reflector screens. The critical approach parameter was the water level.

Seventy one experiments are evaluated and all are considered acceptable for use as benchmark experiments. Thirty eight experiments were performed with lead reflector screens and thirty three with steel reflector screens. Twenty six among the former and twenty one among the latter used absorbing canisters around the four arrays, and the others without any.

The experiments key physical parameters are summarized in Table B-5 through Table B-6.

B.3. Physical Description of the Selected Benchmark Critical Experiments

The benchmark experiments are selected to cover a wide range of code applications for fresh and spent fuel storage analysis. This section provides a summary description of the materials and physical layouts of the 135 critical configurations with fresh and selected actinides for spent fuel. For the fresh fuel assumption, the code is compared to the critical experiments of un-irradiated UO_2 systems with geometric and material characteristics similar to that of fuel storage systems. For the spent fuel assumption with burnup credit, additional comparisons are made to un-irradiated mixed-oxide (MOX) fuel of similar characteristics to spent fuel. The UO_2 experiments address ^{234}U, ^{235}U and ^{238}U. The MOX critical experiments address ^{238}Pu, ^{239}Pu, ^{240}Pu, ^{241}Pu, ^{242}Pu and ^{241}Am. Detailed descriptions of the critical experiments are presented in references [B.6] through [B.12].

Description of the selected critical experiments is summarized in Table B-7.

B.4. References

[B.1] F. Fernex, "Programme HTC – Phase 1 : Réseaux de crayons dans l'eau pure (Water-moderated and reflected simple arrays) Réévaluation des expériences," DSU/SEC/T/2005-33/D.R., Institut de Radioprotection et de Sûreté Nucléaire, 2008.

[B.2] F. Fernex, Programme HTC – Phase 2 : Réseaux simples en eau empoisonnée (bore et gadolinium) (Reflected simple arrays moderated by poisoned water with gadolinium or boron) Réévaluation des expériences," DSU/SEC/T/2005-38/D.R., Institut de Radioprotection et de Sûreté Nucléaire, 2008.

[B.3] F. Fernex, "Programme HTC – Phase 3 : Configurations "stockage en piscine" (Pool storage) Réévaluation des expériences," DSU/SEC/T/2005-37/D.R., Institut de Radioprotection et de Sûreté Nucléaire, 2008.

[B.4] F. Fernex, "Programme HTC – Phase 4 : Configurations "châteaux de transport" (Shipping cask) - Réévaluation des expériences," DSU/SEC/T/2005-36/D.R., Institut de Radioprotection et de Sûreté Nucléaire, 2008.

[B.5] C. Portella, C. Woillard "Programme "HTC" - Expériences de criticité avec des crayons combustibles HTC (type REP à haut taux de combustion) - Résultats de l'étude paramétrique avec de l'eau gadoliniée." [Translation: ""Hbu" program – Criticity Experiments with Hbu fuel rods (LWR type at high burn up) – Results of parametric study with poisoned water with gadolinium."] Note technique IPSN/SRSC n° 90.01.

[B.6] International Handbook of Evaluated Criticality Safety Benchmark Experiments, NEA/NSC/DOC(95)03, NEA Nuclear Science Committee, September 2008 Edition

[B.7] G.S. Hoovier et al., Critical Experiments Supporting Underwater Storage of Tightly Packed Configurations of Spent Fuel Pins, BAW-1645-4, Babcock & Wilcox Company, November 1991.

[B.8] L.W. Newman et al., Urania Gadolinia: Nuclear Model Development and Critical Experiment Benchmark, BAW-1810, Babcock and Wilcox Company, April 1984.

[B.9] J.C. Manaranche et al., "Dissolution and Storage Experimental Program with 4.75% Enriched Uranium-Oxide Rods," Trans. Am. Nucl. Soc. 33: 362-364 (1979).

[B.10] S.R. Bierman, Criticality Experiments with Neutron Flux Traps Containing Voids, PNL-7167, Battelle Pacific Northwest Laboratory, April 1990.

[B.11] S.R. Bierman, Criticality Experiments with Fast Test Reactor Fuel Pins in Organic Moderator, PNL-5803, Battelle Pacific Northwest Laboratory, December 1986.

[B.12] E.G. Taylor et al., Saxton Plutonium Program Critical Experiments for the Saxton Partial Plutonium core, WCAP-3385-54, Westinghouse Electric Corp., Atomic Power Division, December 1965.

[B.13] Evaluation of the French Haut Taux de Combustion (HTC) Critical Experiment Data, NUREG/CR-6979 (ORNL/TM-2007/083), U.S. Nuclear Regulatory Commission, September 2008.

Table B-1 Key Physical Parameters of the HTC Phase 1 Critical Experiments [B.1]

Case	Reference	Experiment number	Pitch (cm)	Number of Rods		Date of experiment	Temperature (°C)	Critical water height (cm) [a]
				Along edge	Total			
1	MIX-COMP-THERM-HTC-001	2327	2.3	50 × 50	2500	05/05/88	22.5	61.41 ± 0.06
2	MIX-COMP-THERM-HTC-002	2335		38 × 37	1406	06/06/88	21.1	87.68 ± 0.06
3	MIX-COMP-THERM-HTC-003	2336		37 × 37	1369	06/07/88	21.0	90.38 ± 0.06
4	MIX-COMP-THERM-HTC-004	2337	1.9	27 × 27	729	06/09/88	20.7	63.77 ± 0.06
5	MIX-COMP-THERM-HTC-005	2339		25 × 25	625	06/13/88	20.5	81.95 ± 0.08
6	MIX-COMP-THERM-HTC-006	2340		25 × 24	600	06/14/88	20.7	90.22 ± 0.06
7	MIX-COMP-THERM-HTC-007	2341	1.7	26 × 26	676	06/15/88	20.2	65.11 ± 0.07
8	MIX-COMP-THERM-HTC-008	2342		25 × 25	625	06/16/88	21.0	74.86 ± 0.06
9	MIX-COMP-THERM-HTC-009	2343		25 × 24	600	06/16/88	20.8	82.25 ± 0.06
10	MIX-COMP-THERM-HTC-010	2345	1.5	29 × 29	841	06/26/88	21.1	59.92 ± 0.06
11	MIX-COMP-THERM-HTC-011	2347		27 × 27	729	06/23/88	21.3	76.72 ± 0.06
12	MIX-COMP-THERM-HTC-012	2348		27 × 26	702	06/23/88	21.1	84.57 ± 0.06
13	MIX-COMP-THERM-HTC-013	2349	1.3	39 × 39	1521	06/29/88	21.3	53.77 ± 0.06
14	MIX-COMP-THERM-HTC-014	2352		34 × 34	1156	07/05/88	21.3	80.16 ± 0.06
15	MIX-COMP-THERM-HTC-015	2353		34 × 33	1122	07/06/88	21.3	86.35 ± 0.06
16	MIX-COMP-THERM-HTC-016	2355	1.7	50 × 18	900	07/19/88	21.0	69.07 ± 0.06
17	MIX-COMP-THERM-HTC-017	2357		50 × 17	850	07/21/88	21.4	83.15 ± 0.08
18	MIX-COMP-THERM-HTC-018	2361		50 × 18 [b]	900	07/28/88	22.4	80.16 ± 0.07

(a) given at a level of confidence of 95%

(b) no-centered array

Table B-2 Key Physical Parameters of the HTC Phase 2 Critical Experiments with Gadolinium Solutions [B.2]

Case	Reference	Experiment number	Pitch (cm)	Number of Rods		Date of experiment	Temperature (°C)	Critical water height (cm) [(a)]	Gadolinium conc. (g/l) [(b)]
				Along edge	Total				
19	MIX-COMP-THERM-HTC-019	2405	1.3	38 × 38	1444	01/20/89	20.3	81.86 ± 0.04	0.052
20	MIX-COMP-THERM-HTC-020	2406		38 × 37	1406	01/23/89	19.7	87.16 ± 0.04	0.052
21	MIX-COMP-THERM-HTC-021	2407		42 × 42	1764	01/23/89	20.1	80.13 ± 0.04	0.100
22	MIX-COMP-THERM-HTC-022	2408		42 × 41	1722	01/25/89	19.7	84.38 ± 0.04	0.099
23	MIX-COMP-THERM-HTC-023	2409		41 × 41	1681	01/25/89	19.6	89.54 ± 0.04	0.099
24	MIX-COMP-THERM-HTC-024	2410		46 × 46	2116	01/26/89	20.1	81.33 ± 0.04	0.151
25	MIX-COMP-THERM-HTC-025	2411		45 × 45	2025	01/27/89	20.0	89.49 ± 0.04	0.148
26	MIX-COMP-THERM-HTC-026	2412		50 × 50	2500	01/30/89	20.7	85.83 ± 0.04	0.200
27	MIX-COMP-THERM-HTC-027	2415		50 × 49	2450	02/01/89	19.6	90.03 ± 0.05	0.197
28	MIX-COMP-THERM-HTC-028	2417	1.5	50 × 50	2500	02/09/89	19.6	89.67 ± 0.04	0.196
29	MIX-COMP-THERM-HTC-029	2419		42 × 42	1764	02/14/89	21.4	85.88 ± 0.05	0.147
30	MIX-COMP-THERM-HTC-030	2420		42 × 41	1722	02/15/89	21.0	90.51 ± 0.05	0.147
31	MIX-COMP-THERM-HTC-031	2422		36 × 36	1296	02/21/89	22.1	83.86 ± 0.05	0.098
32	MIX-COMP-THERM-HTC-032	2423		36 × 35	1260	02/21/89	22.6	89.85 ± 0.04	0.098
33	MIX-COMP-THERM-HTC-033	2425		32 × 32	1024	02/24/89	20.9	73.60 ± 0.05	0.048
34	MIX-COMP-THERM-HTC-034	2427		31 × 31	961	02/27/89	20.6	84.14 ± 0.04	0.048
35	MIX-COMP-THERM-HTC-035	2430	1.7	31 × 30	930	03/01/89	21.1	85.87 ± 0.05	0.048
36	MIX-COMP-THERM-HTC-036	2434	1.9	35 × 35	1225	03/08/89	21.7	89.61 ± 0.04	0.048
37	MIX-COMP-THERM-HTC-037	2436	1.7	39 × 39	1521	03/13/89	22.5	85.86 ± 0.05	0.097
38	MIX-COMP-THERM-HTC-038	2433		50 × 23	1150	03/07/89	21.7	84.35 ± 0.04	0.048

(a) given at a level of confidence of 95%

(b) nominal values given in the report [B.5], not retained

Table B-3 Key Physical Parameters of the HTC Phase 2 Critical Experiments with Boron Solutions [B.2]

Case	Reference	Experiment number	Pitch (cm)	Number of Rods		Date of experiment	Temperature (°C)	Critical water height (cm) [(a)]	Boron conc. (g/l)
				Along edge	Total				
39	MIX-COMP-THERM-HTC-039	2437	1.3	37 × 37	1369	04/17/89	23.0	78.80 ± 0.04	0.100 ± 0.001
40	MIX-COMP-THERM-HTC-040	2438		37 × 36	1332	04/18/89	22.8	83.84 ± 0.04	0.106 ± 0.001
41	MIX-COMP-THERM-HTC-041	2441		39 × 39	1521	04/20/89	23.5	84.04 ± 0.04	0.205 ± 0.002
42	MIX-COMP-THERM-HTC-042	2444		42 × 41	1722	04/26/89	23.0	85.40 ± 0.05	0.299 ± 0.003
43	MIX-COMP-THERM-HTC-043	2446		45 × 44	1980	05/09/89	24.2	84.14 ± 0.04	0.400 ± 0.004
44	MIX-COMP-THERM-HTC-044	2447		44 × 44	1936	05/10/89	24.7	88.63 ± 0.05	0.399 ± 0.004
45	MIX-COMP-THERM-HTC-045	2448		47 × 47	2009	05/11/89	26.3	88.44 ± 0.04	0.486 ± 0.005
46	MIX-COMP-THERM-HTC-046	2449		50 × 50	2500	05/17/89	25.1	90.64 ± 0.04	0.587 ± 0.006
47	MIX-COMP-THERM-HTC-047	2459	1.5	49 × 49	2401	06/05/89	24.7	88.88 ± 0.04	0.595 ± 0.006
48	MIX-COMP-THERM-HTC-048	2468		43 × 43	1849	06/15/89	22.7	89.46 ± 0.04	0.499 ± 0.005
49	MIX-COMP-THERM-HTC-049	2470		39 × 39	1521	06/19/89	23.6	85.37 ± 0.05	0.393 ± 0.004
50	MIX-COMP-THERM-HTC-050	2471		35 × 35	1225	06/21/89	23.6	88.90 ± 0.04	0.295 ± 0.003
51	MIX-COMP-THERM-HTC-051	2473		32 × 32	1024	06/27/89	23.5	87.02 ± 0.04	0.200 ± 0.002
52	MIX-COMP-THERM-HTC-052	2475		30 × 29	870	07/03/89	23.6	82.48 ± 0.04	0.089 ± 0.001
53	MIX-COMP-THERM-HTC-053	2478	1.7	28 × 28	784	07/06/89	23.8	85.10 ± 0.04	0.090 ± 0.001
54	MIX-COMP-THERM-HTC-054	2483		32 × 32	1024	07/19/89	24.2	87.06 ± 0.04	0.194 ± 0.002
55	MIX-COMP-THERM-HTC-055	2485		37 × 37	1369	07/21/89	24.5	89.65 ± 0.04	0.286 ± 0.003
56	MIX-COMP-THERM-HTC-056	2487		45 × 44	1980	08/09/89	23.8	88.72 ± 0.04	0.415 ± 0.004
57	MIX-COMP-THERM-HTC-057	2482		50 × 21	1050	07/17/89	24.0	77.74 ± 0.04	0.100 ± 0.001
58	MIX-COMP-THERM-HTC-058	2490	1.9	39 × 38	1482	09/08/89	22.9	88.41 ± 0.04	0.220 ± 0.002
59	MIX-COMP-THERM-HTC-059	2492		31 × 30	930	09/14/89	22.0	86.95 ± 0.04	0.110 ± 0.001

(a) given at a level of confidence of 95%

Table B-4 Key Physical Parameters of the HTC Phase 3 Critical Experiments (pin pitch 1.6 cm) [B.3]

Case	Reference	Experiment number	Canister Type	Number of Rods		Date of experiment	Temperature (°C)	Critical water height (cm) [(a)]	Water Gap (cm)
				Along edge	Total				
60	MIX-COMP-THERM-HTC-060	2518	Borated Steel	25 × 25	625	01/04/90	18.3	88.83 ± 0.34	3.5
61	MIX-COMP-THERM-HTC-061	2520		25 × 24	600	01/09/90	18.7	49.55 ± 0.34	0.0
62	MIX-COMP-THERM-HTC-062	2521		25 × 24	600	01/10/90	18.8	71.45 ± 0.34	2.0
63	MIX-COMP-THERM-HTC-063	2522		25 × 24	600	01/10/90	19.0	89.96 ± 0.34	3.0
64	MIX-COMP-THERM-HTC-064	2523		25 × 24	600	01/12/90	18.9	58.23 ± 0.34	1.0
65	MIX-COMP-THERM-HTC-065	2514	Boral	25 × 25	625	12/28/89	20.6	90.03 ± 0.34	0.0
66	MIX-COMP-THERM-HTC-066	2511	Cadmium	25 × 25	625	12/21/89	21.1	82.16 ± 0.34	2.0
67	MIX-COMP-THERM-HTC-067	2524		25 × 24	600	01/15/90	18.7	55.33 ± 0.34	0.0
68	MIX-COMP-THERM-HTC-068	2525		25 × 24	600	01/16/90	19.0	67.95 ± 0.34	1.0
69	MIX-COMP-THERM-HTC-069	2526		25 × 24	600	01/17/90	19.1	79.83 ± 0.34	1.5
70	MIX-COMP-THERM-HTC-070	2527		25 × 24	600	01/18/90	19.1	58.66 ± 0.34	0.5
71	MIX-COMP-THERM-HTC-071	2509		25 × 25	625	12/19/89	20.9	84.75 ± 0.34	18.0
72	MIX-COMP-THERM-HTC-072	2531		25 × 24	600	01/23/90	19.0	88.2 ± 0.34	14.5
73	MIX-COMP-THERM-HTC-073	2532		24 × 24	576	01/24/90	19.1	81.18 ± 0.34	11.0
74	MIX-COMP-THERM-HTC-074	2533		24 × 23	552	01/25/90	19.3	82.12 ± 0.34	10.0
75	MIX-COMP-THERM-HTC-075	2534		23 × 23	529	01/26/90	19.4	81.2 ± 0.34	9.0
76	MIX-COMP-THERM-HTC-076	2535		22 × 22	484	01/30/90	19.7	86.17 ± 0.34	8.0
77	MIX-COMP-THERM-HTC-077	2536		20 × 20	400	01/31/90	19.7	82.08 ± 0.34	6.0
78	MIX-COMP-THERM-HTC-078	2537		17 × 17	289	02/01/90	19.9	77.92 ± 0.34	4.0
79	MIX-COMP-THERM-HTC-079	2538		17 × 16	272	02/02/90	20.0	90.28 ± 0.34	4.0
80	MIX-COMP-THERM-HTC-080	2539		14 × 14	196	02/05/90	20.2	75.99 ± 0.34	2.0
81	MIX-COMP-THERM-HTC-081	2541		13 × 13	169	02/06/90	20.0	83.17 ± 0.34	1.0
82	MIX-COMP-THERM-HTC-082	2544		13 × 13	169	02/07/90	20.4	79.46 ± 0.34	0.0
83	MIX-COMP-THERM-HTC-083	2547		25 × 25	625	02/19/90	20.9	29.46 ± 0.34	0.0
84	MIX-COMP-THERM-HTC-084	2548		25 × 25	625	02/20/90	20.9	37.96 ± 0.34	4.0
85	MIX-COMP-THERM-HTC-085	2549		25 × 25	625	02/20/90	21.0	64.43 ± 0.34	10.0

(a) given at a level of confidence of 95%

Table B-5 Key Physical Parameters of the HTC Phase 4 Critical Experiments with the Lead Screen (four 25 × 25 arrays with 1.6 cm pitch) [B.4]

Case	Reference	Experiment number	Canister Type	Date of experiment	Temperature (°C)	Water Gap (cm) [a]	Screen array distance (cm) [b]	Critical water height (cm) [c]
86	MIX-COMP-THERM-HTC-086	2562	Borated Steel	03/16/90	22.8	0.0	0.0	42.53 ± 0.34
87	MIX-COMP-THERM-HTC-087	2563		03/19/90	23.1	0.5	0.0	44.79 ± 0.34
88	MIX-COMP-THERM-HTC-088	2564		03/20/90	23.3	1.0	0.0	47.86 ± 0.34
89	MIX-COMP-THERM-HTC-089	2565		03/21/90	23.1	1.5	0.0	51.3 ± 0.34
90	MIX-COMP-THERM-HTC-090	2566		03/22/90	23.3	2.0	0.0	54.65 ± 0.34
91	MIX-COMP-THERM-HTC-091	2567		03/22/90	23.4	3.0	0.0	62.04 ± 0.34
92	MIX-COMP-THERM-HTC-092	2568		03/23/90	23.6	3.5	0.0	66.10 ± 0.34
93	MIX-COMP-THERM-HTC-093	2569		03/26/90	23.5	2.0	0.5	55.87 ± 0.34
94	MIX-COMP-THERM-HTC-094	2570		03/27/90	23.1	2.0	1.0	57.33 ± 0.34
95	MIX-COMP-THERM-HTC-095	2571		03/27/90	23.0	2.0	1.5	58.68 ± 0.34
96	MIX-COMP-THERM-HTC-096	2572		03/28/90	22.9	2.0	2.0	59.78 ± 0.34
97	MIX-COMP-THERM-HTC-097	2586	Boral	04/23/90	21.9	0.0	0.0	72.47 ± 0.34
98	MIX-COMP-THERM-HTC-098	2587		04/24/90	22.0	0.0	0.0	72.49 ± 0.34
99	MIX-COMP-THERM-HTC-099	2588		04/24/90	22.2	0.0	0.5	74.70 ± 0.34
100	MIX-COMP-THERM-HTC-100	2624		07/13/90	21.6	1.0	0.0	86.06 ± 0.34
101	MIX-COMP-THERM-HTC-101	2625		07/18/90	22.4	0.5	0.0	76.69 ± 0.34
102	MIX-COMP-THERM-HTC-102	2577	Cadmium	04/05/90	22.7	0.0	0.0	46.13 ± 0.34
103	MIX-COMP-THERM-HTC-103	2578		04/05/90	22.6	1.0	0.0	52.89 ± 0.34
104	MIX-COMP-THERM-HTC-104	2579		04/06/90	22.6	2.0	0.0	63.52 ± 0.34
105	MIX-COMP-THERM-HTC-105	2580		04/09/90	22.4	2.5	0.0	69.83 ± 0.34
106	MIX-COMP-THERM-HTC-106	2581		04/11/90	22.5	2.0	0.5	65.84 ± 0.34
107	MIX-COMP-THERM-HTC-107	2582		04/11/90	22.5	2.0	1.0	68.63 ± 0.34
108	MIX-COMP-THERM-HTC-108	2583		04/12/90	22.4	2.0	1.5	71.21 ± 0.34

Case	Reference	Experiment number	Canister Type	Date of experiment	Temperature (°C)	Water Gap (cm) [a]	Screen array distance (cm) [b]	Critical water height (cm) [c]
109	MIX-COMP-THERM-HTC-109	2584		04/12/90	22.4	2.0	2.0	73.36 ± 0.34
110	MIX-COMP-THERM-HTC-110	2621		07/03/90	22.3	3.0	0.0	76.25 ± 0.34
111	MIX-COMP-THERM-HTC-111	2622		07/04/90	22.3	3.5	0.0	83.38 ± 0.34
112	MIX-COMP-THERM-HTC-112	2550	No	02/23/90	21.4	0.0	0.0	27.45 ± 0.34
113	MIX-COMP-THERM-HTC-113	2551		02/26/90	22.1	1.0	0.0	28.00 ± 0.34
114	MIX-COMP-THERM-HTC-114	2552		02/28/90	21.8	2.0	0.0	29.37 ± 0.34
115	MIX-COMP-THERM-HTC-115	2553		03/01/90	21.8	4.0	0.0	34.65 ± 0.34
116	MIX-COMP-THERM-HTC-116	2554		03/02/90	21.3	6.0	0.0	41.60 ± 0.34
117	MIX-COMP-THERM-HTC-117	2555		03/05/90	20.7	8.0	0.0	48.65 ± 0.34
118	MIX-COMP-THERM-HTC-118	2556		03/06/90	20.7	10.0	0.0	54.74 ± 0.34
119	MIX-COMP-THERM-HTC-119	2557		03/07/90	20.9	12.0	0.0	59.57 ± 0.34
120	MIX-COMP-THERM-HTC-120	2558		03/09/90	21.3	2.0	0.5	29.43 ± 0.34
121	MIX-COMP-THERM-HTC-121	2559		03/12/90	21.7	2.0	1.0	29.46 ± 0.34
122	MIX-COMP-THERM-HTC-122	2560		03/13/90	21.9	2.0	1.5	29.55 ± 0.34
123	MIX-COMP-THERM-HTC-123	2561		03/14/90	22.3	2.0	2.0	29.62 ± 0.34

(a) Water gap between arrays.

(b) Water gap between screen and array.

(c) Given at a level of confidence of 95%

Table B-6 Key Physical Parameters of the HTC Phase 4 Critical Experiments with the Steel Screen (four 25 × 25 arrays with 1.6 cm pitch) [B.4]

Case	Reference	Experiment number	Canister Type	Date of experiment	Temperature (°C)	Water Gap (cm) [a]	Screen array distance (cm) [b]	Critical water height (cm) [c]
124	MIX-COMP-THERM-HTC-124	2602	Borated Steel	05/21/90	23.6	0.0	0.0	42.11 ± 0.34
125	MIX-COMP-THERM-HTC-125	2603		05/21/90	23.4	0.5	0.0	44.14 ± 0.34
126	MIX-COMP-THERM-HTC-126	2604		05/22/90	22.9	1.0	0.0	46.96 ± 0.34
127	MIX-COMP-THERM-HTC-127	2605		05/29/90	20.4	1.5	0.0	50.16 ± 0.34
128	MIX-COMP-THERM-HTC-128	2606		05/30/90	20.1	2.0	0.0	53.43 ± 0.34
129	MIX-COMP-THERM-HTC-129	2607		05/31/90	20.0	2.0	0.5	54.71 ± 0.34
130	MIX-COMP-THERM-HTC-130	2608		06/05/90	20.2	2.0	1.0	56.32 ± 0.34
131	MIX-COMP-THERM-HTC-131	2609		06/05/90	20.1	2.0	1.5	57.96 ± 0.34
132	MIX-COMP-THERM-HTC-132	2610		06/06/90	19.7	2.0	2.0	59.16 ± 0.34
133	MIX-COMP-THERM-HTC-133	2611		06/08/90	19.5	3.0	0.0	60.38 ± 0.34
134	MIX-COMP-THERM-HTC-134	2612		06/12/90	20.1	3.5	0.0	64.19 ± 0.34
135	MIX-COMP-THERM-HTC-135	2589	Boral	04/26/90	22.4	0.0	0.0	69.82 ± 0.34
136	MIX-COMP-THERM-HTC-136	2626		07/19/90	22.6	0.5	0.0	73.44 ± 0.34
137	MIX-COMP-THERM-HTC-137	2613	Cadmium	06/13/90	20.5	0.0	0.0	44.70 ± 0.34
138	MIX-COMP-THERM-HTC-138	2614		06/13/90	20.6	1.0	0.0	51.00 ± 0.34
139	MIX-COMP-THERM-HTC-139	2615		06/14/90	20.6	2.0	0.0	60.26 ± 0.34
140	MIX-COMP-THERM-HTC-140	2616		06/15/90	20.7	2.0	0.5	62.54 ± 0.34
141	MIX-COMP-THERM-HTC-141	2617		06/18/90	21.0	2.0	1.0	65.85 ± 0.34
142	MIX-COMP-THERM-HTC-142	2618		06/19/90	21.3	2.0	1.5	68.70 ± 0.34
143	MIX-COMP-THERM-HTC-143	2619		06/20/90	21.5	2.0	2.0	71.00 ± 0.34
144	MIX-COMP-THERM-HTC-144	2620		06/21/90	21.7	2.5	0.0	65.76 ± 0.34
145	MIX-COMP-THERM-HTC-145	2590	No	04/27/90	22.4	0.0	0.0	27.77 ± 0.34
146	MIX-COMP-THERM-HTC-146	2591		05/09/90	24.4	1.0	0.0	28.34 ± 0.34

Case	Reference	Experiment number	Canister Type	Date of experiment	Temperature (°C)	Water Gap (cm) [a]	Screen array distance (cm) [b]	Critical water height (cm) [c]
147	MIX-COMP-THERM-HTC-147	2592		05/10/90	24.4	2.0	0.0	29.74 ± 0.34
148	MIX-COMP-THERM-HTC-148	2593		05/10/90	24.3	2.0	0.5	29.68 ± 0.34
149	MIX-COMP-THERM-HTC-149	2594		05/11/90	24.5	2.0	1.0	29.66 ± 0.34
150	MIX-COMP-THERM-HTC-150	2595		05/11/90	24.4	2.0	1.5	29.68 ± 0.34
151	MIX-COMP-THERM-HTC-151	2596		05/14/90	24.7	2.0	2.0	29.76 ± 0.34
152	MIX-COMP-THERM-HTC-152	2597		05/15/90	24.6	4.0	0.0	35.33 ± 0.34
153	MIX-COMP-THERM-HTC-153	2598		05/15/90	24.6	6.0	0.0	43.24 ± 0.34
154	MIX-COMP-THERM-HTC-154	2599		05/16/90	24.7	8.0	0.0	51.30 ± 0.34
155	MIX-COMP-THERM-HTC-155	2600		05/17/90	24.7	10.0	0.0	58.73 ± 0.34
156	MIX-COMP-THERM-HTC-156	2601		05/18/90	24.6	12.0	0.0	64.84 ± 0.34

(a) Water gap between arrays.

(b) Water gap between screen and array.

(c) Given at a level of confidence of 95%

Table B-7 Description of the Selected Benchmark Critical Experiments [B.6]

Case	Reference	Identification	U, wt%	Pu, wt%	
157	LEU-COMP-THERM-011-001	Core I	2.46	-	
158	LEU-COMP-THERM-011-002	Core II	2.46	-	
159	LEU-COMP-THERM-011-004	Core IIIB	2.46	-	
160	LEU-COMP-THERM-011-015	Core IX	2.46	-	
161	LEU-COMP-THERM-051-001	Core X	2.46	-	
162	LEU-COMP-THERM-051-003	Core XIB	2.46	-	
163	LEU-COMP-THERM-051-009	Core XII	2.46	-	
164	LEU-COMP-THERM-051-010	Core XIII	2.46	-	
165	LEU-COMP-THERM-051-012	Core XIV	2.46	-	
166	LEU-COMP-THERM-051-013	Core XV	2.46	-	
167	LEU-COMP-THERM-051-014	Core XVI	2.46	-	
168	LEU-COMP-THERM-051-015	Core XVII	2.46	-	
169	LEU-COMP-THERM-051-016	Core XVIII	2.46	-	
170	LEU-COMP-THERM-051-017	Core XIX	2.46	-	
171	LEU-COMP-THERM-051-018	Core XX	2.46	-	
172	LEU-COMP-THERM-051-019	Core XXI	2.46	-	
173	BAW-1645-4 [B.7]	S-type Fuel, w/886 ppm B	2.46	-	
174	BAW-1645-4 [B.7]	S-type Fuel, w/746 ppm B	2.46	-	
175	BAW-1645-4 [B.7]	SO-type Fuel, w/1156 ppm B	2.46	-	
176	BAW-1810 [B.8]	Case 1 1337 ppm B	2.46	-	
177	BAW-1810 [B.8]	Case 12 1899 ppm B	2.75	-	
178	French [B.9]	Water Moderator 0 gap	4.75	-	
179	French [B.9]	Water Moderator 2.5 cm gap	4.75	-	
180	French [B.9]	Water Moderator 5 cm gap	4.75	-	
181	French [B.9]	Water Moderator 10 cm gap	4.75	-	
182	LEU-COMP-THERM-017-012	Steel Reflector, 1.321 cm separation	2.35	-	
183	LEU-COMP-THERM-017-013	Steel Reflector, 2.616 cm separation	2.35	-	
184	LEU-COMP-THERM-017-014	Steel Reflector, 3.912 cm separation	2.35	-	
185	LEU-COMP-THERM-001-008	Steel Reflector, Infinite separation	2.35	-	
186	LEU-COMP-THERM-010-016	Steel Reflector, 1.321 cm separation	4.306	-	
187	LEU-COMP-THERM-010-018	Steel Reflector, 2.616 cm separation	4.306	-	
188	LEU-COMP-THERM-010-019	Steel Reflector, 5.405 cm separation	4.306	-	
189	LEU-COMP-THERM-004-010	Steel Reflector, Infinite separation	4.306	-	
190	LEU-COMP-THERM-013-003	Steel Reflector, with Boral Sheets	4.306	-	
191	LEU-COMP-THERM-010-021	Lead Reflector, 0.55 cm sepn.	4.306	-	
192	LEU-COMP-THERM-010-022	Lead Reflector, 1.956 cm sepn.	4.306	-	
193	LEU-COMP-THERM-010-023	Lead Reflector, 5.405 cm sepn.	4.306	-	
194	LEU-COMP-THERM-002-004	Experiment 004/032 – no absorber	4.306	-	
195	LEU-COMP-THERM-009-005	Exp. 009 1.05% Boron Steel plates	4.306	-	

Case	Reference	Identification	U, wt%	Pu, wt%
196	LEU-COMP-THERM-009-007	Exp. 009 1.62% Boron Steel plates	4.306	-
197	LEU-COMP-THERM-009-009	Exp. 031 – Boral plates	4.306	-
198	PNL-7167 [B.10]	Experiment 214R – with flux traps	4.306	-
199	PNL-7167 [B.10]	Experiment 214V3 –with flux trap	4.306	-
200	LEU-COMP-THERM-014-001	Case 173 – 0 ppm B	4.306	-
201	LEU-COMP-THERM-014-005	Case 177 – 2550 ppm B	4.306	-
202	PNL-5803 [B.11]	MOX Fuel – Type 3.2 Exp. 21	0.71	20
203	PNL-5803 [B.11]	MOX Fuel – Type 3.2 Exp. 43	0.71	20
204	PNL-5803 [B.11]	MOX Fuel – Type 3.2 Exp. 13	0.71	20
205	PNL-5803 [B.11]	MOX Fuel – Type 3.2 Exp. 32	0.71	20
206	MIX-COMP-THERM-003-001	Saxton Case 52 PuO2 0.52" pitch	0.72	6.6
207	WCAP-3385 [B.12]	Saxton Case 52 U 0.52" pitch	5.74	-
208	MIX-COMP-THERM-003-002	Saxton Case 56 PuO2 0.56" pitch	0.72	6.6
209	MIX-COMP-THERM-003-003	Saxton Case 56 borated PuO2	0.72	6.6
210	WCAP-3385 [B.12]	Saxton Case 56 U 0.56" pitch	5.74	-
211	MIX-COMP-THERM-003-005	Saxton Case 79 PuO2 0.79" pitch	0.72	6.6
212	WCAP-3385 [B.12]	Saxton Case 79 U 0.79" pitch	5.74	-
213	MIX-COMP-THERM-002-030	0.700-in. pitch 0 ppm B	0.72	2.0
214	MIX-COMP-THERM-002-031	0.700-in. pitch 688 ppm B	0.72	2.0
215	MIX-COMP-THERM-002-032	0.870-in. pitch 0 ppm B	0.72	2.0
216	MIX-COMP-THERM-002-033	0.870-in. pitch 1090 ppm B	0.72	2.0
217	MIX-COMP-THERM-002-034	0.990-in. pitch 0 ppm B	0.72	2.0
218	MIX-COMP-THERM-002-035	0.990-in. pitch 767 ppm B	0.72	2.0
219	MIX-COMP-THERM-003-004	Saxton Case PuO2 0.735" pitch	0.72	6.6
220	MIX-COMP-THERM-003-006	Saxton Case PuO2 1.04" pitch	0.72	6.6
221	MIX-COMP-THERM-006-001	8 wt% 240Pu 0.80" pitch	0.71	2.0
222	MIX-COMP-THERM-006-002	8 wt% 240Pu 0.93" pitch	0.71	2.0
223	MIX-COMP-THERM-006-003	8 wt% 240Pu 1.05" pitch	0.71	2.0
224	MIX-COMP-THERM-006-004	8 wt% 240Pu 1.143" pitch	0.71	2.0
225	MIX-COMP-THERM-006-005	8 wt% 240Pu 1.32" pitch	0.71	2.0
226	MIX-COMP-THERM-006-006	8 wt% 240Pu 1.386" pitch	0.71	2.0
227	MIX-COMP-THERM-007-001	16 wt% 240Pu 0.93" pitch	0.72	2.0
228	MIX-COMP-THERM-007-002	16 wt% 240Pu 1.05" pitch	0.72	2.0
229	MIX-COMP-THERM-007-003	16 wt% 240Pu 1.143" pitch	0.72	2.0
230	MIX-COMP-THERM-007-004	16 wt% 240Pu 1.32" pitch	0.72	2.0
231	MIX-COMP-THERM-008-001	24 wt% 240Pu 0.80" pitch	0.72	2.0
232	MIX-COMP-THERM-008-002	24 wt% 240Pu 0.93" pitch	0.72	2.0
233	MIX-COMP-THERM-008-003	24 wt% 240Pu 1.05" pitch	0.72	2.0
234	MIX-COMP-THERM-008-004	24 wt% 240Pu 1.143" pitch	0.72	2.0
235	MIX-COMP-THERM-008-005	24 wt% 240Pu 1.32" pitch	0.72	2.0

Case	Reference	Identification	U, wt%	Pu, wt%
236	MIX-COMP-THERM-008-006	24 wt% 240Pu 1.386" pitch	0.72	2.0
237	MIX-COMP-THERM-005-001	18 wt% 240Pu 0.85" pitch	0.72	4.0
238	MIX-COMP-THERM-005-002	18 wt% 240Pu 0.93" pitch	0.72	4.0
239	MIX-COMP-THERM-005-003	18 wt% 240Pu 1.05" pitch	0.72	4.0
240	MIX-COMP-THERM-005-004	18 wt% 240Pu 1.143" pitch	0.72	4.0
241	MIX-COMP-THERM-005-005	18 wt% 240Pu 1.386" pitch	0.72	4.0
242	MIX-COMP-THERM-005-006	18 wt% 240Pu 1.60" pitch	0.72	4.0
243	MIX-COMP-THERM-005-007	18 wt% 240Pu 1.70" pitch	0.72	4.0
244	LEU-COMP-THERM-001-001	1 Cluster	2.35	-
245	LEU-COMP-THERM-001-002	3 Clusters, Separation 11.92 cm	2.35	-
246	LEU-COMP-THERM-001-003	3 Clusters, Separation 8.41 cm	2.35	-
247	LEU-COMP-THERM-001-004	3 Clusters, Separation 10.05 cm	2.35	-
248	LEU-COMP-THERM-001-005	3 Clusters, Separation 6.39 cm	2.35	-
249	LEU-COMP-THERM-001-006	3 Clusters, Separation 9.01 cm	2.35	-
250	LEU-COMP-THERM-001-007	3 Clusters, Separation 4.46	2.35	-
251	LEU-COMP-THERM-002-001	1 Cluster, 10x11.51	4.306	-
252	LEU-COMP-THERM-002-002	1 Cluster, 9x13.35	4.306	-
253	LEU-COMP-THERM-002-003	1 Cluster, 8x16.37	4.306	-
254	LEU-COMP-THERM-002-005	3 Clusters, Separation 7.11 cm	4.306	-
255	LEU-COMP-THERM-003-001	1 Cluster, 614.4 Rods, Gd water impurity	2.35	-
256	LEU-COMP-THERM-003-002	1 Cluster, 529.3 Rods	2.35	-
257	LEU-COMP-THERM-003-003	1 Cluster, 523.9 Rods	2.35	-
258	LEU-COMP-THERM-003-004	1 Cluster, 525.3 Rods	2.35	-
259	LEU-COMP-THERM-003-005	1 Cluster, 595.4 Rods	2.35	-
260	LEU-COMP-THERM-003-006	1 Cluster, 485.8 Rods	2.35	-
261	LEU-COMP-THERM-003-007	1 Cluster, 523.8 Rods	2.35	-
262	LEU-COMP-THERM-003-008	1 Cluster, 505.4 Rods	2.35	-
263	LEU-COMP-THERM-003-009	4 Clusters, Separation 2.59 cm	2.35	-
264	LEU-COMP-THERM-003-010	2 Clusters, Separation 1.68 cm	2.35	-
265	LEU-COMP-THERM-003-011	4 Clusters, Separation 4.27 cm	2.35	-
266	LEU-COMP-THERM-003-012	4 Clusters, Separation 5.95 cm	2.35	-
267	LEU-COMP-THERM-003-013	4 Clusters, Separation 5.11 cm	2.35	-
268	LEU-COMP-THERM-003-014	4 Clusters, Separation 6.66 cm	2.35	-
269	LEU-COMP-THERM-003-015	4 Clusters, Separation 7.53 cm	2.35	-
270	LEU-COMP-THERM-003-016	4 Clusters, Separation 9.00 cm	2.35	-
271	LEU-COMP-THERM-003-017	4 Clusters, Separation 9.97 cm	2.35	-
272	LEU-COMP-THERM-003-018	4 Clusters, Separation 11.45 cm	2.35	-
273	LEU-COMP-THERM-003-019	4 Clusters, Separation 13.87 cm	2.35	-
274	LEU-COMP-THERM-003-020	3 Clusters, Separation 9.88 cm	2.35	-
275	LEU-COMP-THERM-003-021	3 Clusters, Separation 6.78 cm	2.35	-

Case	Reference	Identification	U, wt%	Pu, wt%	
276	LEU-COMP-THERM-003-023	3 Clusters, Separation 6.176 cm	2.35	-	
277	LEU-COMP-THERM-004-001	1 Cluster, 225.8 Rods, Gd water impurity	4.306	-	
278	LEU-COMP-THERM-004-002	1 Cluster, 216.2 Rods	4.306	-	
279	LEU-COMP-THERM-004-003	1 Cluster, 216.6 Rods	4.306	-	
280	LEU-COMP-THERM-004-004	1 Cluster, 218.6 Rods	4.306	-	
281	LEU-COMP-THERM-004-005	1 Cluster, 167.85 Rods	4.306	-	
282	LEU-COMP-THERM-004-006	1 Cluster, 203 Rods	4.306	-	
283	LEU-COMP-THERM-004-007	1 Cluster, 173.5 Rods	4.306	-	
284	LEU-COMP-THERM-004-008	2 Clusters, Separation 2.83 cm	4.306	-	
285	LEU-COMP-THERM-004-009	3 Clusters, Separation 12.27 cm	4.306	-	
286	LEU-COMP-THERM-004-011	3 Clusters, Separation 12.493 cm	4.306	-	
287	LEU-COMP-THERM-004-012	4 Clusters, Separation 4.72 cm	4.306	-	
288	LEU-COMP-THERM-004-013	4 Clusters, Separation 8.38 cm	4.306	-	
289	LEU-COMP-THERM-004-014	4 Clusters, Separation 10.86 cm	4.306	-	
290	LEU-COMP-THERM-004-015	4 Clusters, Separation 11.29 cm	4.306	-	
291	LEU-COMP-THERM-004-016	4 Clusters, Separation 12.02 cm	4.306	-	
292	LEU-COMP-THERM-004-017	4 Clusters, Separation 13.64 cm	4.306	-	
293	LEU-COMP-THERM-004-018	4 Clusters, Separation 14.98 cm	4.306	-	
294	LEU-COMP-THERM-004-019	4 Clusters, Separation 19.81 cm	4.306	-	
295	LEU-COMP-THERM-004-020	4 Clusters, Separation 8.50 cm	4.306	-	
296	LEU-COMP-THERM-006-001	19x19, Rod Pitch - 1.849 cm	2.596	-	
297	LEU-COMP-THERM-006-002	20x20, Rod Pitch - 1.849 cm	2.596	-	
298	LEU-COMP-THERM-006-003	21x21, Rod Pitch - 1.849 cm	2.596	-	
299	LEU-COMP-THERM-006-004	17x17, Rod Pitch - 1.956 cm	2.596	-	
300	LEU-COMP-THERM-006-005	18x18, Rod Pitch - 1.956 cm	2.596	-	
301	LEU-COMP-THERM-006-006	19x19, Rod Pitch - 1.956 cm	2.596	-	
302	LEU-COMP-THERM-006-007	20x20, Rod Pitch - 1.956 cm	2.596	-	
303	LEU-COMP-THERM-006-008	21x21, Rod Pitch - 1.956 cm	2.596	-	
304	LEU-COMP-THERM-006-009	16x16, Rod Pitch - 2.15 cm	2.596	-	
305	LEU-COMP-THERM-006-010	17x17, Rod Pitch - 2.15 cm	2.596	-	
306	LEU-COMP-THERM-006-011	18x18, Rod Pitch - 2.15 cm	2.596	-	
307	LEU-COMP-THERM-006-012	19x19, Rod Pitch - 2.15 cm	2.596	-	
308	LEU-COMP-THERM-006-013	20x20, Rod Pitch - 2.15 cm	2.596	-	
309	LEU-COMP-THERM-006-014	15x15, Rod Pitch - 2.293 cm	2.596	-	
310	LEU-COMP-THERM-006-015	16x16, Rod Pitch - 2.293 cm	2.596	-	
311	LEU-COMP-THERM-006-016	17x17, Rod Pitch - 2.293 cm	2.596	-	
312	LEU-COMP-THERM-006-017	18x18, Rod Pitch - 2.293 cm	2.596	-	
313	LEU-COMP-THERM-006-018	19x19, Rod Pitch - 2.293 cm	2.596	-	
314	LEU-COMP-THERM-008-001	Core XI, 1511 ppm	2.459	-	
315	LEU-COMP-THERM-008-002	Core XI, 1335.5 ppm	2.459	-	

Case	Reference	Identification	U, wt%	Pu, wt%
316	LEU-COMP-THERM-008-003	Core XI, 1335.5 ppm	2.459	-
317	LEU-COMP-THERM-008-004	Core XI, 1182 ppm, 36 Pyrex Rods	2.459	-
318	LEU-COMP-THERM-008-005	Core XI, 1182 ppm, 36 Pyrex Rods	2.459	-
319	LEU-COMP-THERM-008-006	Core XI, 1032.5 ppm, 72 Pyrex Rods	2.459	-
320	LEU-COMP-THERM-008-007	Core XI, 1032.5 ppm, 72 Pyrex Rods	2.459	-
321	LEU-COMP-THERM-008-008	Core XI, 794 ppm, 144 Pyrex Rods	2.459	-
322	LEU-COMP-THERM-008-009	Core XI, 779 ppm, 144 Pyrex Rods	2.459	-
323	LEU-COMP-THERM-008-010	Core XI, 1245 ppm, 72 Vicor Rods	2.459	-
324	LEU-COMP-THERM-008-011	Core XI, 1384 ppm, 144 Al_2O_3 Rods	2.459	-
325	LEU-COMP-THERM-008-012	Core XI, 1348 ppm, 36 Al2O3 Rods	2.459	-
326	LEU-COMP-THERM-008-013	Core XI, 1348 ppm, 36 Al2O3 Rods	2.459	-
327	LEU-COMP-THERM-008-014	Core XI, 1363 ppm, 72 Al2O3 Rods	2.459	-
328	LEU-COMP-THERM-008-015	Core XI, 1362 ppm, 72 Al2O3 Rods	2.459	-
329	LEU-COMP-THERM-008-016	Core XI, 1158 ppm	2.459	-
330	LEU-COMP-THERM-008-017	Core XI, 921 ppm	2.459	-
331	LEU-COMP-THERM-009-001	0% Boron Steel plates, dist. 0.245 cm	4.306	-
332	LEU-COMP-THERM-009-002	0% Boron Steel plates, dist. 3.277 cm	4.306	-
333	LEU-COMP-THERM-009-003	0% Boron Steel plates, dist. 0.428 cm	4.306	-
334	LEU-COMP-THERM-009-004	0% Boron Steel plates, dist. 3.277 cm	4.306	-
335	LEU-COMP-THERM-009-006	1.05% Boron Steel plates, dist. 3.277 cm	4.306	-
336	LEU-COMP-THERM-009-008	1.62% Boron Steel plates, dist. 3.277 cm	4.306	-
337	LEU-COMP-THERM-009-024	Al plates, dist. 0.105 cm	4.306	-
338	LEU-COMP-THERM-009-025	Al plates, dist. 3.277 cm	4.306	-
339	LEU-COMP-THERM-009-026	Zircaloy-4 plates, dist. 0.078 cm	4.306	-
340	LEU-COMP-THERM-009-027	Zircaloy-4 plates, dist. 3.277 cm	4.306	-
341	LEU-COMP-THERM-010-001	Lead Reflector, 0 cm separation	4.306	-
342	LEU-COMP-THERM-010-002	Lead Reflector, 0.660 cm separation	4.306	-
343	LEU-COMP-THERM-010-003	Lead Reflector, 1.321 cm separation	4.306	-
344	LEU-COMP-THERM-010-004	Lead Reflector, 5.405 cm separation	4.306	-
345	LEU-COMP-THERM-010-009	Steel Reflector, 0 cm separation	4.306	-
346	LEU-COMP-THERM-010-010	Steel Reflector, 0.660 cm separation	4.306	-
347	LEU-COMP-THERM-010-011	Steel Reflector, 1.321 cm separation	4.306	-
348	LEU-COMP-THERM-010-012	Steel Reflector, 2.616 cm separation	4.306	-
349	LEU-COMP-THERM-010-013	Steel Reflector, 5.405 cm separation	4.306	-
350	LEU-COMP-THERM-010-014	Steel Reflector, 0 cm separation	4.306	-
351	LEU-COMP-THERM-010-015	Steel Reflector, 0.660 cm separation	4.306	-
352	LEU-COMP-THERM-010-017	Steel Reflector, 1.956 cm separation	4.306	-
353	LEU-COMP-THERM-010-020	Lead Reflector, 0 cm separation	4.306	-
354	LEU-COMP-THERM-011-003	Core IIIA	2.46	-
355	LEU-COMP-THERM-011-005	Core IIIC	2.46	-

Case	Reference	Identification	U, wt%	Pu, wt%
356	LEU-COMP-THERM-011-006	Core IIID	2.46	-
357	LEU-COMP-THERM-011-007	Core IIIE	2.46	-
358	LEU-COMP-THERM-011-008	Core IIIF	2.46	-
359	LEU-COMP-THERM-011-009	Core IIIG	2.46	-
360	LEU-COMP-THERM-011-010	Core IV	2.46	-
361	LEU-COMP-THERM-011-011	Core V	2.46	-
362	LEU-COMP-THERM-011-012	Core VI	2.46	-
363	LEU-COMP-THERM-011-013	Core VII	2.46	-
364	LEU-COMP-THERM-011-014	Core VIII	2.46	-
365	LEU-COMP-THERM-012-001	0% Boron Steel plate, Gd water impurity	2.35	-
366	LEU-COMP-THERM-012-002	1.1% Boron Steel plate	2.35	-
367	LEU-COMP-THERM-012-003	1.6% Boron Steel plate	2.35	-
368	LEU-COMP-THERM-012-004	Boral B plate	2.35	-
369	LEU-COMP-THERM-012-005	Boral C plate	2.35	-
370	LEU-COMP-THERM-012-006	Boroflex, 1.84 cm separation	2.35	-
371	LEU-COMP-THERM-012-007	Boroflex, 1.73 cm separation	2.35	-
372	LEU-COMP-THERM-013-001	Steel Reflector, 0% Boron Steel plate	4.306	-
373	LEU-COMP-THERM-013-002	Steel Reflector, 1.1% Boron Steel plate	4.306	-
374	LEU-COMP-THERM-013-004	Steel Reflector, Boroflex, 8.37 cm separation	4.306	-
375	LEU-COMP-THERM-014-002	Borated Water, 490 ppm	4.306	-
376	LEU-COMP-THERM-014-006	Unborated Water	4.306	-
377	LEU-COMP-THERM-014-007	Borated Water, 1030 ppm	4.306	-
378	LEU-COMP-THERM-016-001	0% Boron Steel plates, dist. 0.645 cm	2.35	-
379	LEU-COMP-THERM-016-002	0% Boron Steel plates, dist. 2.732 cm	2.35	-
380	LEU-COMP-THERM-016-003	0% Boron Steel plates, dist. 4.042 cm	2.35	-
381	LEU-COMP-THERM-016-004	0% Boron Steel plates, dist. 0.645 cm	2.35	-
382	LEU-COMP-THERM-016-005	0% Boron Steel plates, dist. 4.042 cm	2.35	-
383	LEU-COMP-THERM-016-006	0% Boron Steel plates, dist. 0.645 cm	2.35	-
384	LEU-COMP-THERM-016-007	0% Boron Steel plates, dist. 4.042 cm	2.35	-
385	LEU-COMP-THERM-016-008	1.05% Boron Steel plates, dist. 0.645 cm	2.35	-
386	LEU-COMP-THERM-016-009	1.05% Boron Steel plates, dist. 4.042 cm	2.35	-
387	LEU-COMP-THERM-016-010	1.62% Boron Steel plates, dist. 0.645 cm	2.35	-
388	LEU-COMP-THERM-016-011	1.62% Boron Steel plates, dist. 4.042 cm	2.35	-
389	LEU-COMP-THERM-016-012	Boral plates, dist. 0.645 cm	2.35	-
390	LEU-COMP-THERM-016-013	Boral plates, dist. 4.442 cm	2.35	-
391	LEU-COMP-THERM-016-014	Boral plates, dist. 0.645 cm	2.35	-
392	LEU-COMP-THERM-016-028	Al plates, dist. 0.645 cm	2.35	-
393	LEU-COMP-THERM-016-029	Al plates, dist. 4.042 cm	2.35	-
394	LEU-COMP-THERM-016-030	Al plates, dist. 4.442 cm	2.35	-
395	LEU-COMP-THERM-016-031	Zircaloy-4 plates, dist. 0.645 cm	2.35	-

Case	Reference	Identification	U, wt%	Pu, wt%
396	LEU-COMP-THERM-016-032	Zircaloy-4 plates, dist. 4.042 cm	2.35	-
397	LEU-COMP-THERM-026-001	Hex, 621 Rods, Temperature 20.1C	4.92	-
398	LEU-COMP-THERM-026-002	Hex, 889 Rods, Temperature 231.4C	4.92	-
399	LEU-COMP-THERM-026-003	Hex, 1951 Rods, Temperature 19.3C	4.92	-
400	LEU-COMP-THERM-026-004	Hex, 2791 Rods, Temperature 206.0C	4.92	-
401	LEU-COMP-THERM-026-005	Hex, 325/680 Rods, Temperature 20.8C	4.92	-
402	LEU-COMP-THERM-026-006	Hex, 325/912 Rods, Temperature 212.1C	4.92	-
403	LEU-COMP-THERM-051-002	Core XIA	2.46	-
404	LEU-COMP-THERM-051-004	Core XIC	2.46	-
405	LEU-COMP-THERM-051-005	Core XID	2.46	-
406	LEU-COMP-THERM-051-006	Core XIE	2.46	-
407	LEU-COMP-THERM-051-007	Core XIF	2.46	-
408	LEU-COMP-THERM-051-008	Core XIG	2.46	-
409	LEU-COMP-THERM-051-011	Core XIIIA	2.46	-
410	LEU-COMP-THERM-062-001	No Boron Steel plates	2.6	-
411	LEU-COMP-THERM-062-002	0% Boron Steel plates, 3 mm, dist. 0	2.6	-
412	LEU-COMP-THERM-062-003	0% Boron Steel plates, 6 mm, dist. 0	2.6	-
413	LEU-COMP-THERM-062-004	0% Boron Steel plates, 6 mm, dist. 0.5	2.6	-
414	LEU-COMP-THERM-062-005	0% Boron Steel plates, 6 mm, dist. 1	2.6	-
415	LEU-COMP-THERM-062-006	0.67% Boron Steel plates, 3 mm, dist. 0	2.6	-
416	LEU-COMP-THERM-062-007	0.67% Boron Steel plates, 6 mm, dist. 0	2.6	-
417	LEU-COMP-THERM-062-008	0.67% Boron Steel plates, 3 mm, dist. 0.5	2.6	-
418	LEU-COMP-THERM-062-009	0.67% Boron Steel plates, 6 mm, dist. 0.5	2.6	-
419	LEU-COMP-THERM-062-010	0.67% Boron Steel plates, 3 mm, dist. 1	2.6	-
420	LEU-COMP-THERM-062-011	0.67% Boron Steel plates, 6 mm, dist. 1	2.6	-
421	LEU-COMP-THERM-062-012	0.98% Boron Steel plates, 3 mm, dist. 0	2.6	-
422	LEU-COMP-THERM-062-013	0.98% Boron Steel plates, 6 mm, dist. 0	2.6	-
423	LEU-COMP-THERM-062-014	0.98% Boron Steel plates, 6 mm, dist. 0.5	2.6	-
424	LEU-COMP-THERM-062-015	0.98% Boron Steel plates, 6 mm, dist. 1	2.6	-
425	LEU-COMP-THERM-065-001	No Boron Steel plates	2.6	-
426	LEU-COMP-THERM-065-002	0% Boron Steel plates, dist. 0	2.6	-
427	LEU-COMP-THERM-065-003	0.67% Boron Steel plates, dist. 0	2.6	-
428	LEU-COMP-THERM-065-004	0.98% Boron Steel plates, dist. 0	2.6	-
429	LEU-COMP-THERM-065-005	No Boron Steel plates	2.6	-
430	LEU-COMP-THERM-065-006	0% Boron Steel plates, dist. 0	2.6	-
431	LEU-COMP-THERM-065-007	0% Boron Steel plates, dist. 0.5	2.6	-
432	LEU-COMP-THERM-065-008	0% Boron Steel plates, dist. 0	2.6	-
433	LEU-COMP-THERM-065-009	0% Boron Steel plates, dist. 0.5	2.6	-
434	LEU-COMP-THERM-065-010	0.67% Boron Steel plates, dist. 0	2.6	-
435	LEU-COMP-THERM-065-011	0.67% Boron Steel plates, dist. 0.5	2.6	-

Case	Reference	Identification	U, wt%	Pu, wt%
436	LEU-COMP-THERM-065-012	0.67% Boron Steel plates, dist. 0	2.6	-
437	LEU-COMP-THERM-065-013	0.67% Boron Steel plates, dist. 0.5	2.6	-
438	LEU-COMP-THERM-065-014	0.98% Boron Steel plates, dist. 0	2.6	-
439	LEU-COMP-THERM-065-015	0.98% Boron Steel plates, dist. 0.5	2.6	-
440	LEU-COMP-THERM-065-016	0.98% Boron Steel plates, dist. 0	2.6	-
441	LEU-COMP-THERM-065-017	0.98% Boron Steel plates, dist. 0.5	2.6	-
442	LEU-COMP-THERM-081-001	Otto Hahn, ZrB_2 and B_4C rods	5.423	-
443	LEU-COMP-THERM-082-001	IPEN/MB-01 (580 pins)	4.3486	-
444	LEU-COMP-THERM-082-002	IPEN/MB-01 (560 pins)	4.3486	-
445	LEU-COMP-THERM-082-003	670 pins, Al_2O_3-B_4C rods	4.3486	-
446	LEU-COMP-THERM-082-004	672 pins, Al_2O_3-B_4C rods	4.3486	-
447	LEU-COMP-THERM-082-005	668 pins, Al_2O_3-B_4C rods	4.3486	-
448	LEU-COMP-THERM-082-006	668 pins, Al_2O_3-B_4C rods	4.3486	-
449	LEU-COMP-THERM-090-001	664 pins, 16 steel rods	4.3486	-
450	LEU-COMP-THERM-090-002	662 pins, 18 steel rods	4.3486	-
451	LEU-COMP-THERM-090-003	658 pins, 14 steel rods	4.3486	-
452	LEU-COMP-THERM-090-004	660 pins, 12 steel rods	4.3486	-
453	LEU-COMP-THERM-090-005	660 pins, 12 steel rods	4.3486	-
454	LEU-COMP-THERM-090-006	661 pins, 17 steel rods	4.3486	-
455	LEU-COMP-THERM-090-007	662 pins, 16 steel rods	4.3486	-
456	LEU-COMP-THERM-090-008	634 pins, 12 steel rods	4.3486	-
457	LEU-COMP-THERM-090-009	620 pins, 26 steel rods	4.3486	-
458	LEU-COMP-THERM-091-001	668 pins, 0 steel rods, 4 Gd_2O_3 rods	4.3486	-
459	LEU-COMP-THERM-091-002	648 pins, 0 steel rods, 8 Gd_2O_3 rods	4.3486	-
460	LEU-COMP-THERM-091-003	672 pins, 0 steel rods, 4 Gd_2O_3 rods	4.3486	-
461	LEU-COMP-THERM-091-004	646 pins, 4 steel rods, 4 Gd_2O_3 rods	4.3486	-
462	LEU-COMP-THERM-091-005	656 pins, 4 steel rods, 4 Gd_2O_3 rods	4.3486	-
463	LEU-COMP-THERM-091-006	664 pins, 4 steel rods, 2 Gd_2O_3 rods	4.3486	-
464	LEU-COMP-THERM-091-007	670 pins, 2 steel rods, 2 Gd_2O_3 rods	4.3486	-
465	LEU-COMP-THERM-091-008	664 pins, 2 steel rods, 2 Gd_2O_3 rods	4.3486	-
466	LEU-COMP-THERM-091-009	656 pins, 0 steel rods, 2 Gd_2O_3 rods	4.3486	-
467	MIX-COMP-THERM-004-001	23x23, 1.825 cm pitch	0.72	3.01
468	MIX-COMP-THERM-004-002	23x23, 1.825 cm pitch	0.72	3.01
469	MIX-COMP-THERM-004-003	23x23, 1.825 cm pitch	0.72	3.01
470	MIX-COMP-THERM-004-004	21x21, 1.956 cm pitch	0.72	3.01
471	MIX-COMP-THERM-004-005	21x21, 1.956 cm pitch	0.72	3.01
472	MIX-COMP-THERM-004-006	21x21, 1.956 cm pitch	0.72	3.01
473	MIX-COMP-THERM-004-007	20x20, 2.225 cm pitch	0.72	3.01

Case	Reference	Identification	U, wt%	Pu, wt%
474	MIX-COMP-THERM-004-008	20x20, 2.225 cm pitch	0.72	3.01
475	MIX-COMP-THERM-004-009	20x20, 2.225 cm pitch	0.72	3.01
476	MIX-COMP-THERM-004-010	21x21, 2.474 cm pitch	0.72	3.01
477	MIX-COMP-THERM-004-011	21x21, 2.474 cm pitch	0.72	3.01
478	MIX-COMP-THERM-006-007	8 wt% 240Pu 1.05" pitch, Al Rods	0.72	2.0
479	MIX-COMP-THERM-006-013	8 wt% 240Pu 1.05" pitch, B4 Rods	0.72	2.0
480	MIX-COMP-THERM-006-014	8 wt% 240Pu 1.05" pitch, B3 Rods	0.72	2.0
481	MIX-COMP-THERM-006-015	8 wt% 240Pu 1.05" pitch, B2 Rods	0.72	2.0
482	MIX-COMP-THERM-006-016	8 wt% 240Pu 1.05" pitch, B1 Rods	0.72	2.0
483	MIX-COMP-THERM-006-017	8 wt% 240Pu 1.05" pitch, Al+Cd Rods	0.72	2.0
484	MIX-COMP-THERM-006-023	8 wt% 240Pu 1.05" pitch, B4+Cd Rods	0.72	2.0
485	MIX-COMP-THERM-006-024	8 wt% 240Pu 1.05" pitch, B3+Cd Rods	0.72	2.0
486	MIX-COMP-THERM-006-025	8 wt% 240Pu 1.05" pitch, B2+Cd Rods	0.72	2.0
487	MIX-COMP-THERM-006-026	8 wt% 240Pu 1.05" pitch, B1+Cd Rods	0.72	2.0
488	MIX-COMP-THERM-006-027	8 wt% 240Pu 1.05" pitch, Air+Cd Rods	0.72	2.0
489	MIX-COMP-THERM-006-028	8 wt% 240Pu 1.05" pitch, H2O+Cd Rods	0.72	2.0
490	MIX-COMP-THERM-006-029	8 wt% 240Pu 1.32" pitch, Al Rods	0.72	2.0
491	MIX-COMP-THERM-006-035	8 wt% 240Pu 1.32" pitch, B4 Rods	0.72	2.0
492	MIX-COMP-THERM-006-036	8 wt% 240Pu 1.32" pitch, B3 Rods	0.72	2.0
493	MIX-COMP-THERM-006-037	8 wt% 240Pu 1.32" pitch, B2 Rods	0.72	2.0
494	MIX-COMP-THERM-006-038	8 wt% 240Pu 1.32" pitch, B1 Rods	0.72	2.0
495	MIX-COMP-THERM-006-039	8 wt% 240Pu 1.32" pitch, Al+Cd Rods	0.72	2.0
496	MIX-COMP-THERM-006-045	8 wt% 240Pu 1.32" pitch, B4+Cd Rods	0.72	2.0
497	MIX-COMP-THERM-006-046	8 wt% 240Pu 1.32" pitch, B3+Cd Rods	0.72	2.0
498	MIX-COMP-THERM-006-047	8 wt% 240Pu 1.32" pitch, B2+Cd Rods	0.72	2.0
499	MIX-COMP-THERM-006-048	8 wt% 240Pu 1.32" pitch, B1+Cd Rods	0.72	2.0
500	MIX-COMP-THERM-006-049	8 wt% 240Pu 1.32" pitch, Air+Cd Rods	0.72	2.0
501	MIX-COMP-THERM-006-050	8 wt% 240Pu 1.32" pitch, H2O+Cd Rods	0.72	2.0
502	MIX-COMP-THERM-007-005	16 wt% 240Pu 1.386" pitch	0.72	2.0
503	MIX-COMP-THERM-007-006	16 wt% 240Pu 1.05" pitch, Al Rods	0.72	2.0
504	MIX-COMP-THERM-007-012	16 wt% 240Pu 1.05" pitch, B4 Rods	0.72	2.0
505	MIX-COMP-THERM-007-013	16 wt% 240Pu 1.05" pitch, B3 Rods	0.72	2.0
506	MIX-COMP-THERM-007-014	16 wt% 240Pu 1.05" pitch, B2 Rods	0.72	2.0
507	MIX-COMP-THERM-007-015	16 wt% 240Pu 1.05" pitch, B1 Rods	0.72	2.0
508	MIX-COMP-THERM-007-016	16 wt% 240Pu 1.05" pitch, Al+Cd Rods	0.72	2.0
509	MIX-COMP-THERM-007-022	16 wt% 240Pu 1.05" pitch, B4+Cd Rods	0.72	2.0
510	MIX-COMP-THERM-007-023	16 wt% 240Pu 1.05" pitch, B3+Cd Rods	0.72	2.0
511	MIX-COMP-THERM-007-024	16 wt% 240Pu 1.05" pitch, B2+Cd Rods	0.72	2.0
512	MIX-COMP-THERM-007-025	16 wt% 240Pu 1.05" pitch, B1+Cd Rods	0.72	2.0
513	MIX-COMP-THERM-007-026	16 wt% 240Pu 1.05" pitch, Air+Cd Rods	0.72	2.0

Case	Reference	Identification	U, wt%	Pu, wt%
514	MIX-COMP-THERM-007-027	16 wt% 240Pu 1.05" pitch, H2O+Cd Rods	0.72	2.0
515	MIX-COMP-THERM-008-007	24 wt% 240Pu 1.05" pitch, Al Rods	0.72	2.0
516	MIX-COMP-THERM-008-013	24 wt% 240Pu 1.05" pitch, B4 Rods	0.72	2.0
517	MIX-COMP-THERM-008-014	24 wt% 240Pu 1.05" pitch, B3 Rods	0.72	2.0
518	MIX-COMP-THERM-008-015	24 wt% 240Pu 1.05" pitch, B2 Rods	0.72	2.0
519	MIX-COMP-THERM-008-016	24 wt% 240Pu 1.05" pitch, B1 Rods	0.72	2.0
520	MIX-COMP-THERM-008-017	24 wt% 240Pu 1.05" pitch, Al+Cd Rods	0.72	2.0
521	MIX-COMP-THERM-008-023	24 wt% 240Pu 1.05" pitch, B4+Cd Rods	0.72	2.0
522	MIX-COMP-THERM-008-024	24 wt% 240Pu 1.05" pitch, B3+Cd Rods	0.72	2.0
523	MIX-COMP-THERM-008-025	24 wt% 240Pu 1.05" pitch, B2+Cd Rods	0.72	2.0
524	MIX-COMP-THERM-008-026	24 wt% 240Pu 1.05" pitch, B1+Cd Rods	0.72	2.0
525	MIX-COMP-THERM-008-027	24 wt% 240Pu 1.05" pitch, Air+Cd Rods	0.72	2.0
526	MIX-COMP-THERM-008-028	24 wt% 240Pu 1.05" pitch, H2O+Cd Rods	0.72	2.0
527	MIX-COMP-THERM-009-001	8 wt% 240Pu 0.55" pitch	0.16	1.5
528	MIX-COMP-THERM-009-002	8 wt% 240Pu 0.60" pitch	0.16	1.5
529	MIX-COMP-THERM-009-003	8 wt% 240Pu 0.71" pitch	0.16	1.5
530	MIX-COMP-THERM-009-004	8 wt% 240Pu 0.80" pitch	0.16	1.5
531	MIX-COMP-THERM-009-005	8 wt% 240Pu 0.90" pitch	0.16	1.5
532	MIX-COMP-THERM-009-006	8 wt% 240Pu 0.93" pitch	0.16	1.5

Appendix C

Benchmark of MCNP5-1.51 with ENDF/B-V

(total number of pages: 27 including this page)

C.1 Introduction

This Appendix presents the analysis of the validation results for MCNP5-1.51 code and includes the results of the calculations, normality test, the detailed statistical trending analysis, calculation bias and bias uncertainty for each distinct area of applicability of the parameters of interest.

C.2 Computer Code Parameter Data

The computer code MCNP5-1.51 [C.1] is the continuous energy Monte Carlo codes and treats an arbitrary three-dimensional configuration of materials in geometric cells bounded by first- and second-degree surfaces and fourth-degree elliptical tori. Thermal neutrons are described by both the free gas and S(α,β) models. All calculations were performed using the default data libraries provided with the code: the default continuous energy neutron transport data predominantly based on ENDF/B-V. The list of ZAIDs that were used in the analysis is presented in Table C.2-1. The criticality source card was set to accumulate a total of 1.8 million neutron histories for every individual run. The neutrons start from an arbitrary distribution, causing a generally very large variance of results from the first cycles in comparison with the following cycles. Therefore, the results from the first 50 cycles were skipped when calculating the average k_{eff}. The calculated k_{eff} values have associated uncertainties due to the statistical nature of the Monte Carlo codes.

C.3 Analysis of MCNP5-1.51 Validation Results

C.3.1. Calculational Results

The calculation results for the 156 HTC critical experiments and for the 135 selected critical experiments described in Appendix B are presented and discussed in this section. The calculation results are summarized by grouping the experiments in terms of the categories as set forth in Appendix B. Calculation results, including $k_{eff\text{-}I}$, $\sigma_{calc\text{-}i}$ and EALF, measurement uncertainties (σ_{exp}) and the calculation and measurement combined uncertainty (σ_i) are shown in Table C.3-1 through Table C.3-5.

Figure C.3-1 and C.3-2 are histograms showing the frequency of calculated k_{eff} and EALF for all 291 benchmarks. The nominal calculated k_{eff} values range from [redacted]. The EALF results values show a range between [redacted].

Descriptive statistics for the different group of experiments is summarized in Table C.3-6.

C.3.2. Normality Test

In order to assess the normality assumption, Shapiro and Wilk [5] test has been used for groups with fewer than 50 samples while the Pearson's chi-square (χ^2) test [4] has been used for samples larger than 20 samples. The tests are applied to the group of experiments in terms of the categories as set forth in Appendix B.

For the Shapiro and Wilk test, Table C.3-7 shows the computed *Wtest* value, and *W* value that can be obtained for the number of experiments from [5] to accept the normality hypothesis. If W

is less than the test statistic, *Wtest*, then the data is considered normally distributed. For the χ^2 test, it is concluded normal for $\chi^2 \leq n$, where n is a number of bins for the group of experiments. The probability $P_d(\tilde{\chi}^2 \geq \tilde{\chi}_0{}^2)$ of obtaining a value of $\tilde{\chi}^2 \geq \tilde{\chi}_0{}^2$ in an experiment with d degrees of freedom to confirm quantitatively that the agreement is satisfactory was taken or interpolated, if necessary, from Appendix D in Reference [4]. Thus, if $P_d(\tilde{\chi}^2 \geq \tilde{\chi}_0{}^2)$ is large, the obtained and expected distributions are consistent; if it is small, they probably disagree. In particular, if $P_d(\tilde{\chi}^2 \geq \tilde{\chi}_0{}^2)$ is less than 5%, we say that the disagreement is significant and reject the assumed distributions at the 5% level. If it is less than 1%, the disagreement is called highly significant, and we reject the assumed distributions at the 1% level.

As it is shown in Table C.3-7, all cases except Phase 1 test normal. Nevertheless, the group with all 291 experiments shows an agreement with the assumed normal distribution with the probability $P_d = 7.36\%$.

C.3.3. Trending Analysis

Trends are determined through the use of regression fits to the calculated results. The equations used to identify trends are given below:

$$Y(x) = a + bx \tag{7-1}$$

$$a = \frac{1}{\Delta}\left(\sum\frac{x_i^2}{\sigma_i^2}\sum\frac{y_i}{\sigma_i^2} - \sum\frac{x_i}{\sigma_i^2}\sum\frac{x_i y_i}{\sigma_i^2}\right) \tag{7-2}$$

$$b = \frac{1}{\Delta}\left(\sum\frac{1}{\sigma_i^2}\sum\frac{x_i y_i}{\sigma_i^2} - \sum\frac{x_i}{\sigma_i^2}\sum\frac{y_i}{\sigma_i^2}\right) \tag{7-3}$$

$$\Delta = \sum\frac{1}{\sigma_i^2}\sum\frac{x_i^2}{\sigma_i^2} - \left(\sum\frac{x_i}{\sigma_i^2}\right)^2 \tag{7-4}$$

The squared term of the linear correlation factor r defined below (from Reference [5]) is used to quantitatively measure the degree to which a linear relationship exist between two variables.

$$r = \frac{\Sigma\frac{1}{\sigma_i^2}(x_i - \bar{x})(y_i - \bar{y})}{\sqrt{\left[\Sigma\frac{1}{\sigma_i^2}(x_i - \bar{x})^2\right]\left[\Sigma\frac{1}{\sigma_i^2}(y_i - \bar{y})^2\right]}} \tag{7-5}$$

The closer r^2 approaches the value of 1, the better the fit of the data to the linear equation. A more quantitative measure of the fit can be found by using Appendix C in Reference [4]. The interpolation was applied, if necessary. For any given observed value r_0, $P_N(|r| \geq |r_0|)$ is the probability that N measurements of two uncorrelated variables would give a coefficient r as large as r_0. Thus, if we obtain a coefficient r_0 for which $P_N(|r| \geq |r_0|)$ is small, it is correspondingly unlikely that our variables are uncorrelated; that is, a correlation indicated. In particular, if

$P_N(|r| \geq |r_0|) \leq 5\%$, the correlation is called significant; if it is less than 1%, the correlation is called highly significant.

The validation results are analyzed by grouping the experiments in terms of the categories as set forth in Appendix B. Independent variables used in the trending analysis by group, correlation coefficients and trending analysis results are summarized in Table C.3-8. The linear regression equations for the independent parameter with the significant correlation of k_{eff} were presented in Table C.3-8.

C.3.4. Bias and Bias Uncertainty

In this section, benchmark results are analyzed using the statistical method described in section 2.2.

The first step is to evaluate whether the four HTC phases and selected experiments, should be reduced to a single set. The mean k_{eff} of the Phase 1 data set is [redacted], the mean k_{eff} of the Phase 2 data set is [redacted], the mean k_{eff} of the Phase 3 data set is [redacted], the mean k_{eff} of the Phase 4 data set is [redacted] and the mean k_{eff} of the selected experiments data is [redacted]. The maximum difference between the means is just [redacted] which is less than the uncertainty. These sets are water moderated uranium or mixed plutonium-uranium dioxide lattices. The addition of a absorber rods, separator plates or reflector plates is not introducing a significant increase in the ability to calculate k_{eff}. The Phase 1 through Phase 4 sets and the selected experiments are considered one large set of 291 experiments from now on.

The analysis of the correlation coefficient in Table C.3-8 (combined set) and the plot of data trend (Figure C.3-3) show that there is a significant trend a function of the rod pitch. This is discussed in the Section C.3.5.2.

The total bias (systematic error or mean of the deviation from a keff of exactly 1.000) of the MCNP5-1.51 code is shown in the table below

Calculational Bias of the MCNP5-1.51 code		
Description	Total Bias	Bias Uncertainty
HTC and Selected Experiments	[redacted]	[redacted]

C.3.5. Applicability of MCNP5-1.51 Validation Results

This subsection contains a more detailed evaluation of the set of critical experiments. Regarding the selected experiments, the following subjects are discussed:

- Neutron absorber and neutron reflector materials
- Fuel rod pitch trend
- Neutron absorber geometry

- Fuel burnup
- Unborated and borated water.

The general focus is to justify that using the full set of critical experiments is appropriate. In some cases, subsets of full set of experiments are established. For those subsets, statistical evaluations are performed to determine bias, bias uncertainty, normality and trends. Trends are evaluated for fuel rod outer diameter, fuel rod pitch, fuel density, and EALF.

C.3.5.1. Neutron Absorber and Neutron Reflector Materials

The HTC and Selected Experiments consider the following neutron absorbers and reflectors:

- Absorbers
  - Boron, in the form of soluble boron in the water, boron in solid form (B_4C), and boron in borated steel
  - Soluble gadolinium in water
  - Cadmium
- Reflectors
  - Steel
  - Lead
  - Water

Some typical configurations do not contain gadolinium or cadmium neutron absorbers or lead reflectors. To verify that including those materials does not have a significant effect on the results of the benchmarking analyses, a subset without those experiments containing those materials was analyzed. The comparison with the full set is presented in Table C.3-9 and shows no significant differences when those materials are excluded. However, in both cases, a significant trend is observed, as a function of the rod pitch in the experiment. This is discussed in the next section.

C.3.5.2. Fuel Rod Pitch Trend

To better understand the observed rod pitch trend, the results for all 291 experiments are shown in Figure C.3-4 as a function of rod pitch. It appears that the trend is due to the experiments at higher rod pitch value (> 2 cm), which consistently show k_{eff} values well above 1.0. To evaluate the impact of those experiments at larger rod pitches, the Table C.3-10 shows a comparison of results with and without those experiments. When results above 2 cm rod pitch are excluded, a slightly higher absolute bias is observed, in this case with a lower uncertainty, and no significant rod pitch trend. Based on those results it could be concluded that the trend is only caused by the experiments at higher rod pitch values. To ensure that a potential trend would not be ignored, all following evaluations are performed for the two conditions used above, i.e. for all rod pitch values, and for experiments with rod pitch values limited to no more than 2 cm.

C.3.5.3. Absorber Geometry

The criticality experiments analyzed in this report include experiments with Boron in the form of plates, absorber rods and soluble boron in water. No trend relating to these experiments is observed.

C.3.5.4. Fuel Burnup

The full set of critical experiments contains experiments with fresh UO_2 fuel, with simulated spent fuel (37.5 GWd/MTU), and MOX fuel with Pu content between 2 and 20%, which is even higher than typically found in spent fuel. The experiments are therefore reasonably representative of burned fuel at different burnup levels. To verify that the experiments cover the burnup range sufficiently, the experiments are subdivided into fresh UO_2 fuel, HTC experiments and MOX experiments, and compared to the results of the entire set. The comparison is shown in Table C.3-11. The comparison shows no significant differences between the entire set and the UO_2 and HTC subsets, but for MOX the bias is now positive (i.e. truncated bias of 0.0), with a larger uncertainty, and some trends. However, this is based on relatively small sets of experiments. Bias values are comparable between sets with and without rod pitch values above 2 cm, with a maximum absolute value of [redacted].

C.3.5.5. Unborated and Borated Water

The full set of critical experiments contains both experiments with and without soluble boron. The entire set of analyses shows no significant trend when analyzed as a function of the soluble boron level. Nevertheless, sets with and without soluble boron are analyzed and compared to the full set that contains all experiments. The results are shown in Table C.3-12. Similar to the previous subsection, the comparison shows no significant differences between those subsets. Bias values are comparable between sets with and without rod pitch values above 2 cm, with a maximum absolute value of [redacted].

C.4 Summary

A set of 291 critical experiments has been selected and has been used for the validation of the Holtec International criticality safety methodology. The similarity between the chosen experiments and the actual systems has been based on a set of screening criteria as is stated in the NUREG/CR-6698 [5]. Experiments have been categorized by common features as Phase 1 through Phase 4 and selected experiments and parameterized by key variables such as lattice pitch / assembly pitch, absorber solution concentration, number of fuel rods, rod outer diameter, fuel density, screen array distance, fuel enrichment and EALF. Benchmark calculations have been performed using the Monte Carlo code MCNP5-1.51. It was determined that Phase 1 through Phase 4 and selected experiments are in sufficient agreement that this sets are lumped together as a single set of 291 experiments. The bias and bias uncertainty are presented in section C.3.4. The applicability of validation results is considered in section C.3.5.

The range of key parameters for the design application, benchmarks and validated AOA are summarized in Table C.3-13. A point by point comparison between design application and benchmarks shows that the experimental range covers all the parameters. The soluble boron

concentration is extrapolated generously since ^{10}B is a 1/v absorber (as permitted on Table 2.3 of [5]).

As for the fuel density, Table 2.3 of Reference [5] states there is "no requirement" and that "experiments should be as close to the desired concentration as possible". Since the experiment fuel density is 9.2 – 10.4 g/cm^3 and the design application one is around 10.0 – 10.7 g/cm^3, it is considered that the values are very close so the validated AOA covers the design application range.

The fuel enrichment can be up to 5%. The experiments used go up to 5.74 wt% ^{235}U. Therefore, it is considered that the validated AOA covers the design application range.

C.5 References

[C.1] "MCNP - A General Monte Carlo N-Particle Transport Code, Version 5"; Los Alamos National Laboratory, LA-UR-03-1987 (Revised 2/1/2008).

Table C.2-1 MCNP5-1.51 ZAIDs Used for Each Nuclide

Nuclide	ZAID
^{1}H	1001.50c
^{10}B	5010.50c
^{11}B	5011.55c
C	6000.50c
^{14}N	7014.50c
^{16}O	8016.50c
^{23}Na	11023.51c
Mg	12000.50c
^{27}Al	13027.50c
Si	14000.51c
^{31}P	15031.50c
^{32}S	16032.51c
Ca	20000.51c
Ti	22000.50c
Cr	24000.50c
^{55}Mn	25055.51c
Fe	26000.55c
^{59}Co	27059.50c
Ni	28000.50c
Cu	29000.50c
Zn	30000.40c
Zr	40000.56c
Mo	42000.50c
Cd	48000.50c
Sn	50000.40c
Gd	64000.35c
Pb	82000.50c
^{234}U	92234.50c
^{235}U	92235.50c
^{236}U	92236.50c
^{238}U	92238.50c
^{238}Pu	94238.50c
^{239}Pu	94239.50c
^{240}Pu	94240.50c
^{241}Pu	94241.50c
^{242}Pu	94242.50c
^{241}Am	95241.50c

Table C.3-1 The MCNP5-1.51 Calculational Results and Measurements Uncertainties for Phase 1 Critical Experiments: Water-Moderated and Reflected Arrays

Case	Evaluation Identification	File-name	k_{eff-i}	$\pm \sigma_{calc-i}$	$\pm \sigma_{exp}$	$\pm \sigma_i$	EALF (eV)
1	MIX-COMP-THERM-HTC-001	[redacted]	[redacted]	[redacted]	[redacted]	[redacted]	[redacted]
2	MIX-COMP-THERM-HTC-002	[redacted]	[redacted]	[redacted]	[redacted]	[redacted]	[redacted]
3	MIX-COMP-THERM-HTC-003	[redacted]	[redacted]	[redacted]	[redacted]	[redacted]	[redacted]
4	MIX-COMP-THERM-HTC-004	[redacted]	[redacted]	[redacted]	[redacted]	[redacted]	[redacted]
5	MIX-COMP-THERM-HTC-005	[redacted]	[redacted]	[redacted]	[redacted]	[redacted]	[redacted]
6	MIX-COMP-THERM-HTC-006	[redacted]	[redacted]	[redacted]	[redacted]	[redacted]	[redacted]
7	MIX-COMP-THERM-HTC-007	[redacted]	[redacted]	[redacted]	[redacted]	[redacted]	[redacted]
8	MIX-COMP-THERM-HTC-008	[redacted]	[redacted]	[redacted]	[redacted]	[redacted]	[redacted]
9	MIX-COMP-THERM-HTC-009	[redacted]	[redacted]	[redacted]	[redacted]	[redacted]	[redacted]
10	MIX-COMP-THERM-HTC-010	[redacted]	[redacted]	[redacted]	[redacted]	[redacted]	[redacted]
11	MIX-COMP-THERM-HTC-011	[redacted]	[redacted]	[redacted]	[redacted]	[redacted]	[redacted]
12	MIX-COMP-THERM-HTC-012	[redacted]	[redacted]	[redacted]	[redacted]	[redacted]	[redacted]
13	MIX-COMP-THERM-HTC-013	[redacted]	[redacted]	[redacted]	[redacted]	[redacted]	[redacted]
14	MIX-COMP-THERM-HTC-014	[redacted]	[redacted]	[redacted]	[redacted]	[redacted]	[redacted]
15	MIX-COMP-THERM-HTC-015	[redacted]	[redacted]	[redacted]	[redacted]	[redacted]	[redacted]
16	MIX-COMP-THERM-HTC-016	[redacted]	[redacted]	[redacted]	[redacted]	[redacted]	[redacted]
17	MIX-COMP-THERM-HTC-017	[redacted]	[redacted]	[redacted]	[redacted]	[redacted]	[redacted]
18	MIX-COMP-THERM-HTC-018	[redacted]	[redacted]	[redacted]	[redacted]	[redacted]	[redacted]

Table C.3-2 The MCNP5-1.51 Calculational Results and Measurements Uncertainties for Phase 2 Critical Experiments: Reflected Simple Arrays Moderated by Poisoned Water with Gadolinium or Boron

Case	Evaluation Identification	File-name	k_{eff-i}	$\pm \sigma_{calc-i}$	$\pm \sigma_{exp}$	$\pm \sigma_i$	EALF (eV)
19	MIX-COMP-THERM-HTC-019						
20	MIX-COMP-THERM-HTC-020						
21	MIX-COMP-THERM-HTC-021						
22	MIX-COMP-THERM-HTC-022						
23	MIX-COMP-THERM-HTC-023						
24	MIX-COMP-THERM-HTC-024						
25	MIX-COMP-THERM-HTC-025						
26	MIX-COMP-THERM-HTC-026						
27	MIX-COMP-THERM-HTC-027						
28	MIX-COMP-THERM-HTC-028						
29	MIX-COMP-THERM-HTC-029						
30	MIX-COMP-THERM-HTC-030						
31	MIX-COMP-THERM-HTC-031						
32	MIX-COMP-THERM-HTC-032						
33	MIX-COMP-THERM-HTC-033						
34	MIX-COMP-THERM-HTC-034						
35	MIX-COMP-THERM-HTC-035						
36	MIX-COMP-THERM-HTC-036						
37	MIX-COMP-THERM-HTC-037						
38	MIX-COMP-THERM-HTC-038						
39	MIX-COMP-THERM-HTC-039						
40	MIX-COMP-THERM-HTC-040						
41	MIX-COMP-THERM-HTC-041						
42	MIX-COMP-THERM-HTC-042						
43	MIX-COMP-THERM-HTC-043						
44	MIX-COMP-THERM-HTC-044						
45	MIX-COMP-THERM-HTC-045						
46	MIX-COMP-THERM-HTC-046						
47	MIX-COMP-THERM-HTC-047						
48	MIX-COMP-THERM-HTC-048						
49	MIX-COMP-THERM-HTC-049						
50	MIX-COMP-THERM-HTC-050						
51	MIX-COMP-THERM-HTC-051						
52	MIX-COMP-THERM-HTC-052						
53	MIX-COMP-THERM-HTC-053						
54	MIX-COMP-THERM-HTC-054						
55	MIX-COMP-THERM-HTC-055						

Case	Evaluation Identification	File-name	k_{eff-i}	$\pm \sigma_{calc-i}$	$\pm \sigma_{exp}$	$\pm \sigma_i$	EALF (eV)
56	MIX-COMP-THERM-HTC-056	[redacted]	[redacted]	[redacted]	[redacted]	[redacted]	[redacted]
57	MIX-COMP-THERM-HTC-057	[redacted]	[redacted]	[redacted]	[redacted]	[redacted]	[redacted]
58	MIX-COMP-THERM-HTC-058	[redacted]	[redacted]	[redacted]	[redacted]	[redacted]	[redacted]
59	MIX-COMP-THERM-HTC-059	[redacted]	[redacted]	[redacted]	[redacted]	[redacted]	[redacted]

Table C.3-3 The MCNP5-1.51 Calculational Results and Measurements Uncertainties for Phase 3 Critical Experiments: Pool Storage

Case	Evaluation Identification	File-name	k_{eff-i}	$\pm \sigma_{calc-i}$	$\pm \sigma_{exp}$	$\pm \sigma_i$	EALF (eV)
60	MIX-COMP-THERM-HTC-060	[redacted]	[redacted]	[redacted]	[redacted]	[redacted]	[redacted]
61	MIX-COMP-THERM-HTC-061	[redacted]	[redacted]	[redacted]	[redacted]	[redacted]	[redacted]
62	MIX-COMP-THERM-HTC-062	[redacted]	[redacted]	[redacted]	[redacted]	[redacted]	[redacted]
63	MIX-COMP-THERM-HTC-063	[redacted]	[redacted]	[redacted]	[redacted]	[redacted]	[redacted]
64	MIX-COMP-THERM-HTC-064	[redacted]	[redacted]	[redacted]	[redacted]	[redacted]	[redacted]
65	MIX-COMP-THERM-HTC-065	[redacted]	[redacted]	[redacted]	[redacted]	[redacted]	[redacted]
66	MIX-COMP-THERM-HTC-066	[redacted]	[redacted]	[redacted]	[redacted]	[redacted]	[redacted]
67	MIX-COMP-THERM-HTC-067	[redacted]	[redacted]	[redacted]	[redacted]	[redacted]	[redacted]
68	MIX-COMP-THERM-HTC-068	[redacted]	[redacted]	[redacted]	[redacted]	[redacted]	[redacted]
69	MIX-COMP-THERM-HTC-069	[redacted]	[redacted]	[redacted]	[redacted]	[redacted]	[redacted]
70	MIX-COMP-THERM-HTC-070	[redacted]	[redacted]	[redacted]	[redacted]	[redacted]	[redacted]
71	MIX-COMP-THERM-HTC-071	[redacted]	[redacted]	[redacted]	[redacted]	[redacted]	[redacted]
72	MIX-COMP-THERM-HTC-072	[redacted]	[redacted]	[redacted]	[redacted]	[redacted]	[redacted]
73	MIX-COMP-THERM-HTC-073	[redacted]	[redacted]	[redacted]	[redacted]	[redacted]	[redacted]
74	MIX-COMP-THERM-HTC-074	[redacted]	[redacted]	[redacted]	[redacted]	[redacted]	[redacted]
75	MIX-COMP-THERM-HTC-075	[redacted]	[redacted]	[redacted]	[redacted]	[redacted]	[redacted]
76	MIX-COMP-THERM-HTC-076	[redacted]	[redacted]	[redacted]	[redacted]	[redacted]	[redacted]
77	MIX-COMP-THERM-HTC-077	[redacted]	[redacted]	[redacted]	[redacted]	[redacted]	[redacted]
78	MIX-COMP-THERM-HTC-078	[redacted]	[redacted]	[redacted]	[redacted]	[redacted]	[redacted]
79	MIX-COMP-THERM-HTC-079	[redacted]	[redacted]	[redacted]	[redacted]	[redacted]	[redacted]
80	MIX-COMP-THERM-HTC-080	[redacted]	[redacted]	[redacted]	[redacted]	[redacted]	[redacted]
81	MIX-COMP-THERM-HTC-081	[redacted]	[redacted]	[redacted]	[redacted]	[redacted]	[redacted]
82	MIX-COMP-THERM-HTC-082	[redacted]	[redacted]	[redacted]	[redacted]	[redacted]	[redacted]
83	MIX-COMP-THERM-HTC-083	[redacted]	[redacted]	[redacted]	[redacted]	[redacted]	[redacted]
84	MIX-COMP-THERM-HTC-084	[redacted]	[redacted]	[redacted]	[redacted]	[redacted]	[redacted]
85	MIX-COMP-THERM-HTC-085	[redacted]	[redacted]	[redacted]	[redacted]	[redacted]	[redacted]

Table C.3-4 The MCNP5-1.51 Calculational Results and Measurements Uncertainties for Phase 4 Critical Experiments: Shipping Cask

Case	Evaluation Identification	File-name	k_{eff-i}	$\pm \sigma_{calc-i}$	$\pm \sigma_{exp}$	$\pm \sigma_i$	EALF (eV)
86	MIX-COMP-THERM-HTC-086	[redacted]	[redacted]	[redacted]	[redacted]	[redacted]	[redacted]
87	MIX-COMP-THERM-HTC-087	[redacted]	[redacted]	[redacted]	[redacted]	[redacted]	[redacted]
88	MIX-COMP-THERM-HTC-088	[redacted]	[redacted]	[redacted]	[redacted]	[redacted]	[redacted]
89	MIX-COMP-THERM-HTC-089	[redacted]	[redacted]	[redacted]	[redacted]	[redacted]	[redacted]
90	MIX-COMP-THERM-HTC-090	[redacted]	[redacted]	[redacted]	[redacted]	[redacted]	[redacted]
91	MIX-COMP-THERM-HTC-091	[redacted]	[redacted]	[redacted]	[redacted]	[redacted]	[redacted]
92	MIX-COMP-THERM-HTC-092	[redacted]	[redacted]	[redacted]	[redacted]	[redacted]	[redacted]
93	MIX-COMP-THERM-HTC-093	[redacted]	[redacted]	[redacted]	[redacted]	[redacted]	[redacted]
94	MIX-COMP-THERM-HTC-094	[redacted]	[redacted]	[redacted]	[redacted]	[redacted]	[redacted]
95	MIX-COMP-THERM-HTC-095	[redacted]	[redacted]	[redacted]	[redacted]	[redacted]	[redacted]
96	MIX-COMP-THERM-HTC-096	[redacted]	[redacted]	[redacted]	[redacted]	[redacted]	[redacted]
97	MIX-COMP-THERM-HTC-097	[redacted]	[redacted]	[redacted]	[redacted]	[redacted]	[redacted]
98	MIX-COMP-THERM-HTC-098	[redacted]	[redacted]	[redacted]	[redacted]	[redacted]	[redacted]
99	MIX-COMP-THERM-HTC-099	[redacted]	[redacted]	[redacted]	[redacted]	[redacted]	[redacted]
100	MIX-COMP-THERM-HTC-100	[redacted]	[redacted]	[redacted]	[redacted]	[redacted]	[redacted]
101	MIX-COMP-THERM-HTC-101	[redacted]	[redacted]	[redacted]	[redacted]	[redacted]	[redacted]
102	MIX-COMP-THERM-HTC-102	[redacted]	[redacted]	[redacted]	[redacted]	[redacted]	[redacted]
103	MIX-COMP-THERM-HTC-103	[redacted]	[redacted]	[redacted]	[redacted]	[redacted]	[redacted]
104	MIX-COMP-THERM-HTC-104	[redacted]	[redacted]	[redacted]	[redacted]	[redacted]	[redacted]
105	MIX-COMP-THERM-HTC-105	[redacted]	[redacted]	[redacted]	[redacted]	[redacted]	[redacted]
106	MIX-COMP-THERM-HTC-106	[redacted]	[redacted]	[redacted]	[redacted]	[redacted]	[redacted]
107	MIX-COMP-THERM-HTC-107	[redacted]	[redacted]	[redacted]	[redacted]	[redacted]	[redacted]
108	MIX-COMP-THERM-HTC-108	[redacted]	[redacted]	[redacted]	[redacted]	[redacted]	[redacted]
109	MIX-COMP-THERM-HTC-109	[redacted]	[redacted]	[redacted]	[redacted]	[redacted]	[redacted]
110	MIX-COMP-THERM-HTC-110	[redacted]	[redacted]	[redacted]	[redacted]	[redacted]	[redacted]
111	MIX-COMP-THERM-HTC-111	[redacted]	[redacted]	[redacted]	[redacted]	[redacted]	[redacted]
112	MIX-COMP-THERM-HTC-112	[redacted]	[redacted]	[redacted]	[redacted]	[redacted]	[redacted]
113	MIX-COMP-THERM-HTC-113	[redacted]	[redacted]	[redacted]	[redacted]	[redacted]	[redacted]
114	MIX-COMP-THERM-HTC-114	[redacted]	[redacted]	[redacted]	[redacted]	[redacted]	[redacted]
115	MIX-COMP-THERM-HTC-115	[redacted]	[redacted]	[redacted]	[redacted]	[redacted]	[redacted]
116	MIX-COMP-THERM-HTC-116	[redacted]	[redacted]	[redacted]	[redacted]	[redacted]	[redacted]
117	MIX-COMP-THERM-HTC-117	[redacted]	[redacted]	[redacted]	[redacted]	[redacted]	[redacted]
118	MIX-COMP-THERM-HTC-118	[redacted]	[redacted]	[redacted]	[redacted]	[redacted]	[redacted]
119	MIX-COMP-THERM-HTC-119	[redacted]	[redacted]	[redacted]	[redacted]	[redacted]	[redacted]
120	MIX-COMP-THERM-HTC-120	[redacted]	[redacted]	[redacted]	[redacted]	[redacted]	[redacted]
121	MIX-COMP-THERM-HTC-121	[redacted]	[redacted]	[redacted]	[redacted]	[redacted]	[redacted]
122	MIX-COMP-THERM-HTC-122	[redacted]	[redacted]	[redacted]	[redacted]	[redacted]	[redacted]
123	MIX-COMP-THERM-HTC-123	[redacted]	[redacted]	[redacted]	[redacted]	[redacted]	[redacted]

Case	Evaluation Identification	File-name	k_{eff-i}	$\pm \sigma_{calc-i}$	$\pm \sigma_{exp}$	$\pm \sigma_i$	EALF (eV)
124	MIX-COMP-THERM-HTC-124	[redacted]	[redacted]	[redacted]	[redacted]	[redacted]	[redacted]
125	MIX-COMP-THERM-HTC-125	[redacted]	[redacted]	[redacted]	[redacted]	[redacted]	[redacted]
126	MIX-COMP-THERM-HTC-126	[redacted]	[redacted]	[redacted]	[redacted]	[redacted]	[redacted]
127	MIX-COMP-THERM-HTC-127	[redacted]	[redacted]	[redacted]	[redacted]	[redacted]	[redacted]
128	MIX-COMP-THERM-HTC-128	[redacted]	[redacted]	[redacted]	[redacted]	[redacted]	[redacted]
129	MIX-COMP-THERM-HTC-129	[redacted]	[redacted]	[redacted]	[redacted]	[redacted]	[redacted]
130	MIX-COMP-THERM-HTC-130	[redacted]	[redacted]	[redacted]	[redacted]	[redacted]	[redacted]
131	MIX-COMP-THERM-HTC-131	[redacted]	[redacted]	[redacted]	[redacted]	[redacted]	[redacted]
132	MIX-COMP-THERM-HTC-132	[redacted]	[redacted]	[redacted]	[redacted]	[redacted]	[redacted]
133	MIX-COMP-THERM-HTC-133	[redacted]	[redacted]	[redacted]	[redacted]	[redacted]	[redacted]
134	MIX-COMP-THERM-HTC-134	[redacted]	[redacted]	[redacted]	[redacted]	[redacted]	[redacted]
135	MIX-COMP-THERM-HTC-135	[redacted]	[redacted]	[redacted]	[redacted]	[redacted]	[redacted]
136	MIX-COMP-THERM-HTC-136	[redacted]	[redacted]	[redacted]	[redacted]	[redacted]	[redacted]
137	MIX-COMP-THERM-HTC-137	[redacted]	[redacted]	[redacted]	[redacted]	[redacted]	[redacted]
138	MIX-COMP-THERM-HTC-138	[redacted]	[redacted]	[redacted]	[redacted]	[redacted]	[redacted]
139	MIX-COMP-THERM-HTC-139	[redacted]	[redacted]	[redacted]	[redacted]	[redacted]	[redacted]
140	MIX-COMP-THERM-HTC-140	[redacted]	[redacted]	[redacted]	[redacted]	[redacted]	[redacted]
141	MIX-COMP-THERM-HTC-141	[redacted]	[redacted]	[redacted]	[redacted]	[redacted]	[redacted]
142	MIX-COMP-THERM-HTC-142	[redacted]	[redacted]	[redacted]	[redacted]	[redacted]	[redacted]
143	MIX-COMP-THERM-HTC-143	[redacted]	[redacted]	[redacted]	[redacted]	[redacted]	[redacted]
144	MIX-COMP-THERM-HTC-144	[redacted]	[redacted]	[redacted]	[redacted]	[redacted]	[redacted]
145	MIX-COMP-THERM-HTC-145	[redacted]	[redacted]	[redacted]	[redacted]	[redacted]	[redacted]
146	MIX-COMP-THERM-HTC-146	[redacted]	[redacted]	[redacted]	[redacted]	[redacted]	[redacted]
147	MIX-COMP-THERM-HTC-147	[redacted]	[redacted]	[redacted]	[redacted]	[redacted]	[redacted]
148	MIX-COMP-THERM-HTC-148	[redacted]	[redacted]	[redacted]	[redacted]	[redacted]	[redacted]
149	MIX-COMP-THERM-HTC-149	[redacted]	[redacted]	[redacted]	[redacted]	[redacted]	[redacted]
150	MIX-COMP-THERM-HTC-150	[redacted]	[redacted]	[redacted]	[redacted]	[redacted]	[redacted]
151	MIX-COMP-THERM-HTC-151	[redacted]	[redacted]	[redacted]	[redacted]	[redacted]	[redacted]
152	MIX-COMP-THERM-HTC-152	[redacted]	[redacted]	[redacted]	[redacted]	[redacted]	[redacted]
153	MIX-COMP-THERM-HTC-153	[redacted]	[redacted]	[redacted]	[redacted]	[redacted]	[redacted]
154	MIX-COMP-THERM-HTC-154	[redacted]	[redacted]	[redacted]	[redacted]	[redacted]	[redacted]
155	MIX-COMP-THERM-HTC-155	[redacted]	[redacted]	[redacted]	[redacted]	[redacted]	[redacted]
156	MIX-COMP-THERM-HTC-156	[redacted]	[redacted]	[redacted]	[redacted]	[redacted]	[redacted]

Table C.3-5 The MCNP5-1.51 Calculational Results and Measurements Uncertainties for Selected Critical Experiments

Case	Evaluation Identification	File-name	k_{eff-i}	$\pm \sigma_{calc-i}$	$\pm \sigma_{exp}$	$\pm \sigma_i$	EALF (eV)
157	Core I						
158	Core II						
159	Core III						
160	Core IX						
161	Core X						
162	Core XI						
163	Core XII						
164	Core XIII						
165	Core XIV						
166	Core XV						
167	Core XVI						
168	Core XVII						
169	Core XVIII						
170	Core XIX						
171	Core XX						
172	Core XXI						
173	S-type Fuel, w/886 ppm B						
174	S-type Fuel, w/746 ppm B						
175	SO-type Fuel, w/1156 ppm B						
176	Case 1 1337 ppm B						
177	Case 12 1899 ppm B						
178	Water Moderator 0 gap						
179	Water Moderator 2.5 cm gap						
180	Water Moderator 5 cm gap						
181	Water Moderator 10 cm gap						
182	Steel Reflector, 1.321 cm separation						
183	Steel Reflector, 2.616 cm separation						
184	Steel Reflector, 3.912 cm separation						
185	Steel Reflector, Infinite separation						
186	Steel Reflector, 1.321 cm separation						
187	Steel Reflector, 2.616 cm separation						
188	Steel Reflector, 5.405 cm separation						
189	Steel Reflector, Infinite separation						
190	Steel Reflector, with Boral Sheets						
191	Lead Reflector, 0.55 cm sepn.						
192	Lead Reflector, 1.956 cm sepn.						
193	Lead Reflector, 5.405 cm sepn.						
194	Experiment 004/032 – no absorber						

Case	Evaluation Identification	File-name	k_{eff-i}	$\pm \sigma_{calc-i}$	$\pm \sigma_{exp}$	$\pm \sigma_i$	EALF (eV)
195	Exp. 009 1.05% Boron Steel plates						
196	Exp. 009 1.62% Boron Steel plates						
197	Exp. 031 – Boral plates						
198	Experiment 214R – with flux traps						
199	Experiment 214V3 –with flux trap						
200	Case 173 – 0 ppm B						
201	Case 177 – 2550 ppm B						
202	MOX Fuel – Type 3.2 Exp. 21						
203	MOX Fuel – Type 3.2 Exp. 43						
204	MOX Fuel – Type 3.2 Exp. 13						
205	MOX Fuel – Type 3.2 Exp. 32						
206	Saxton Case 52 PuO2 0.52" pitch						
207	Saxton Case 52 U 0.52" pitch						
208	Saxton Case 56 PuO2 0.56" pitch						
209	Saxton Case 56 borated PuO2						
210	Saxton Case 56 U 0.56" pitch						
211	Saxton Case 79 PuO2 0.79" pitch						
212	Saxton Case 79 U 0.79" pitch						
213	0.700-in. pitch 0 ppm B						
214	0.700-in. pitch 688 ppm B						
215	0.870-in. pitch 0 ppm B						
216	0.870-in. pitch 1090 ppm B						
217	0.990-in. pitch 0 ppm B						
218	0.990-in. pitch 767 ppm B						
219	Saxton Case PuO2 0.735" pitch						
220	Saxton Case PuO2 1.04" pitch						
221	8 wt% 240Pu 0.80" pitch						
222	8 wt% 240Pu 0.93" pitch						
223	8 wt% 240Pu 1.05" pitch						
224	8 wt% 240Pu 1.143" pitch						
225	8 wt% 240Pu 1.32" pitch						
226	8 wt% 240Pu 1.386" pitch						
227	16 wt% 240Pu 0.93" pitch						
228	16 wt% 240Pu 1.05" pitch						
229	16 wt% 240Pu 1.143" pitch						
230	16 wt% 240Pu 1.32" pitch						
231	24 wt% 240Pu 0.80" pitch						
232	24 wt% 240Pu 0.93" pitch						
233	24 wt% 240Pu 1.05" pitch						
234	24 wt% 240Pu 1.143" pitch						

Case	Evaluation Identification	File-name	k_{eff-i}	$\pm \sigma_{calc-i}$	$\pm \sigma_{exp}$	$\pm \sigma_i$	EALF (eV)
235	24 wt% 240Pu 1.32" pitch						
236	24 wt% 240Pu 1.386" pitch						
237	18 wt% 240Pu 0.85" pitch						
238	18 wt% 240Pu 0.93" pitch						
239	18 wt% 240Pu 1.05" pitch						
240	18 wt% 240Pu 1.143" pitch						
241	18 wt% 240Pu 1.386" pitch						
242	18 wt% 240Pu 1.60" pitch						
243	18 wt% 240Pu 1.70" pitch						
317	Core XI, 1182 ppm, 36 Pyrex Rods						
318	Core XI, 1182 ppm, 36 Pyrex Rods						
319	Core XI, 1032.5 ppm, 72 Pyrex Rods						
320	Core XI, 1032.5 ppm, 72 Pyrex Rods						
321	Core XI, 794 ppm, 144 Pyrex Rods						
322	Core XI, 779 ppm, 144 Pyrex Rods						
323	Core XI, 1245 ppm, 72 Vicor Rods						
360	Core IV						
361	Core V						
362	Core VI						
363	Core VII						
364	Core VIII						
445	670 pins, Al2O3-B4C rods						
446	672 pins, Al2O3-B4C rods						
447	668 pins, Al2O3-B4C rods						
448	668 pins, Al2O3-B4C rods						
479	8 wt% 240Pu 1.05" pitch, B4 Rods						
480	8 wt% 240Pu 1.05" pitch, B3 Rods						
481	8 wt% 240Pu 1.05" pitch, B2 Rods						
482	8 wt% 240Pu 1.05" pitch, B1 Rods						
484	8 wt% 240Pu 1.05" pitch, B4+Cd Rods						
485	8 wt% 240Pu 1.05" pitch, B3+Cd Rods						
486	8 wt% 240Pu 1.05" pitch, B2+Cd Rods						
487	8 wt% 240Pu 1.05" pitch, B1+Cd Rods						
491	8 wt% 240Pu 1.32" pitch, B4 Rods						
492	8 wt% 240Pu 1.32" pitch, B3 Rods						
493	8 wt% 240Pu 1.32" pitch, B2 Rods						
494	8 wt% 240Pu 1.32" pitch, B1 Rods						

Case	Evaluation Identification	File-name	k_{eff-i}	$\pm \sigma_{calc-i}$	$\pm \sigma_{exp}$	$\pm \sigma_i$	EALF (eV)
496	8 wt% 240Pu 1.32" pitch, B4+Cd Rods						
497	8 wt% 240Pu 1.32" pitch, B3+Cd Rods						
498	8 wt% 240Pu 1.32" pitch, B2+Cd Rods						
499	8 wt% 240Pu 1.32" pitch, B1+Cd Rods						
504	16 wt% 240Pu 1.05" pitch, B4 Rods						
505	16 wt% 240Pu 1.05" pitch, B3 Rods						
506	16 wt% 240Pu 1.05" pitch, B2 Rods						
507	16 wt% 240Pu 1.05" pitch, B1 Rods						
509	16 wt% 240Pu 1.05" pitch, B4+Cd Rods						
510	16 wt% 240Pu 1.05" pitch, B3+Cd Rods						
511	16 wt% 240Pu 1.05" pitch, B2+Cd Rods						
512	16 wt% 240Pu 1.05" pitch, B1+Cd Rods						
516	24 wt% 240Pu 1.05" pitch, B4 Rods						
517	24 wt% 240Pu 1.05" pitch, B3 Rods						
518	24 wt% 240Pu 1.05" pitch, B2 Rods						
519	24 wt% 240Pu 1.05" pitch, B1 Rods						
521	24 wt% 240Pu 1.05" pitch, B4+Cd Rods						
522	24 wt% 240Pu 1.05" pitch, B3+Cd Rods						
523	24 wt% 240Pu 1.05" pitch, B2+Cd Rods						
524	24 wt% 240Pu 1.05" pitch, B1+Cd Rods						

Table C.3-6 Descriptive Statistics of the MCNP5-1.51 Calculational Results

Experiment Description	No. of exp.	k_{eff} range	EALF (eV) range
Phase 1	18	[redacted]	[redacted]
Phase 2	41	[redacted]	[redacted]
Phase 3	26	[redacted]	[redacted]
Phase 4	71	[redacted]	[redacted]
Selected Experiments	135	[redacted]	[redacted]
All experiments	291	[redacted]	[redacted]

Table C.3-7 Normality Test Results for the MCNP5-1.51 calculations

Experiment Description	No. of exp.	Shapiro-Wilk		Pearson's chi-square (χ^2)			
		Wtest	W	χ^2	n	$P_d(\chi^2;d)$	Normal
Phase 1	18	[redacted]	[redacted]	[redacted]	[redacted]	[redacted]	[redacted]
Phase 2	41	[redacted]	[redacted]	[redacted]	[redacted]	[redacted]	[redacted]
Phase 3	26	[redacted]	[redacted]	[redacted]	[redacted]	[redacted]	[redacted]
Phase 4	71	[redacted]	[redacted]	[redacted]	[redacted]	[redacted]	[redacted]
HTC Experiments	156	[redacted]	[redacted]	[redacted]	[redacted]	[redacted]	[redacted]
Selected Experiments	135	[redacted]	[redacted]	[redacted]	[redacted]	[redacted]	[redacted]
All experiments	291	[redacted]	[redacted]	[redacted]	[redacted]	[redacted]	[redacted]

Table C.3-8 Trending Analysis Results for the MCNP5-1.51 calculations

Experiment Description	No. of exp.	Correlated Parameter, x	Correlation Coefficient, r^2	Probability, Pd(N;r)	Correlation	Regression Equation, k(x)
Phase 1	18	EALF				
		Pitch				
		Number of Rods				
Phase 2	41	EALF				
		Pitch				
		Number of Rods				
		Gadolinium Conc.				
		Boron Conc.				
Phase 3	26	EALF				
		Water Gap				
		Number of Rods				
Phase 4	71	EALF				
		Water Gap				
		Screen Array Distance				
Selected Experiments	135	EALF				
		Pitch				
		Rod OD				
		Fuel Density				
		U Enrichment				
		Pu Enrichment				
All experiments	291	EALF				
		Pitch				
		Rod OD				
		Fuel Density				

Table C.3-9 Analysis of Neutron Absorbers and Reflector Materials for the MCNP5-1. 51 calculations

Experiment Description	No. of exp.	Bias	Bias Uncertainty	Normality χ^2 ($P_d(\chi^2;d)$)	Significant Trends
All experiments	291				
All except those with Gadolinium, Cadmium and Lead	201				

Table C.3-10 Analysis of Fuel Rod Pitch Trend for the MCNP5-1. 51 calculations

Experiment Description	Rod Pitch	Bias	Bias Uncertainty	Normality χ^2 ($P_d(\chi^2;d)$)	Significant Trends
All experiments	All (291 total)				
	<=2 cm (218 total)				
All except those with Gadolinium, Cadmium and Lead	All (201 total)				
	<=2 cm (144 total)				

Table C.3-11 Analysis of Fuel Burnup for the MCNP5-1. 51 calculations

Experiment Description	Rod Pitch	Bias	Bias Uncertainty	Normality χ^2 ($P_d(\chi^2;d)$)	Significant Trends
All except those with Gadolinium, Cadmium and Lead†	All (201 total)				
	<=2 cm (144 total)				
Fresh UO_2 Fuel	All (61 total)				
	<=2 cm (52 total)				
HTC Experiments	All (85 total)				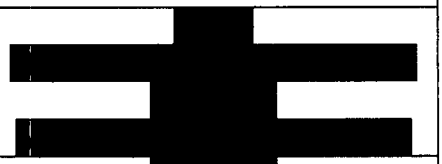
	<=2 cm (82 total)				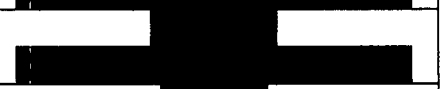
MOX Experiments	All (55 total)				
	<=2 cm (10 total)				

†Note: Critical experiments with Gadolinium, Cadmium and Lead were excluded from all subsequent subsets.

Table C.3-12 Analysis of the Unborated and Borated Water for the MCNP5-1.51 calculations

Experiment Description	Rod Pitch	Bias	Bias Uncertainty	Normality χ^2 ($P_d(\chi^2;d)$)	Significant Trends
All except those with Gadolinium, Cadmium and Lead†	All (201 total)				
	<=2 cm (144 total)				
All with Fresh Water	All (149 total)				
	<=2 cm (94 total)				
All with Borated Water	All (52 total)				
	<=2 cm (50 total)				

†Note: Critical experiments with Gadolinium, Cadmium and Lead were excluded from all subsequent subsets.

Table C.3-13 Comparison of Key Parameters and Definition of Validated AOA

Parameter	Design Application	Benchmarks	Validated
Fissionable Material	^{235}U, ^{239}Pu, ^{241}Pu	^{235}U, ^{239}Pu, ^{241}Pu	^{235}U, ^{239}Pu, ^{241}Pu
Isotopic Composition			
$^{235}U/Ut$	< 5.0wt%	1.57 – 5.74%	< 5wt%
Pu/(U+Pu)	< 20wt%	1.104 - 20 %	< 20wt%
Physical Form	UO_2, MOX	UO_2, MOX	UO_2, MOX
Fuel Density (g/cm^3)	10.0 – 10.7	9.2 – 10.4	9.2 – 10.7
Moderator Material (coolant)	H	H	H
Physical Form	H_20	H_20	H_20
Density (g/cm^3)	around 1.0 g/cm^3	around 1.0 g/cm^3	around 1.0 g/cm^3
Reflector Material	H	H	H
Physical Form	H_20	H_20	H_20
Density (g/cm^3)	around 1.0 g/cm^3	around 1.0 g/cm^3	around 1.0 g/cm^3
Interstitial Reflector Material			
Plate	Steel or Lead	Steel or Lead	Steel or Lead
Absorber Material			
Soluble	None, Boron or Gadolinium	None, Boron (89 - 595 ppm) or Gadolinium (49.2 – 199.7 ppm)	None, Boron (0 - 1000 ppm) or Gadolinium (0 to 1000 ppm)
Rods	Boron	Pyrex®, Vicor® or B-Al	Boron
Separating Material			
Plate	Water, B-SS, Boral or Cadmium	Water, B-SS, Boral or Cadmium	Water, B-SS, Boral or Cadmium
Geometry			
Lattice type	Square	Square, Triangle	Square, Triangle
Lattice Pitch (cm)	1.26 – 1.47 (PWR) 1.24 – 1.88 (BWR)	0.968 to 4.318	0.968 to 4.318
Neutron Energy	Thermal spectrum	Thermal spectrum	Thermal spectrum

Figure Proprietary

Figure C.3-1 Frequency Chart for Calculated k_{eff} of the Selected 243 Benchmarks for the MCNP5-1.51 code

Figure Proprietary

Figure C.3-2 Frequency Chart for Calculated EALF (eV) of the Selected 243 Benchmarks for the MCNP5-1.51 code

Figure Proprietary

Figure C.3-3 MCNP5-1.51 Calculated k_{eff} Values for Various Values of the Spectral Index (All Experiments)

Figure Proprietary

Figure C.3-4 MCNP5-1.51 Calculated k_{eff} Values as a Function of Rod Pitch (All Experiments)

Appendix D

Benchmark of MCNP5-1.51 with ENDF/B-VII

(total number of pages: 51 including this page)

D.1 Introduction

This Appendix presents the analysis of the validation results for MCNP5-1.51 code and includes the results of the calculations, normality test, the detailed statistical trending analysis, calculation bias and bias uncertainty for each distinct area of applicability of the parameters of interest.

D.2 Computer Code Parameter Data

The computer code MCNP5-1.51 [D.1] is the continuous energy Monte Carlo codes and treats an arbitrary three-dimensional configuration of materials in geometric cells bounded by first- and second-degree surfaces and fourth-degree elliptical tori. Thermal neutrons are described by both the free gas and S(α,β) models. All calculations were performed using the default data libraries provided with the code: the default continuous energy neutron transport data based on ENDF/B-VII. The list of ZAIDs that were used in the analysis is presented in Table D.2-1. The neutrons start from an arbitrary distribution, causing a generally very large variance of results from the first cycles in comparison with the following cycles. Therefore, all MCNP5-1.51 calculations are performed with 12,000 histories per cycle, 50 skipped cycles before averaging, and 100 cycles that are accumulated. The calculated k_{eff} values have associated uncertainties due to the statistical nature of the Monte Carlo codes.

D.3 Analysis of MCNP5-1.51 Validation Results

D.3.1. Calculational Results

The calculation results for the 156 HTC critical experiments and for the 376 selected critical experiments described in Appendix B are presented and discussed in this section. The calculation results are summarized by grouping the experiments in terms of the categories as set forth in Appendix B. Calculation results, including $k_{eff\text{-}I}$, $\sigma_{calc\text{-}i}$ and EALF, measurement uncertainties (σ_{exp}) and the calculation and measurement combined uncertainty (σ_i) are shown in Table D.3-1 through Table D.3-5.

Figure D.3-1 and D.3-2 are histograms showing the frequency of calculated k_{eff} and EALF for all 532 benchmarks. The nominal calculated k_{eff} values range from 0[redacted]. The EALF results values show a range between [redacted].

Descriptive statistics for the different group of experiments is summarized in Table D.3-6.

D.3.2. Normality Test

In order to assess the normality assumption, Shapiro and Wilk [5] test has been used for groups with fewer than 50 samples while the Pearson's chi-square (χ^2) test [4] has been used for samples larger than 20 samples. The tests are applied to the group of experiments in terms of the categories as set forth in Appendix B.

For the Shapiro and Wilk test, Table D.3-7 shows the computed *Wtest* value, and *W* value that can be obtained for the number of experiments from [5] to accept the normality hypothesis. If W

is less than the test statistic, *Wtest*, then the data is considered normally distributed. For the χ^2 test, it is concluded normal for $\chi^2 \leq n$, where n is a number of bins for the group of experiments. The probability $P_d(\tilde{\chi}^2 \geq \tilde{\chi}_0{}^2)$ of obtaining a value of $\tilde{\chi}^2 \geq \tilde{\chi}_0{}^2$ in an experiment with d degrees of freedom to confirm quantitatively that the agreement is satisfactory was taken or interpolated, if necessary, from Appendix D in Reference [4]. Thus, if $P_d(\tilde{\chi}^2 \geq \tilde{\chi}_0{}^2)$ is large, the obtained and expected distributions are consistent; if it is small, they probably disagree. In particular, if $P_d(\tilde{\chi}^2 \geq \tilde{\chi}_0{}^2)$ is less than 5%, we say that the disagreement is significant and reject the assumed distributions at the 5% level. If it is less than 1%, the disagreement is called highly significant, and we reject the assumed distributions at the 1% level.

D.3.3. Trending Analysis

Trends are determined through the use of regression fits to the calculated results. The equations used to identify trends are given below:

$$Y(x) = a + bx \tag{7-1}$$

$$a = \frac{1}{\Delta}\left(\sum \frac{x_i^2}{\sigma_i^2}\sum \frac{y_i}{\sigma_i^2} - \sum \frac{x_i}{\sigma_i^2}\sum \frac{x_i y_i}{\sigma_i^2}\right) \tag{7-2}$$

$$b = \frac{1}{\Delta}\left(\sum \frac{1}{\sigma_i^2}\sum \frac{x_i y_i}{\sigma_i^2} - \sum \frac{x_i}{\sigma_i^2}\sum \frac{y_i}{\sigma_i^2}\right) \tag{7-3}$$

$$\Delta = \sum \frac{1}{\sigma_i^2}\sum \frac{x_i^2}{\sigma_i^2} - \left(\sum \frac{x_i}{\sigma_i^2}\right)^2 \tag{7-4}$$

The squared term of the linear correlation factor r defined below (from Reference [5]) is used to quantitatively measure the degree to which a linear relationship exist between two variables.

$$r = \frac{\Sigma \frac{1}{\sigma_i^2}(x_i - \bar{x})(y_i - \bar{y})}{\sqrt{\left[\Sigma \frac{1}{\sigma_i^2}(x_i - \bar{x})^2\right]\left[\Sigma \frac{1}{\sigma_i^2}(y_i - \bar{y})^2\right]}} \tag{7-5}$$

The closer r^2 approaches the value of 1, the better the fit of the data to the linear equation. A more quantitative measure of the fit can be found by using Appendix C in Reference [4]. The interpolation was applied, if necessary. For any given observed value r_0, $P_N(|r| \geq |r_0|)$ is the probability that N measurements of two uncorrelated variables would give a coefficient r as large as r_0. Thus, if we obtain a coefficient r_0 for which $P_N(|r| \geq |r_0|)$ is small, it is correspondingly unlikely that our variables are uncorrelated; that is, a correlation indicated. In particular, if $P_N(|r| \geq |r_0|) \leq 5\%$, the correlation is called significant; if it is less than 1%, the correlation is called highly significant.

The validation results are analyzed for the group of all experiments. Independent variables used in the trending analysis, correlation coefficients and trending analysis results are summarized in Table D.3-8.

D.3.4. Bias and Bias Uncertainty

In this section, benchmark results are analyzed using the statistical method described in section 2.2.

The first step is to evaluate whether the HTC experiments and selected experiments, should be reduced to a single set. The mean k_{eff} of the HTC data set is [redacted] and the mean k_{eff} of the selected experiments data is [redacted]. The difference between the means is just 0.0010 which is less than the uncertainty. These sets are water moderated uranium or mixed plutonium-uranium dioxide lattices. The HTC sets of experiments and the selected experiments are considered one large set of 532 experiments from now on.

The normality test in Table D.3-7 and in Figure D.3-1 shows that the data is not normally distributed. Therefore, the distribution free approach [6] is used for all subsets with the rejected normality distribution. The lower tolerance limit with 95% probability and 95% confidence level is determined for order data [6] and the difference between weighted average k_{eff} and this lower tolerance limit is used to determine the bias uncertainty. This is conservative since the data is close to the normal distribution. The distribution free bias uncertainty is also provided in all subsequent tables for the subsets with the rejected normality assumption.

The analysis of the correlation coefficient in Table D.3-8 and the plot of data trend (Figure D.3-3) show that there is not a clear trend in the data.

The total bias (systematic error or mean of the deviation from a keff of exactly 1.000) of the MCNP5-1.51 code is shown in the table below

Calculational Bias of the MCNP5-1.51 code		
Description	Total Bias	Bias Uncertainty
HTC and Selected Experiments	[redacted]	[redacted]

D.3.5. Applicability of MCNP5-1.51 Validation Results

This subsection contains a more detailed evaluation of the set of critical experiments. Regarding the selected experiments, the following subjects are discussed:

- Neutron absorber and neutron reflector materials
- Neutron absorber geometry
- Fuel burnup
- Unborated and borated water

- Various Combinations of Fuel Burnup and Unborated/Borated Water.

The general focus is to justify that using the full set of critical experiments is appropriate. In some cases, subsets of full set of experiments are established. For those subsets, statistical evaluations are performed to determine bias, bias uncertainty, normality and trends. Trends are evaluated for fuel rod outer diameter, fuel rod pitch, fuel density, boron content, U or Pu enrichment and EALF. To estimate a significance of observed trend, the residuals from the trend equation were tested for a normal distribution [D.2]. If residuals are normally distributed then there is a significant trend, otherwise there is no linear trend as this violets the basic assumptions of linear regression. For each significant linear correlation, the bias and bias uncertainty were calculated as a function of the independent parameter.

D.3.5.1. Neutron Absorber and Neutron Reflector Materials

The HTC and Selected Experiments consider the following neutron absorbers and reflectors:

- Absorbers
  - Boron, in the form of soluble boron in the water, boron in solid form (B_4C), and boron in borated steel, Pyrex, Boroflex and borated aluminum
  - Soluble gadolinium in water and Gd_2O_3 rods
  - Cadmium
- Reflectors
  - Steel
  - Lead
  - Water

Some typical configurations do not contain gadolinium or cadmium neutron absorbers or lead reflectors. To verify that including those materials does not have a significant effect on the results of the benchmarking analyses, a subset without those experiments containing those materials was analyzed. In addition, according to recommendations of NUREG-6979 [B.13], the following HTC experiments were also excluded: 61, 65, 67, 86, 97, 98, 99, 102, 124, 135, and 137. The comparison with the full set is presented in Table D.3-9 and shows no significant differences when those materials are excluded. However, a significant correlation as a function of EALF was determined by the residuals normality test. This correlation is presented in the Figure D.3-4. The bias and bias uncertainty as a function of the EALF were calculated for this trend and shown in Table D.3-10, with a maximum absolute value of [redacted].

D.3.5.2. Absorber Geometry

The criticality experiments analyzed in this report include experiments with Boron in the form of plates, absorber rods and soluble boron in water. No trend relating to these experiments is observed.

D.3.5.3. Fuel Burnup

The full set of critical experiments contains experiments with fresh UO_2 fuel, with simulated spent fuel (37.5 GWd/MTU), and MOX fuel with Pu content between 1.5 and 20%, which is

even higher than typically found in spent fuel. The experiments are therefore reasonably representative of burned fuel at different burnup levels. To verify that the experiments cover the burnup range sufficiently, the experiments are subdivided into fresh UO_2 fuel and spent fuel with HTC and MOX experiments, and compared to the results of the entire set. The comparison is shown in Table D.3-11. The comparison shows no significant differences between the entire set and the fresh and spent fuel subsets. However, in some cases, the correlations are observed. The significant trends as a function of EALF and Pu enrichment were determined in the spent fuel subset by the residuals normality test. These correlations are presented in the Figure D.3-5 and Figure D.3-6. The bias and bias uncertainty as a function of the EALF and Pu enrichment were calculated for these trends and shown in Table D.3-12, with a maximum absolute value of -[redacted].

D.3.5.4. Unborated and Borated Water

The full set of critical experiments contains both experiments with and without soluble boron. The entire set of analyses shows no significant trend when analyzed as a function of the soluble boron level. Nevertheless, sets with and without soluble boron are analyzed and compared to the full set that contains all experiments. The results are shown in Table D.3-13. Similar to the previous subsection, the comparison shows no significant differences between those subsets. However, there are significant trends in the fresh water subset as a function of EALF and U enrichment and in the borated water subset as a function of fuel density that were determined by the residuals normality test. These correlations are presented in the Figure D.3-7 through Figure D.3-9. The bias and bias uncertainty as a function of the EALF, U enrichment and fuel density were calculated for these trends and shown in Table D.3-14, with a maximum absolute value of -[redacted].

D.3.5.5. Various Combinations of Fuel Burnup and Unborated/Borated Water

To perform more detailed evaluation of the set of critical experiments, the additional four subsets with different combinations of fuel burnup and unborated/borated water were analyzed. The results are shown in Table D.3-15. There are significant EALF trend in the subset of fresh UO_2 fuel with fresh water, significant trends in the subset of spent fuel with fresh water as a function of EALF and Pu enrichment and significant trends in the subset of spent fuel with borated water as a function of rod OD and fuel density, that were determined by the residuals normality test. These correlations are presented in the Figure D.3-10 through Figure D.3-14.The bias and bias uncertainty as a function of the EALF, Pu enrichment, rod OD and fuel density were calculated for these trends and shown in Table D.3-16, with a maximum absolute value of [redacted].

D.4 Summary

A set of 532 critical experiments has been selected and has been used for the validation of the Holtec International criticality safety methodology. The similarity between the chosen experiments and the actual systems has been based on a set of screening criteria as is stated in the NUREG/CR-6698 [5]. Experiments have been categorized by fuel burnup as fresh UO_2 fuel and spent fuel with HTC and MOX experiments or by unborated and borated water condition and

parameterized by key variables such as lattice pitch / assembly pitch, absorber solution concentration, number of fuel rods, rod outer diameter, fuel density, screen array distance, fuel enrichment and EALF. Benchmark calculations have been performed using the Monte Carlo code MCNP5-1.51. It was determined that HTC experiments and selected experiments are in sufficient agreement that this sets are lumped together as a single set of 532 experiments. The bias and bias uncertainty are presented in section D.3.4. The applicability of validation results is considered in section D.3.5.

The range of key parameters for the design application, benchmarks and validated AOA are summarized in Table D.3-17. A point by point comparison between design application and benchmarks shows that the experimental range covers all the parameters. The soluble boron concentration is extrapolated generously since ^{10}B is a 1/v absorber (as permitted on Table 2.3 of [5]).

As for the fuel density, Table 2.3 of Reference [5] states there is "no requirement" and that "experiments should be as close to the desired concentration as possible". Since the experiment fuel density is 9.2 – 10.4 g/cm^3 and the design application one is around 10.0 – 10.7 g/cm^3, it is considered that the values are very close so the validated AOA covers the design application range.

The fuel enrichment can be up to 5%. The experiments used go up to 5.74 wt% ^{235}U. Therefore, it is considered that the validated AOA covers the design application range.

D.5 References

[D.1] "MCNP - A General Monte Carlo N-Particle Transport Code, Version 5"; Los Alamos National Laboratory, LA-UR-03-1987 (Revised 2/1/2008).

[D.2] J. W. Barnes, "Statistical Analysis for Engineers and Scientists", McGraw-Hill Inc., 1988

Table D.2-1 ZAIDs Used for Each Nuclide

Nuclide	MCNP5.1.51 ZAID	Nuclide	MCNP5.1.51 ZAID	Nuclide	MCNP5.1.51 ZAID
^{1}H	1001.70c	^{48}Ti	22048.70c	^{100}Mo	42100.70c
^{2}H	1002.70c	^{49}Ti	22049.70c	^{107}Ag	47107.70c
^{4}He	2004.70c	^{50}Ti	22050.70c	^{109}Ag	47109.70c
^{10}B	5010.70c	^{50}Cr	24050.70c	^{106}Cd	48106.70c
^{11}B	5011.70c	^{52}Cr	24052.70c	^{108}Cd	48108.70c
C	6000.70c	^{53}Cr	24053.70c	^{110}Cd	48110.70c
^{14}N	7014.70c	^{54}Cr	24054.70c	^{111}Cd	48111.70c
^{16}O	8016.70c	^{55}Mn	25055.70c	^{112}Cd	48112.70c
^{20}Ne	10020.42c	^{54}Fe	26054.70c	^{113}Cd	48113.70c
^{23}Na	11023.70c	^{56}Fe	26056.70c	^{114}Cd	48114.70c
^{24}Mg	12024.70c	^{57}Fe	26057.70c	^{116}Cd	48116.70c
^{25}Mg	12025.70c	^{58}Fe	26058.70c	^{113}In	49113.70c
^{26}Mg	12026.70c	^{59}Co	27059.70c	^{115}In	49115.70c
^{27}Al	13027.70c	^{58}Ni	28058.70c	^{112}Sn	50112.70c
^{28}Si	14028.70c	^{60}Ni	28060.70c	^{114}Sn	50114.70c
^{29}Si	14029.70c	^{61}Ni	28061.70c	^{115}Sn	50115.70c
^{30}Si	14030.70c	^{62}Ni	28062.70c	^{116}Sn	50116.70c
^{31}P	15031.70c	^{64}Ni	28064.70c	^{117}Sn	50117.70c
^{32}S	16032.70c	^{63}Cu	29063.70c	^{118}Sn	50118.70c
^{36}Ar	18036.70c	^{65}Cu	29065.70c	^{119}Sn	50119.70c
^{38}Ar	18038.70c	Zn	30000.70c	^{120}Sn	50120.70c
^{40}Ar	18040.70c	^{90}Zr	40090.70c	^{122}Sn	50122.70c
^{39}K	19039.70c	^{91}Zr	40091.70c	^{124}Sn	50124.70c
^{40}K	19040.70c	^{92}Zr	40092.70c	^{144}Sm	62144.70c
^{41}K	19041.70c	^{94}Zr	40094.70c	^{147}Sm	62147.70c
^{40}Ca	20040.70c	^{96}Zr	40096.70c	^{148}Sm	62148.70c
^{42}Ca	20042.70c	^{93}Nb	41093.70c	^{149}Sm	62149.70c
^{43}Ca	20043.70c	^{92}Mo	42092.70c	^{150}Sm	62150.70c
^{44}Ca	20044.70c	^{94}Mo	42094.70c	^{152}Sm	62152.70c
^{46}Ca	20046.70c	^{95}Mo	42095.70c	^{154}Sm	62154.70c
^{48}Ca	20048.70c	^{96}Mo	42096.70c	^{152}Gd	64152.70c
^{46}Ti	22046.70c	^{97}Mo	42097.70c	^{154}Gd	64154.70c
^{47}Ti	22047.70c	^{98}Mo	42098.70c	^{155}Gd	64155.70c

Nuclide	MCNP5.1.51 ZAID	Nuclide	MCNP5.1.51 ZAID	Nuclide	MCNP5.1.51 ZAID
^{156}Gd	64156.70c	^{179}Hf	72179.70c	^{236}U	92236.70c
^{157}Gd	64157.70c	^{180}Hf	72180.70c	^{238}U	92238.70c
^{158}Gd	64158.70c	^{204}Pb	82204.70c	^{238}Pu	94238.70c
^{160}Gd	64160.70c	^{206}Pb	82206.70c	^{239}Pu	94239.70c
^{174}Hf	72174.70c	^{207}Pb	82207.70c	^{240}Pu	94240.70c
^{176}Hf	72176.70c	^{208}Pb	82208.70c	^{241}Pu	94241.70c
^{177}Hf	72177.70c	^{234}U	92234.70c	^{242}Pu	94242.70c
^{178}Hf	72178.70c	^{235}U	92235.70c	^{241}Am	95241.70c

Table D.3-1 The MCNP5-1.51 Calculational Results and Measurements Uncertainties for Phase 1 Critical Experiments: Water-Moderated and Reflected Arrays

Case	Evaluation Identification	File-name	k_{eff-i}	$\pm \sigma_{calc-i}$	$\pm \sigma_{exp}$	$\pm \sigma_i$	EALF (eV)
1	MIX-COMP-THERM-HTC-001	[redacted]	[redacted]	[redacted]	[redacted]	[redacted]	[redacted]
2	MIX-COMP-THERM-HTC-002	[redacted]	[redacted]	[redacted]	[redacted]	[redacted]	[redacted]
3	MIX-COMP-THERM-HTC-003	[redacted]	[redacted]	[redacted]	[redacted]	[redacted]	[redacted]
4	MIX-COMP-THERM-HTC-004	[redacted]	[redacted]	[redacted]	[redacted]	[redacted]	[redacted]
5	MIX-COMP-THERM-HTC-005	[redacted]	[redacted]	[redacted]	[redacted]	[redacted]	[redacted]
6	MIX-COMP-THERM-HTC-006	[redacted]	[redacted]	[redacted]	[redacted]	[redacted]	[redacted]
7	MIX-COMP-THERM-HTC-007	[redacted]	[redacted]	[redacted]	[redacted]	[redacted]	[redacted]
8	MIX-COMP-THERM-HTC-008	[redacted]	[redacted]	[redacted]	[redacted]	[redacted]	[redacted]
9	MIX-COMP-THERM-HTC-009	[redacted]	[redacted]	[redacted]	[redacted]	[redacted]	[redacted]
10	MIX-COMP-THERM-HTC-010	[redacted]	[redacted]	[redacted]	[redacted]	[redacted]	[redacted]
11	MIX-COMP-THERM-HTC-011	[redacted]	[redacted]	[redacted]	[redacted]	[redacted]	[redacted]
12	MIX-COMP-THERM-HTC-012	[redacted]	[redacted]	[redacted]	[redacted]	[redacted]	[redacted]
13	MIX-COMP-THERM-HTC-013	[redacted]	[redacted]	[redacted]	[redacted]	[redacted]	[redacted]
14	MIX-COMP-THERM-HTC-014	[redacted]	[redacted]	[redacted]	[redacted]	[redacted]	[redacted]
15	MIX-COMP-THERM-HTC-015	[redacted]	[redacted]	[redacted]	[redacted]	[redacted]	[redacted]
16	MIX-COMP-THERM-HTC-016	[redacted]	[redacted]	[redacted]	[redacted]	[redacted]	[redacted]
17	MIX-COMP-THERM-HTC-017	[redacted]	[redacted]	[redacted]	[redacted]	[redacted]	[redacted]
18	MIX-COMP-THERM-HTC-018	[redacted]	[redacted]	[redacted]	[redacted]	[redacted]	[redacted]

Table D.3-2 The MCNP5-1.51 Calculational Results and Measurements Uncertainties for Phase 2 Critical Experiments: Reflected Simple Arrays Moderated by Poisoned Water with Gadolinium or Boron

Case	Evaluation Identification	File-name	k_{eff-i}	$\pm \sigma_{calc-i}$	$\pm \sigma_{exp}$	$\pm \sigma_i$	EALF (eV)
19	MIX-COMP-THERM-HTC-019						
20	MIX-COMP-THERM-HTC-020						
21	MIX-COMP-THERM-HTC-021						
22	MIX-COMP-THERM-HTC-022						
23	MIX-COMP-THERM-HTC-023						
24	MIX-COMP-THERM-HTC-024						
25	MIX-COMP-THERM-HTC-025						
26	MIX-COMP-THERM-HTC-026						
27	MIX-COMP-THERM-HTC-027						
28	MIX-COMP-THERM-HTC-028						
29	MIX-COMP-THERM-HTC-029						
30	MIX-COMP-THERM-HTC-030						
31	MIX-COMP-THERM-HTC-031						
32	MIX-COMP-THERM-HTC-032						
33	MIX-COMP-THERM-HTC-033						
34	MIX-COMP-THERM-HTC-034						
35	MIX-COMP-THERM-HTC-035						
36	MIX-COMP-THERM-HTC-036						
37	MIX-COMP-THERM-HTC-037						
38	MIX-COMP-THERM-HTC-038						
39	MIX-COMP-THERM-HTC-039						
40	MIX-COMP-THERM-HTC-040						
41	MIX-COMP-THERM-HTC-041						
42	MIX-COMP-THERM-HTC-042						
43	MIX-COMP-THERM-HTC-043						
44	MIX-COMP-THERM-HTC-044						
45	MIX-COMP-THERM-HTC-045						
46	MIX-COMP-THERM-HTC-046						
47	MIX-COMP-THERM-HTC-047						
48	MIX-COMP-THERM-HTC-048						
49	MIX-COMP-THERM-HTC-049						
50	MIX-COMP-THERM-HTC-050						
51	MIX-COMP-THERM-HTC-051						
52	MIX-COMP-THERM-HTC-052						
53	MIX-COMP-THERM-HTC-053						
54	MIX-COMP-THERM-HTC-054						
55	MIX-COMP-THERM-HTC-055						

Case	Evaluation Identification	File-name	k_{eff-i}	$\pm \sigma_{calc-i}$	$\pm \sigma_{exp}$	$\pm \sigma_i$	EALF (eV)
56	MIX-COMP-THERM-HTC-056	[redacted]	[redacted]	[redacted]	[redacted]	[redacted]	[redacted]
57	MIX-COMP-THERM-HTC-057	[redacted]	[redacted]	[redacted]	[redacted]	[redacted]	[redacted]
58	MIX-COMP-THERM-HTC-058	[redacted]	[redacted]	[redacted]	[redacted]	[redacted]	[redacted]
59	MIX-COMP-THERM-HTC-059	[redacted]	[redacted]	[redacted]	[redacted]	[redacted]	[redacted]

Table D.3-3 The MCNP5-1.51 Calculational Results and Measurements Uncertainties for Phase 3 Critical Experiments: Pool Storage

Case	Evaluation Identification	File-name	k_{eff-i}	$\pm \sigma_{calc-i}$	$\pm \sigma_{exp}$	$\pm \sigma_i$	EALF (eV)
60	MIX-COMP-THERM-HTC-060	[redacted]	[redacted]	[redacted]	[redacted]	[redacted]	[redacted]
61	MIX-COMP-THERM-HTC-061	[redacted]	[redacted]	[redacted]	[redacted]	[redacted]	[redacted]
62	MIX-COMP-THERM-HTC-062	[redacted]	[redacted]	[redacted]	[redacted]	[redacted]	[redacted]
63	MIX-COMP-THERM-HTC-063	[redacted]	[redacted]	[redacted]	[redacted]	[redacted]	[redacted]
64	MIX-COMP-THERM-HTC-064	[redacted]	[redacted]	[redacted]	[redacted]	[redacted]	[redacted]
65	MIX-COMP-THERM-HTC-065	[redacted]	[redacted]	[redacted]	[redacted]	[redacted]	[redacted]
66	MIX-COMP-THERM-HTC-066	[redacted]	[redacted]	[redacted]	[redacted]	[redacted]	[redacted]
67	MIX-COMP-THERM-HTC-067	[redacted]	[redacted]	[redacted]	[redacted]	[redacted]	[redacted]
68	MIX-COMP-THERM-HTC-068	[redacted]	[redacted]	[redacted]	[redacted]	[redacted]	[redacted]
69	MIX-COMP-THERM-HTC-069	[redacted]	[redacted]	[redacted]	[redacted]	[redacted]	[redacted]
70	MIX-COMP-THERM-HTC-070	[redacted]	[redacted]	[redacted]	[redacted]	[redacted]	[redacted]
71	MIX-COMP-THERM-HTC-071	[redacted]	[redacted]	[redacted]	[redacted]	[redacted]	[redacted]
72	MIX-COMP-THERM-HTC-072	[redacted]	[redacted]	[redacted]	[redacted]	[redacted]	[redacted]
73	MIX-COMP-THERM-HTC-073	[redacted]	[redacted]	[redacted]	[redacted]	[redacted]	[redacted]
74	MIX-COMP-THERM-HTC-074	[redacted]	[redacted]	[redacted]	[redacted]	[redacted]	[redacted]
75	MIX-COMP-THERM-HTC-075	[redacted]	[redacted]	[redacted]	[redacted]	[redacted]	[redacted]
76	MIX-COMP-THERM-HTC-076	[redacted]	[redacted]	[redacted]	[redacted]	[redacted]	[redacted]
77	MIX-COMP-THERM-HTC-077	[redacted]	[redacted]	[redacted]	[redacted]	[redacted]	[redacted]
78	MIX-COMP-THERM-HTC-078	[redacted]	[redacted]	[redacted]	[redacted]	[redacted]	[redacted]
79	MIX-COMP-THERM-HTC-079	[redacted]	[redacted]	[redacted]	[redacted]	[redacted]	[redacted]
80	MIX-COMP-THERM-HTC-080	[redacted]	[redacted]	[redacted]	[redacted]	[redacted]	[redacted]
81	MIX-COMP-THERM-HTC-081	[redacted]	[redacted]	[redacted]	[redacted]	[redacted]	[redacted]
82	MIX-COMP-THERM-HTC-082	[redacted]	[redacted]	[redacted]	[redacted]	[redacted]	[redacted]
83	MIX-COMP-THERM-HTC-083	[redacted]	[redacted]	[redacted]	[redacted]	[redacted]	[redacted]
84	MIX-COMP-THERM-HTC-084	[redacted]	[redacted]	[redacted]	[redacted]	[redacted]	[redacted]
85	MIX-COMP-THERM-HTC-085	[redacted]	[redacted]	[redacted]	[redacted]	[redacted]	[redacted]

Table D.3-4 The MCNP5-1.51 Calculational Results and Measurements Uncertainties for Phase 4 Critical Experiments: Shipping Cask

Case	Evaluation Identification	File-name	k_{eff-i}	$\pm \sigma_{calc-i}$	$\pm \sigma_{exp}$	$\pm \sigma_i$	EALF (eV)
86	MIX-COMP-THERM-HTC-086						
87	MIX-COMP-THERM-HTC-087						
88	MIX-COMP-THERM-HTC-088						
89	MIX-COMP-THERM-HTC-089						
90	MIX-COMP-THERM-HTC-090						
91	MIX-COMP-THERM-HTC-091						
92	MIX-COMP-THERM-HTC-092						
93	MIX-COMP-THERM-HTC-093						
94	MIX-COMP-THERM-HTC-094						
95	MIX-COMP-THERM-HTC-095						
96	MIX-COMP-THERM-HTC-096						
97	MIX-COMP-THERM-HTC-097						
98	MIX-COMP-THERM-HTC-098						
99	MIX-COMP-THERM-HTC-099						
100	MIX-COMP-THERM-HTC-100						
101	MIX-COMP-THERM-HTC-101						
102	MIX-COMP-THERM-HTC-102						
103	MIX-COMP-THERM-HTC-103						
104	MIX-COMP-THERM-HTC-104						
105	MIX-COMP-THERM-HTC-105						
106	MIX-COMP-THERM-HTC-106						
107	MIX-COMP-THERM-HTC-107						
108	MIX-COMP-THERM-HTC-108						
109	MIX-COMP-THERM-HTC-109						
110	MIX-COMP-THERM-HTC-110						
111	MIX-COMP-THERM-HTC-111						
112	MIX-COMP-THERM-HTC-112						
113	MIX-COMP-THERM-HTC-113						
114	MIX-COMP-THERM-HTC-114						
115	MIX-COMP-THERM-HTC-115						
116	MIX-COMP-THERM-HTC-116						
117	MIX-COMP-THERM-HTC-117						
118	MIX-COMP-THERM-HTC-118						
119	MIX-COMP-THERM-HTC-119						
120	MIX-COMP-THERM-HTC-120						
121	MIX-COMP-THERM-HTC-121						
122	MIX-COMP-THERM-HTC-122						
123	MIX-COMP-THERM-HTC-123						

Case	Evaluation Identification	File-name	k_{eff-i}	$\pm \sigma_{calc-i}$	$\pm \sigma_{exp}$	$\pm \sigma_i$	EALF (eV)
124	MIX-COMP-THERM-HTC-124						
125	MIX-COMP-THERM-HTC-125						
126	MIX-COMP-THERM-HTC-126						
127	MIX-COMP-THERM-HTC-127						
128	MIX-COMP-THERM-HTC-128						
129	MIX-COMP-THERM-HTC-129						
130	MIX-COMP-THERM-HTC-130						
131	MIX-COMP-THERM-HTC-131						
132	MIX-COMP-THERM-HTC-132						
133	MIX-COMP-THERM-HTC-133						
134	MIX-COMP-THERM-HTC-134						
135	MIX-COMP-THERM-HTC-135						
136	MIX-COMP-THERM-HTC-136						
137	MIX-COMP-THERM-HTC-137						
138	MIX-COMP-THERM-HTC-138						
139	MIX-COMP-THERM-HTC-139						
140	MIX-COMP-THERM-HTC-140						
141	MIX-COMP-THERM-HTC-141						
142	MIX-COMP-THERM-HTC-142						
143	MIX-COMP-THERM-HTC-143						
144	MIX-COMP-THERM-HTC-144						
145	MIX-COMP-THERM-HTC-145						
146	MIX-COMP-THERM-HTC-146						
147	MIX-COMP-THERM-HTC-147						
148	MIX-COMP-THERM-HTC-148						
149	MIX-COMP-THERM-HTC-149						
150	MIX-COMP-THERM-HTC-150						
151	MIX-COMP-THERM-HTC-151						
152	MIX-COMP-THERM-HTC-152						
153	MIX-COMP-THERM-HTC-153						
154	MIX-COMP-THERM-HTC-154						
155	MIX-COMP-THERM-HTC-155						
156	MIX-COMP-THERM-HTC-156						

Table D.3-5 The MCNP5-1.51 Calculational Results and Measurements Uncertainties for Selected Critical Experiments

Case	Evaluation Identification	File-name	k_{eff-i}	$\pm \sigma_{calc-i}$	$\pm \sigma_{exp}$	$\pm \sigma_i$	EALF (eV)
157	Core I						
158	Core II						
159	Core III						
160	Core IX						
161	Core X						
162	Core XI						
163	Core XII						
164	Core XIII						
165	Core XIV						
166	Core XV						
167	Core XVI						
168	Core XVII						
169	Core XVIII						
170	Core XIX						
171	Core XX						
172	Core XXI						
173	S-type Fuel, w/886 ppm B						
174	S-type Fuel, w/746 ppm B						
175	SO-type Fuel, w/1156 ppm B						
176	Case 1 1337 ppm B						
177	Case 12 1899 ppm B						
178	Water Moderator 0 gap						
179	Water Moderator 2.5 cm gap						
180	Water Moderator 5 cm gap						
181	Water Moderator 10 cm gap						
182	Steel Reflector, 1.321 cm separation						
183	Steel Reflector, 2.616 cm separation						
184	Steel Reflector, 3.912 cm separation						
185	Steel Reflector, Infinite separation						
186	Steel Reflector, 1.321 cm separation						
187	Steel Reflector, 2.616 cm separation						
188	Steel Reflector, 5.405 cm separation						
189	Steel Reflector, Infinite separation						
190	Steel Reflector, with Boral Sheets						
191	Lead Reflector, 0.55 cm sepn.						
192	Lead Reflector, 1.956 cm sepn.						
193	Lead Reflector, 5.405 cm sepn.						
194	Experiment 004/032 – no absorber						

Case	Evaluation Identification	File-name	k_{eff-i}	$\pm \sigma_{calc-i}$	$\pm \sigma_{exp}$	$\pm \sigma_i$	EALF (eV)
195	Exp. 009 1.05% Boron Steel plates						
196	Exp. 009 1.62% Boron Steel plates						
197	Exp. 031 – Boral plates						
198	Experiment 214R – with flux traps						
199	Experiment 214V3 –with flux trap						
200	Case 173 – 0 ppm B						
201	Case 177 – 2550 ppm B						
202	MOX Fuel – Type 3.2 Exp. 21						
203	MOX Fuel – Type 3.2 Exp. 43						
204	MOX Fuel – Type 3.2 Exp. 13						
205	MOX Fuel – Type 3.2 Exp. 32						
206	Saxton Case 52 PuO2 0.52" pitch						
207	Saxton Case 52 U 0.52" pitch						
208	Saxton Case 56 PuO2 0.56" pitch						
209	Saxton Case 56 borated PuO2						
210	Saxton Case 56 U 0.56" pitch						
211	Saxton Case 79 PuO2 0.79" pitch						
212	Saxton Case 79 U 0.79" pitch						
213	0.700-in. pitch 0 ppm B						
214	0.700-in. pitch 688 ppm B						
215	0.870-in. pitch 0 ppm B						
216	0.870-in. pitch 1090 ppm B						
217	0.990-in. pitch 0 ppm B						
218	0.990-in. pitch 767 ppm B						
219	Saxton Case PuO2 0.735" pitch						
220	Saxton Case PuO2 1.04" pitch						
221	8 wt% 240Pu 0.80" pitch						
222	8 wt% 240Pu 0.93" pitch						
223	8 wt% 240Pu 1.05" pitch						
224	8 wt% 240Pu 1.143" pitch						
225	8 wt% 240Pu 1.32" pitch						
226	8 wt% 240Pu 1.386" pitch						
227	16 wt% 240Pu 0.93" pitch						
228	16 wt% 240Pu 1.05" pitch						
229	16 wt% 240Pu 1.143" pitch						
230	16 wt% 240Pu 1.32" pitch						
231	24 wt% 240Pu 0.80" pitch						
232	24 wt% 240Pu 0.93" pitch						
233	24 wt% 240Pu 1.05" pitch						
234	24 wt% 240Pu 1.143" pitch						

Case	Evaluation Identification	File-name	k_{eff-i}	$\pm \sigma_{calc-i}$	$\pm \sigma_{exp}$	$\pm \sigma_i$	EALF (eV)
235	24 wt% 240Pu 1.32" pitch						
236	24 wt% 240Pu 1.386" pitch						
237	18 wt% 240Pu 0.85" pitch						
238	18 wt% 240Pu 0.93" pitch						
239	18 wt% 240Pu 1.05" pitch						
240	18 wt% 240Pu 1.143" pitch						
241	18 wt% 240Pu 1.386" pitch						
242	18 wt% 240Pu 1.60" pitch						
243	18 wt% 240Pu 1.70" pitch						
244	1 Cluster						
245	3 Clusters, Separation 11.92 cm						
246	3 Clusters, Separation 8.41 cm						
247	3 Clusters, Separation 10.05 cm						
248	3 Clusters, Separation 6.39 cm						
249	3 Clusters, Separation 9.01 cm						
250	3 Clusters, Separation 4.46						
251	1 Cluster, 10x11.51						
252	1 Cluster, 9x13.35						
253	1 Cluster, 8x16.37						
254	3 Clusters, Separation 7.11 cm						
255	1 Cluster, 614.4 Rods, Gd water impurity						
256	1 Cluster, 529.3 Rods						
257	1 Cluster, 523.9 Rods						
258	1 Cluster, 525.3 Rods						
259	1 Cluster, 595.4 Rods						
260	1 Cluster, 485.8 Rods						
261	1 Cluster, 523.8 Rods						
262	1 Cluster, 505.4 Rods						
263	4 Clusters, Separation 2.59 cm						
264	2 Clusters, Separation 1.68 cm						
265	4 Clusters, Separation 4.27 cm						
266	4 Clusters, Separation 5.95 cm						
267	4 Clusters, Separation 5.11 cm						
268	4 Clusters, Separation 6.66 cm						
269	4 Clusters, Separation 7.53 cm						
270	4 Clusters, Separation 9.00 cm						
271	4 Clusters, Separation 9.97 cm						
272	4 Clusters, Separation 11.45 cm						
273	4 Clusters, Separation 13.87 cm						

Case	Evaluation Identification	File-name	k_{eff-i}	$\pm \sigma_{calc-i}$	$\pm \sigma_{exp}$	$\pm \sigma_i$	EALF (eV)
274	3 Clusters, Separation 9.88 cm						
275	3 Clusters, Separation 6.78 cm						
276	3 Clusters, Separation 6.176 cm						
277	1 Cluster, 225.8 Rods, Gd water impurity						
278	1 Cluster, 216.2 Rods						
279	1 Cluster, 216.6 Rods						
280	1 Cluster, 218.6 Rods						
281	1 Cluster, 167.85 Rods						
282	1 Cluster, 203 Rods						
283	1 Cluster, 173.5 Rods						
284	2 Clusters, Separation 2.83 cm						
285	3 Clusters, Separation 12.27 cm						
286	3 Clusters, Separation 12.493 cm						
287	4 Clusters, Separation 4.72 cm						
288	4 Clusters, Separation 8.38 cm						
289	4 Clusters, Separation 10.86 cm						
290	4 Clusters, Separation 11.29 cm						
291	4 Clusters, Separation 12.02 cm						
292	4 Clusters, Separation 13.64 cm						
293	4 Clusters, Separation 14.98 cm						
294	4 Clusters, Separation 19.81 cm						
295	4 Clusters, Separation 8.50 cm						
296	19x19, Rod Pitch - 1.849 cm						
297	20x20, Rod Pitch - 1.849 cm						
298	21x21, Rod Pitch - 1.849 cm						
299	17x17, Rod Pitch - 1.956 cm						
300	18x18, Rod Pitch - 1.956 cm						
301	19x19, Rod Pitch - 1.956 cm						
302	20x20, Rod Pitch - 1.956 cm						
303	21x21, Rod Pitch - 1.956 cm						
304	16x16, Rod Pitch - 2.15 cm						
305	17x17, Rod Pitch - 2.15 cm						
306	18x18, Rod Pitch - 2.15 cm						
307	19x19, Rod Pitch - 2.15 cm						
308	20x20, Rod Pitch - 2.15 cm						
309	15x15, Rod Pitch - 2.293 cm						
310	16x16, Rod Pitch - 2.293 cm						
311	17x17, Rod Pitch - 2.293 cm						
312	18x18, Rod Pitch - 2.293 cm						

Case	Evaluation Identification	File-name	k_{eff-i}	$\pm \sigma_{calc-i}$	$\pm \sigma_{exp}$	$\pm \sigma_i$	EALF (eV)
313	19x19, Rod Pitch - 2.293 cm						
314	Core XI, 1511 ppm						
315	Core XI, 1335.5 ppm						
316	Core XI, 1335.5 ppm						
317	Core XI, 1182 ppm, 36 Pyrex Rods						
318	Core XI, 1182 ppm, 36 Pyrex Rods						
319	Core XI, 1032.5 ppm, 72 Pyrex Rods						
320	Core XI, 1032.5 ppm, 72 Pyrex Rods						
321	Core XI, 794 ppm, 144 Pyrex Rods						
322	Core XI, 779 ppm, 144 Pyrex Rods						
323	Core XI, 1245 ppm, 72 Vicor Rods						
324	Core XI, 1384 ppm, 144 Al_2O_3 Rods						
325	Core XI, 1348 ppm, 36 Al2O3 Rods						
326	Core XI, 1348 ppm, 36 Al2O3 Rods						
327	Core XI, 1363 ppm, 72 Al2O3 Rods						
328	Core XI, 1362 ppm, 72 Al2O3 Rods						
329	Core XI, 1158 ppm						
330	Core XI, 921 ppm						
331	0% Boron Steel plates, dist. 0.245 cm						
332	0% Boron Steel plates, dist. 3.277 cm						
333	0% Boron Steel plates, dist. 0.428 cm						
334	0% Boron Steel plates, dist. 3.277 cm						
335	1.05% Boron Steel plates, dist. 3.277 cm						
336	1.62% Boron Steel plates, dist. 3.277 cm						
337	Al plates, dist. 0.105 cm						
338	Al plates, dist. 3.277 cm						
339	Zircaloy-4 plates, dist. 0.078 cm						
340	Zircaloy-4 plates, dist. 3.277 cm						
341	Lead Reflector, 0 cm separation						
342	Lead Reflector, 0.660 cm separation						
343	Lead Reflector, 1.321 cm separation						
344	Lead Reflector, 5.405 cm separation						
345	Steel Reflector, 0 cm separation						
346	Steel Reflector, 0.660 cm separation						
347	Steel Reflector, 1.321 cm separation						
348	Steel Reflector, 2.616 cm separation						
349	Steel Reflector, 5.405 cm separation						
350	Steel Reflector, 0 cm separation						

Case	Evaluation Identification	File-name	k_{eff-i}	$\pm \sigma_{calc-i}$	$\pm \sigma_{exp}$	$\pm \sigma_i$	EALF (eV)
351	Steel Reflector, 0.660 cm separation						
352	Steel Reflector, 1.956 cm separation						
353	Lead Reflector, 0 cm separation						
354	Core IIIA						
355	Core IIIC						
356	Core IIID						
357	Core IIIE						
358	Core IIIF						
359	Core IIIG						
360	Core IV						
361	Core V						
362	Core VI						
363	Core VII						
364	Core VIII						
365	0% Boron Steel plate, Gd water impurity						
366	1.1% Boron Steel plate						
367	1.6% Boron Steel plate						
368	Boral B plate						
369	Boral C plate						
370	Boroflex, 1.84 cm separation						
371	Boroflex, 1.73 cm separation						
372	Steel Reflector, 0% Boron Steel plate						
373	Steel Reflector, 1.1% Boron Steel plate						
374	Steel Reflector, Boroflex, 8.37 cm separation						
375	Borated Water, 490 ppm						
376	Unborated Water						
377	Borated Water, 1030 ppm						
378	0% Boron Steel plates, dist. 0.645 cm						
379	0% Boron Steel plates, dist. 2.732 cm						
380	0% Boron Steel plates, dist. 4.042 cm						
381	0% Boron Steel plates, dist. 0.645 cm						
382	0% Boron Steel plates, dist. 4.042 cm						
383	0% Boron Steel plates, dist. 0.645 cm						
384	0% Boron Steel plates, dist. 4.042 cm						
385	1.05% Boron Steel plates, dist. 0.645 cm						
386	1.05% Boron Steel plates, dist. 4.042 cm						

Case	Evaluation Identification	File-name	k_{eff-i}	$\pm \sigma_{calc-i}$	$\pm \sigma_{exp}$	$\pm \sigma_i$	EALF (eV)
387	1.62% Boron Steel plates, dist. 0.645 cm						
388	1.62% Boron Steel plates, dist. 4.042 cm						
389	Boral plates, dist. 0.645 cm						
390	Boral plates, dist. 4.442 cm						
391	Boral plates, dist. 0.645 cm						
392	Al plates, dist. 0.645 cm						
393	Al plates, dist. 4.042 cm						
394	Al plates, dist. 4.442 cm						
395	Zircaloy-4 plates, dist. 0.645 cm						
396	Zircaloy-4 plates, dist. 4.042 cm						
397	Hex, 621 Rods, Temperature 20.1C						
398	Hex, 889 Rods, Temperature 231.4C						
399	Hex, 1951 Rods, Temperature 19.3C						
400	Hex, 2791 Rods, Temperature 206.0C						
401	Hex, 325/680 Rods, Temperature 20.8C						
402	Hex, 325/912 Rods, Temperature 212.1C						
403	Core XIA						
404	Core XIC						
405	Core XID						
406	Core XIE						
407	Core XIF						
408	Core XIG						
409	Core XIIIA						
410	No Boron Steel plates						
411	0% Boron Steel plates, 3 mm, dist. 0						
412	0% Boron Steel plates, 6 mm, dist. 0						
413	0% Boron Steel plates, 6 mm, dist. 0.5						
414	0% Boron Steel plates, 6 mm, dist. 1						
415	0.67% Boron Steel plates, 3 mm, dist. 0						
416	0.67% Boron Steel plates, 6 mm, dist. 0						
417	0.67% Boron Steel plates, 3 mm, dist. 0.5						
418	0.67% Boron Steel plates, 6 mm, dist. 0.5						
419	0.67% Boron Steel plates, 3 mm, dist. 1						
420	0.67% Boron Steel plates, 6 mm, dist.						

Case	Evaluation Identification	File-name	k_{eff-i}	$\pm \sigma_{calc-i}$	$\pm \sigma_{exp}$	$\pm \sigma_i$	EALF (eV)
	1						
421	0.98% Boron Steel plates, 3 mm, dist. 0	[redacted]	[redacted]	[redacted]	[redacted]	[redacted]	[redacted]
422	0.98% Boron Steel plates, 6 mm, dist. 0	[redacted]	[redacted]	[redacted]	[redacted]	[redacted]	[redacted]
423	0.98% Boron Steel plates, 6 mm, dist. 0.5	[redacted]	[redacted]	[redacted]	[redacted]	[redacted]	[redacted]
424	0.98% Boron Steel plates, 6 mm, dist. 1	[redacted]	[redacted]	[redacted]	[redacted]	[redacted]	[redacted]
425	No Boron Steel plates	[redacted]	[redacted]	[redacted]	[redacted]	[redacted]	[redacted]
426	0% Boron Steel plates, dist. 0	[redacted]	[redacted]	[redacted]	[redacted]	[redacted]	[redacted]
427	0.67% Boron Steel plates, dist. 0	[redacted]	[redacted]	[redacted]	[redacted]	[redacted]	[redacted]
428	0.98% Boron Steel plates, dist. 0	[redacted]	[redacted]	[redacted]	[redacted]	[redacted]	[redacted]
429	No Boron Steel plates	[redacted]	[redacted]	[redacted]	[redacted]	[redacted]	[redacted]
430	0% Boron Steel plates, dist. 0	[redacted]	[redacted]	[redacted]	[redacted]	[redacted]	[redacted]
431	0% Boron Steel plates, dist. 0.5	[redacted]	[redacted]	[redacted]	[redacted]	[redacted]	[redacted]
432	0% Boron Steel plates, dist. 0	[redacted]	[redacted]	[redacted]	[redacted]	[redacted]	[redacted]
433	0% Boron Steel plates, dist. 0.5	[redacted]	[redacted]	[redacted]	[redacted]	[redacted]	[redacted]
434	0.67% Boron Steel plates, dist. 0	[redacted]	[redacted]	[redacted]	[redacted]	[redacted]	[redacted]
435	0.67% Boron Steel plates, dist. 0.5	[redacted]	[redacted]	[redacted]	[redacted]	[redacted]	[redacted]
436	0.67% Boron Steel plates, dist. 0	[redacted]	[redacted]	[redacted]	[redacted]	[redacted]	[redacted]
437	0.67% Boron Steel plates, dist. 0.5	[redacted]	[redacted]	[redacted]	[redacted]	[redacted]	[redacted]
438	0.98% Boron Steel plates, dist. 0	[redacted]	[redacted]	[redacted]	[redacted]	[redacted]	[redacted]
439	0.98% Boron Steel plates, dist. 0.5	[redacted]	[redacted]	[redacted]	[redacted]	[redacted]	[redacted]
440	0.98% Boron Steel plates, dist. 0	[redacted]	[redacted]	[redacted]	[redacted]	[redacted]	[redacted]
441	0.98% Boron Steel plates, dist. 0.5	[redacted]	[redacted]	[redacted]	[redacted]	[redacted]	[redacted]
442	Otto Hahn, ZrB_2 and B_4C rods	[redacted]	[redacted]	[redacted]	[redacted]	[redacted]	[redacted]
443	IPEN/MB-01 (580 pins)	[redacted]	[redacted]	[redacted]	[redacted]	[redacted]	[redacted]
444	IPEN/MB-01 (560 pins)	[redacted]	[redacted]	[redacted]	[redacted]	[redacted]	[redacted]
445	670 pins, Al_2O_3-B_4C rods	[redacted]	[redacted]	[redacted]	[redacted]	[redacted]	[redacted]
446	672 pins, Al_2O_3-B_4C rods	[redacted]	[redacted]	[redacted]	[redacted]	[redacted]	[redacted]
447	668 pins, Al_2O_3-B_4C rods	[redacted]	[redacted]	[redacted]	[redacted]	[redacted]	[redacted]
448	668 pins, Al_2O_3-B_4C rods	[redacted]	[redacted]	[redacted]	[redacted]	[redacted]	[redacted]
449	664 pins, 16 steel rods	[redacted]	[redacted]	[redacted]	[redacted]	[redacted]	[redacted]
450	662 pins, 18 steel rods	[redacted]	[redacted]	[redacted]	[redacted]	[redacted]	[redacted]
451	658 pins, 14 steel rods	[redacted]	[redacted]	[redacted]	[redacted]	[redacted]	[redacted]
452	660 pins, 12 steel rods	[redacted]	[redacted]	[redacted]	[redacted]	[redacted]	[redacted]
453	660 pins, 12 steel rods	[redacted]	[redacted]	[redacted]	[redacted]	[redacted]	[redacted]
454	661 pins, 17 steel rods	[redacted]	[redacted]	[redacted]	[redacted]	[redacted]	[redacted]
455	662 pins, 16 steel rods	[redacted]	[redacted]	[redacted]	[redacted]	[redacted]	[redacted]
456	634 pins, 12 steel rods	[redacted]	[redacted]	[redacted]	[redacted]	[redacted]	[redacted]

Case	Evaluation Identification	File-name	k_{eff-i}	$\pm \sigma_{calc-i}$	$\pm \sigma_{exp}$	$\pm \sigma_i$	EALF (eV)
457	620 pins, 26 steel rods						
458	668 pins, 0 steel rods, 4 Gd_2O_3 rods						
459	648 pins, 0 steel rods, 8 Gd_2O_3 rods						
460	672 pins, 0 steel rods, 4 Gd_2O_3 rods						
461	646 pins, 4 steel rods, 4 Gd_2O_3 rods						
462	656 pins, 4 steel rods, 4 Gd_2O_3 rods						
463	664 pins, 4 steel rods, 2 Gd_2O_3 rods						
464	670 pins, 2 steel rods, 2 Gd_2O_3 rods						
465	664 pins, 2 steel rods, 2 Gd_2O_3 rods						
466	656 pins, 0 steel rods, 2 Gd_2O_3 rods						
467	23x23, 1.825 cm pitch						
468	23x23, 1.825 cm pitch						
469	23x23, 1.825 cm pitch						
470	21x21, 1.956 cm pitch						
471	21x21, 1.956 cm pitch						
472	21x21, 1.956 cm pitch						
473	20x20, 2.225 cm pitch						
474	20x20, 2.225 cm pitch						
475	20x20, 2.225 cm pitch						
476	21x21, 2.474 cm pitch						
477	21x21, 2.474 cm pitch						
478	8 wt% 240Pu 1.05" pitch, Al Rods						
479	8 wt% 240Pu 1.05" pitch, B4 Rods						
480	8 wt% 240Pu 1.05" pitch, B3 Rods						
481	8 wt% 240Pu 1.05" pitch, B2 Rods						
482	8 wt% 240Pu 1.05" pitch, B1 Rods						
483	8 wt% 240Pu 1.05" pitch, Al+Cd Rods						
484	8 wt% 240Pu 1.05" pitch, B4+Cd Rods						
485	8 wt% 240Pu 1.05" pitch, B3+Cd Rods						
486	8 wt% 240Pu 1.05" pitch, B2+Cd Rods						
487	8 wt% 240Pu 1.05" pitch, B1+Cd Rods						
488	8 wt% 240Pu 1.05" pitch, Air+Cd Rods						
489	8 wt% 240Pu 1.05" pitch, H2O+Cd Rods						
490	8 wt% 240Pu 1.32" pitch, Al Rods						
491	8 wt% 240Pu 1.32" pitch, B4 Rods						

Case	Evaluation Identification	File-name	k_{eff-i}	$\pm \sigma_{calc-i}$	$\pm \sigma_{exp}$	$\pm \sigma_i$	EALF (eV)
492	8 wt% 240Pu 1.32" pitch, B3 Rods						
493	8 wt% 240Pu 1.32" pitch, B2 Rods						
494	8 wt% 240Pu 1.32" pitch, B1 Rods						
495	8 wt% 240Pu 1.32" pitch, Al+Cd Rods						
496	8 wt% 240Pu 1.32" pitch, B4+Cd Rods						
497	8 wt% 240Pu 1.32" pitch, B3+Cd Rods						
498	8 wt% 240Pu 1.32" pitch, B2+Cd Rods						
499	8 wt% 240Pu 1.32" pitch, B1+Cd Rods						
500	8 wt% 240Pu 1.32" pitch, Air+Cd Rods						
501	8 wt% 240Pu 1.32" pitch, H2O+Cd Rods						
502	16 wt% 240Pu 1.386" pitch						
503	16 wt% 240Pu 1.05" pitch, Al Rods						
504	16 wt% 240Pu 1.05" pitch, B4 Rods						
505	16 wt% 240Pu 1.05" pitch, B3 Rods						
506	16 wt% 240Pu 1.05" pitch, B2 Rods						
507	16 wt% 240Pu 1.05" pitch, B1 Rods						
508	16 wt% 240Pu 1.05" pitch, Al+Cd Rods						
509	16 wt% 240Pu 1.05" pitch, B4+Cd Rods						
510	16 wt% 240Pu 1.05" pitch, B3+Cd Rods						
511	16 wt% 240Pu 1.05" pitch, B2+Cd Rods						
512	16 wt% 240Pu 1.05" pitch, B1+Cd Rods						
513	16 wt% 240Pu 1.05" pitch, Air+Cd Rods						
514	16 wt% 240Pu 1.05" pitch, H2O+Cd Rods						
515	24 wt% 240Pu 1.05" pitch, Al Rods						
516	24 wt% 240Pu 1.05" pitch, B4 Rods						
517	24 wt% 240Pu 1.05" pitch, B3 Rods						
518	24 wt% 240Pu 1.05" pitch, B2 Rods						
519	24 wt% 240Pu 1.05" pitch, B1 Rods						
520	24 wt% 240Pu 1.05" pitch, Al+Cd Rods						
521	24 wt% 240Pu 1.05" pitch, B4+Cd						

Case	Evaluation Identification	File-name	k_{eff-i}	$\pm \sigma_{calc-i}$	$\pm \sigma_{exp}$	$\pm \sigma_i$	EALF (eV)
	Rods						
522	24 wt% 240Pu 1.05" pitch, B3+Cd Rods	[redacted]	[redacted]	[redacted]	[redacted]	[redacted]	[redacted]
523	24 wt% 240Pu 1.05" pitch, B2+Cd Rods	[redacted]	[redacted]	[redacted]	[redacted]	[redacted]	[redacted]
524	24 wt% 240Pu 1.05" pitch, B1+Cd Rods	[redacted]	[redacted]	[redacted]	[redacted]	[redacted]	[redacted]
525	24 wt% 240Pu 1.05" pitch, Air+Cd Rods	[redacted]	[redacted]	[redacted]	[redacted]	[redacted]	[redacted]
526	24 wt% 240Pu 1.05" pitch, H2O+Cd Rods	[redacted]	[redacted]	[redacted]	[redacted]	[redacted]	[redacted]
527	8 wt% 240Pu 0.55" pitch	[redacted]	[redacted]	[redacted]	[redacted]	[redacted]	[redacted]
528	8 wt% 240Pu 0.60" pitch	[redacted]	[redacted]	[redacted]	[redacted]	[redacted]	[redacted]
529	8 wt% 240Pu 0.71" pitch	[redacted]	[redacted]	[redacted]	[redacted]	[redacted]	[redacted]
530	8 wt% 240Pu 0.80" pitch	[redacted]	[redacted]	[redacted]	[redacted]	[redacted]	[redacted]
531	8 wt% 240Pu 0.90" pitch	[redacted]	[redacted]	[redacted]	[redacted]	[redacted]	[redacted]
532	8 wt% 240Pu 0.93" pitch	[redacted]	[redacted]	[redacted]	[redacted]	[redacted]	[redacted]

Table D.3-6 Descriptive Statistics of the MCNP5-1.51 Calculational Results

Experiment Description	No. of exp.	k_{eff} range	EALF (eV) range
HTC Experiments	156	[redacted]	[redacted]
Selected Experiments	376	[redacted]	[redacted]
All experiments	532	[redacted]	[redacted]

Table D.3-7 Normality Test Results for the MCNP5-1.51 calculations

Experiment Description	No. of exp.	Shapiro-Wilk		Pearson's chi-square (χ^2)			
		Wtest	W	χ^2	n	$P_d(\chi^2;d)$	Normal
HTC Experiments	156	N/A	N/A	[redacted]	[redacted]	[redacted]	[redacted]
Selected Experiments	376	N/A	N/A	[redacted]	[redacted]	[redacted]	[redacted]
All experiments	532	N/A	N/A	[redacted]	[redacted]	[redacted]	[redacted]

Table D.3-8 Trending Analysis Results for the MCNP5-1.51 calculations

Experiment Description	No. of exp.	Correlated Parameter, x	Correlation Coefficient, r^2	Probability, Pd(N;r)	Correlation	Regression Equation, k(x)
All experiments	532	EALF	[redacted]	[redacted]	[redacted]	[redacted]
		Pitch	[redacted]	[redacted]	[redacted]	[redacted]
		Rod OD	[redacted]	[redacted]	[redacted]	[redacted]
		Fuel Density	[redacted]	[redacted]	[redacted]	[redacted]

Table D.3-9 Analysis of Neutron Absorbers and Reflector Materials for the MCNP5-1.51 calculations

Experiment Description	No. of exp.	Bias	Bias Uncertainty	Normality χ^2 ($P_d(\chi^2;d)$)	Linear Correlation	Residuals Normality, ($P_d(\chi^2;d)$)
All experiments	532					
All except those with Gadolinium, Cadmium and Lead	365					

Table D.3-10 Bias and Bias Uncertainty as a Function of Independent Parameter

Experiment Description	Independent Parameter, x	Calculated k_{eff}	Bias	Bias Uncertainty
All except those with Gadolinium, Cadmium and Lead	EALF			
	[redacted]	[redacted]	[redacted]	[redacted]
	[redacted]	[redacted]	[redacted]	[redacted]
	[redacted]	[redacted]	[redacted]	[redacted]
	[redacted]	[redacted]	[redacted]	[redacted]
	[redacted]	[redacted]	[redacted]	[redacted]
	[redacted]	[redacted]	[redacted]	[redacted]
	[redacted]	[redacted]	[redacted]	[redacted]
	[redacted]	[redacted]	[redacted]	[redacted]
	[redacted]	[redacted]	[redacted]	[redacted]
	[redacted]	[redacted]	[redacted]	[redacted]
	[redacted]	[redacted]	[redacted]	[redacted]
	[redacted]	[redacted]	[redacted]	[redacted]
	[redacted]	[redacted]	[redacted]	[redacted]
	[redacted]	[redacted]	[redacted]	[redacted]
	[redacted]	[redacted]	[redacted]	[redacted]
	[redacted]	[redacted]	[redacted]	[redacted]
	[redacted]	[redacted]	[redacted]	[redacted]
	[redacted]	[redacted]	[redacted]	[redacted]
	[redacted]	[redacted]	[redacted]	[redacted]
	[redacted]	[redacted]	[redacted]	[redacted]
	[redacted]	[redacted]	[redacted]	[redacted]

Table D.3-11 Analysis of Fuel Burnup for the MCNP5-1.51 calculations

Experiment Description	No. of exp.	Bias	Bias Uncertainty	Normality χ^2 ($P_d(\chi^2;d)$)	Linear Correlation	Residuals Normality, ($P_d(\chi^2;d)$)
All except those with Gadolinium, Cadmium and Lead[†]	365					
Fresh UO_2 Fuel	207					
HTC + MOX Experiments	158				 	 

Table D.3-12 Bias and Bias Uncertainty as a Function of Independent Parameter

Experiment Description	Independent Parameter, x	Calculated k_{eff}	Bias	Bias Uncertainty	Independent Parameter, x	Calculated k_{eff}	Bias	Bias Uncertainty
HTC + MOX Experiments	EALF				Pu Enrichment			
	[redacted]							

Table D.3-13 Analysis of the Unborated and Borated Water for the MCNP5-1.51 calculations

Experiment Description	No. of exp.	Bias	Bias Uncertainty	Normality χ^2 ($P_d(\chi^2;d)$)	Linear Correlation	Residuals Normality, ($P_d(\chi^2;d)$)
All except those with Gadolinium, Cadmium and Lead†	365					
All with Fresh Water	287				 	 
All with Borated Water	78				  	  

†Note: Critical experiments with Gadolinium, Cadmium and Lead were excluded from all subsequent subsets.

Table D.3-14 Bias and Bias Uncertainty as a Function of Independent Parameter

Experiment Description	Independent Parameter, x	Calculated k_{eff}	Bias	Bias Uncertainty	Independent Parameter, x	Calculated k_{eff}	Bias	Bias Uncertainty
All with Fresh Water	EALF				U Enrichment			
	[redacted]							
All with Borated Water	Density				N/A			
	[redacted]							

Experiment Description	Independent Parameter, x	Calculated k_{eff}	Bias	Bias Uncertainty	Independent Parameter, x	Calculated k_{eff}	Bias	Bias Uncertainty
	[redacted]	[redacted]	[redacted]	[redacted]				
	[redacted]	[redacted]	[redacted]	[redacted]				
	[redacted]	[redacted]	[redacted]	[redacted]				
	[redacted]	[redacted]	[redacted]	[redacted]				
	[redacted]	[redacted]	[redacted]	[redacted]				
	[redacted]	[redacted]	[redacted]	[redacted]				
	[redacted]	[redacted]	[redacted]	[redacted]				
	[redacted]	[redacted]	[redacted]	[redacted]				
	[redacted]	[redacted]	[redacted]	[redacted]				

Table D.3-15 Analysis of the Combinations of Fuel Burnup and Unborated/Borated Water for the MCNP5-1.51 calculations

Experiment Description	No. of exp.	Bias	Bias Uncertainty	Normality χ^2 ($P_d(\chi^2;d)$)	Linear Correlation	Residuals Normality, ($P_d(\chi^2;d)$)
All except those with Gadolinium, Cadmium and Lead†	365					
Fresh UO_2 Fuel with Fresh Water	154					
Fresh UO_2 Fuel with Borated Water	53					
HTC + MOX Fuel with Fresh Water	133				 	 
HTC + MOX Fuel with Borated Water	25				 	 

†Note: Critical experiments with Gadolinium, Cadmium and Lead were excluded from all subsequent subsets.

Table D.3-16 Bias and Bias Uncertainty as a Function of Independent Parameter

Experiment Description	Independent Parameter, x	Calculated k_{eff}	Bias	Bias Uncertainty	Independent Parameter, x	Calculated k_{eff}	Bias	Bias Uncertainty
Fresh UO_2 Fuel with Fresh Water	EALF				N/A			
	[redacted]							
HTC + MOX Fuel with Fresh Water	EALF				Pu Enrichment			
	[redacted]							

Experiment Description	Independent Parameter, x	Calculated k_{eff}	Bias	Bias Uncertainty	Independent Parameter, x	Calculated k_{eff}	Bias	Bias Uncertainty
	[redacted]	[redacted]	[redacted]	[redacted]	[redacted]	[redacted]	[redacted]	[redacted]
HTC + MOX Fuel with Borated Water	Rod OD				Density			
	[redacted]	[redacted]	[redacted]	[redacted]	[redacted]	[redacted]	[redacted]	[redacted]

Table D.3-17 Comparison of Key Parameters and Definition of Validated AOA

Parameter	Design Application	Benchmarks	Validated
Fissionable Material	^{235}U, ^{239}Pu, ^{241}Pu	^{235}U, ^{239}Pu, ^{241}Pu	^{235}U, ^{239}Pu, ^{241}Pu
Isotopic Composition			
$^{235}U/Ut$	< 5.0wt%	1.57 – 5.74%	< 5wt%
Pu/(U+Pu)	< 20wt%	1.104 - 20 %	< 20wt%
Physical Form	UO_2, MOX	UO_2, MOX	UO_2, MOX
Fuel Density (g/cm^3)	10.0 – 10.7	9.2 – 10.4	9.2 – 10.7
Moderator Material (coolant)	H	H	H
Physical Form	H_20	H_20	H_20
Density (g/cm^3)	around 1.0 g/cm^3	around 1.0 g/cm^3	around 1.0 g/cm^3
Reflector Material	H	H	H
Physical Form	H_20	H_20	H_20
Density (g/cm^3)	around 1.0 g/cm^3	around 1.0 g/cm^3	around 1.0 g/cm^3
Interstitial Reflector Material			
Plate	Steel or Lead	Steel or Lead	Steel or Lead
Absorber Material			
Soluble	None, Boron or Gadolinium	None, Boron (15 - 2550 ppm) or Gadolinium (48 – 197 ppm)	None, Boron (0 - 2550 ppm) or Gadolinium (48 to 197 ppm)
Rods	Boron	Pyrex®, Vicor®, Steel or B-Al	Boron
Separating Material			
Plate	Water, B-SS, Boral or Cadmium	Water, B-SS, Boral, Boroflex, Zircaloy or Cadmium	Water, B-SS, Boral, Boroflex, Zircaloy or Cadmium
Geometry			
Lattice type	Square	Square, Triangle	Square, Triangle
Lattice Pitch (cm)	1.26 – 1.47 (PWR) 1.24 – 1.88 (BWR)	0.968 to 4.318	0.968 to 4.318
Neutron Energy	Thermal spectrum	Thermal spectrum	Thermal spectrum

Figure Proprietary

Figure D.3-1 Frequency Chart for Calculated k_{eff} of the Selected 532 Benchmarks for the MCNP5-1.51 code

Figure Proprietary

Figure D.3-2 Frequency Chart for Calculated EALF (eV) of the Selected 532 Benchmarks for the MCNP5-1.51 code

Figure Proprietary

Figure D.3-3 MCNP5-1.51 Calculated k_{eff} Values for Various Values of the Spectral Index (All Experiments)

Figure Proprietary

Figure D.3-4 MCNP5-1.51 Calculated k_{eff} Values for Various Values of the Spectral Index

Figure Proprietary

Figure D.3-5 MCNP5-1.51 Calculated k_{eff} Values for Various Values of the Spectral Index

Figure Proprietary

Figure D.3-6 MCNP5-1.51 Calculated k_{eff} Values for Various Values of the Pu Enrichment

Figure Proprietary

Figure D.3-7 MCNP5-1.51 Calculated k_{eff} Values for Various Values of the Spectral Index

Figure Proprietary

Figure D.3-8 MCNP5-1.51 Calculated k_{eff} Values for Various Values of the U Enrichment

Figure Proprietary

Figure D.3-9 MCNP5-1.51 Calculated k_{eff} Values for Various Values of the Fuel Density

Figure Proprietary

Figure D.3-10 MCNP5-1.51 Calculated k_{eff} Values for Various Values of the Spectral Index

Figure Proprietary

Figure D.3-11 MCNP5-1.51 Calculated k_{eff} Values for Various Values of the Spectral Index

Figure Proprietary

Figure D.3-12 MCNP5-1.51 Calculated k_{eff} Values for Various Values of the Pu Enrichment

Figure Proprietary

Figure D.3-13 MCNP5-1.51 Calculated k_{eff} Values for Various Values of the Rod OD

Figure Proprietary

Figure D.3-14 MCNP5-1.51 Calculated k_{eff} Values for Various Values of the Fuel Density

ATTACHMENT 5

Holtec International Report No. HI-2125245, Revision 4,
"Licensing Report for Quad Cities Criticality
Analysis for Inserts – Non Proprietary Version"

HOLTEC
INTERNATIONAL

Holtec Center, 555 Lincoln Drive West, Marlton, NJ 08053
Telephone (856) 797- 0900
Fax (856) 797 - 0909

Licensing Report for Quad Cities Criticality Analysis for Inserts - Non Proprietary Version

FOR

Exelon

Holtec Report No: HI-2125245

Holtec Project No: 2127

Sponsoring Holtec Division: HTS

Report Class : SAFETY RELATED

Summary of Revisions:

Revision 0: Original Issue

Revision 1: Supplement 1 was added to cover a new revision of NETCO-SNAP-IN® rack insert.

Revision 2: All Revision 1 revision bars were removed. No other changes were made.

Revision 3: Sections 2.3.8, 2.7, 7.6, 8.0 and Appendix B were revised. All changes were marked by revision bars.

Revision 4: Minor editorial changes to page 4 description of Table 7.1(c) and Table 2.1(c) was move up one line. Neither change marked by revision bar. All Revision 3 revision bars removed.

Table of Contents

[redacted]

List of Tables

List of Figures

Figure	Description	Page
[redacted]	[redacted]	105
[redacted]	[redacted]	106
[redacted]	[redacted]	107
[redacted]	[redacted]	108
[redacted]	[redacted]	109
[redacted]	[redacted]	110
[redacted]	[redacted]	111
[redacted]	[redacted]	112
[redacted]	[redacted]	113
[redacted]	[redacted]	114
[redacted]	[redacted]	115
[redacted]	[redacted]	116
[redacted]	[redacted]	117
[redacted]	[redacted]	118
[redacted]	[redacted]	B-24
[redacted]	[redacted]	B-25
[redacted]	[redacted]	B-26
[redacted]	[redacted]	B-27
[redacted]	[redacted]	B-28
[redacted]	[redacted]	B-29
[redacted]	[redacted]	B-30
[redacted]	[redacted]	B-31

1. INTRODUCTION

This report documents the criticality safety evaluation for the storage of spent BWR fuel in the Unit 1 and Unit 2 spent fuel pools (SFPs) at Quad Cities Station operated by Exelon. The Unit 1 and Unit 2 SFP racks are identical and are designed to accommodate BWR fuel. Currently, the SFP racks credit BORAFLEX for reactivity control. This new analysis will not credit the BORAFLEX but will instead credit new NETCO-SNAP-IN® rack inserts, which are new to Quad Cities but not new relative to their use for spent fuel pool reactivity control. This analysis will demonstrate that with credit for the inserts the effective neutron multiplication factor (k_{eff}) in the SFP racks fully loaded with fuel of the highest anticipated reactivity, at a temperature corresponding to the highest reactivity, is less than 0.95 with a 95% probability at a 95% confidence level. Reactivity effects of abnormal and accident conditions are also evaluated to assure that under all credible abnormal and accident conditions, the reactivity will not exceed the regulatory limit.

Criticality control in the SFP, as credited in this analysis, relies on the following:

- Fixed neutron absorbers
  - NETCO-SNAP-IN® rack inserts in SFP rack cells
- Integrated neutron absorbers
  - Gadolinium (Gd) in the fuel (peak reactivity isotopic composition).

Criticality control in the SFP, as credited in this analysis, does not rely on the following:

- Burnup credit
- BORAFLEX.

2. METHODOLOGY

2.1 *General Approach*

The analysis is performed consistent with regulatory requirements and guidance. The calculations are performed using either the worst case bounding approach or the statistical analysis approach with respect to the various calculation parameters. The approach considered for each parameter is discussed below.

2.2 *Computer Codes and Cross Section Libraries*

2.2.1 MCNP5-1.51

MCNP5-1.51 is a three-dimensional Monte Carlo code developed at the Los Alamos National Laboratory [1]. MCNP5-1.51 calculations use continuous energy cross-section data based on ENDF/B-VII. MCNP is selected because it has history of successful use in fuel storage criticality analyses and has most of the necessary features (except for fuel depletion analysis) for the analysis to be performed for Quad Cities Station SFP.

The convergence of a Monte Carlo criticality problem is sensitive to the following parameters: (1) number of histories per cycle, (2) the number of cycles skipped before averaging, (3) the total number of cycles and (4) the initial source distribution. All MCNP5 calculations are performed with a minimum of 12,000 histories per cycle, a minimum of 150 skipped cycles before averaging, and a minimum of 150 cycles that are accumulated. The initial source is specified as uniform over the fueled regions (assemblies). [redacted]

2.2.1.1 MCNP5-1.51 Validation

[redacted]

[redacted]

[redacted]

[redacted]

2.2.2 CASMO-4

Fuel depletion analyses during core operation are performed with CASMO-4 Version 2.05.14 (using the 70-group cross-section library), which has been approved by the NRC for reactor analysis (depletion) when providing reactivity data for specific 3D simulator codes. CASMO-4 is a two-dimensional multigroup transport theory code based on the Method of Characteristics and it is developed by Studsvik of Sweden [4]. CASMO-4 is used to perform depletion calculations and to perform various sensitivity studies. The uncertainty on the isotopic composition of the fuel (i.e., the number density) is considered as discussed below (see Section 2.3.3). A validation for CASMO-4 to develop a bias and bias uncertainty is not necessary because the results of the CASMO-4 sensitivity studies are not used as input into the k_{eff} calculations. However, the code authors have validated CASMO-4 against MCNP and various critical experiments [5].

The version of the CASMO-4 code used in this application has a built-in limitation in a number of isotopes that may be extracted for specific pins. Therefore, two independent CASMO-4 depletion calculations were performed to separately extract the actinides and fission products. The extracted isotopes were further combined and used in MCNP5-1.51 calculations.

2.3 *Analysis Methods*

2.3.1 Design Basis Fuel Assembly

There are various fuel designs stored in the Quad Cities SFP. For the purpose of this analysis, the reactivity of each design is evaluated and the most reactive fuel bundle lattice is determined for use as the design basis fuel assembly to determine k_{eff} at the 95/95 level. This approach follows the guidance in [2] and [6], and is further described below.

2.3.1.1 Peak Reactivity

The BWR fuel designs used at the Quad Cities Station use Gd as an integral burnable absorber. Initially, the Gd in the fuel assembly holds down the fresh fuel assembly reactivity and then, as core depletion occurs, the Gd begins to burnout until it is essentially fully depleted. As the Gd depletes the reactivity of the fuel assembly increases until it reaches a peak. This peak reactivity is the fuel assembly's most reactive condition. Note that most BWR fuel designs are composed of various axial lattices (including blankets) that can have different axial lengths, uranium loadings (also mixed oxide loading, for MOX fuel), fuel pin arrangements including partial or part-length rods, Gd pin locations and loading, etc. These various lattice components can all effect at what burnup the peak reactivity occurs and the magnitude of the peak reactivity. The axial lattices within a single fuel assembly can therefore all have different peak reactivity.

[redacted]

[redacted]

2.3.1.1.1 Peak Reactivity and Fuel Assembly Burnup

Typically, a spent fuel assembly is characterized by its assembly average burnup (over all lattices or nodes). In this analysis methodology the fuel assembly average burnup is of no concern and is not credited for reactivity control. Rather, the methodology credits the residual Gd and other depletion isotopic compositions at the fuel assembly peak reactivity (most reactive lattice peak reactivity). While the peak reactivity occurs at some specific *lattice burnup*, the peak reactivity lattice burnup varies from lattice to lattice within a fuel design. Therefore, independent calculations with MCNP5-1.51 using pin specific compositions (see Section 2.3.1.1.2) are performed for *every lattice* of the SVEA-96 Optima2 fuel assembly (as will be seen in Section 7, this is the fuel assembly with the design basis lattice) over a burnup range to determine the burnup at peak reactivity for every lattice. Since each lattice is considered at its peak reactivity (and therefore the lattice or nodal burnup at which that occurs), the fuel assembly average burnup or fuel assembly burnup profile is not applicable because the analysis already considers each lattice at its most reactive composition, independent of the fuel assembly average burnup.

2.3.1.1.2 [redacted]

[redacted]

[redacted]

[redacted]

2.3.1.2 [redacted]

[redacted]

[redacted]

[redacted]

[redacted]

[redacted]

[redacted]

[redacted]

2.3.1.3 Determination of the Design Basis Fuel Assembly Lattice

[redacted]

2.3.1.4 Optima2 CASMO-4 Model Simplification Effect

As previously discussed in Section 2.3.1.2, various fuel designs were provided. Of these fuel designs, the SVEA-96 Optima2 designs were specified to be bounding. The Optima2 model in CASMO-4 is described as the SVEA-96 model provided in the CASMO-4 manual [4]. This CASMO-4 internal model is slightly different from the actual fuel assembly geometry. Therefore, it is important to evaluate and if necessary quantify the reactivity effect of the CASMO-4 model simplifications inherent in the code. The CASMO-4 model geometry of the SVEA-96 Optima2 fuel differs from the SVEA-96 Optima2 fuel as follows:

[redacted]

With respect to the fuel assembly geometry models, the amount of zirconium (and therefore the amount of water) in the CASMO-4 model of the SVEA-96 Optima2 fuel is reasonably similar to that of the actual SVEA-96 Optima2 fuel and therefore these built-in CASMO-4 simplifications are acceptable. However, to evaluate the CASMO-4 model geometry simplification effect on reactivity, an applicable set of code-to-code comparisons is performed. The following cases are evaluated.

For the purpose of showing that the two codes calculate an equivalent reactivity the following comparisons are made:

- Case 2.3.1.4.1 is compared to Case 2.3.1.4.2 at 0 GWD/MTU to show that the two codes calculate similar results with respect to the fuel assembly and storage rack geometry.

- Case 2.3.1.4.1 is compared to Case 2.3.1.4.2 at peak reactivity burnup to quantify the reactivity difference due to the effect of the spent fuel. The two codes use different cross section library versions and calculation sequences. The main calculation sequence difference between the two codes is that CASMO-4 uses a thermal expansion of spent fuel pellet which effects the fuel density [4]. The actual density is conservatively used in MCNP5-1.51. The results are expected to show that the MCNP5-1.51 code is conservative with respect to the CASMO-4 code. Any non-conservative result would be treated as a bias.

- Case 2.3.1.4.3 is compared to Case 2.3.1.4.2 to show the reactivity difference between the simplified MCNP5-1.51 model and the design basis model that is slightly modified to be similar to the CASMO-4 insert orientation. This case is expected to show that the design basis model with respect to the fuel pin pitch (and subsequent sub-bundle pitch) is conservative. This is expected to be conservative because the design basis model fuel compositions are taken from the average fuel pin pitch CASMO-4 calculations and used in the MCNP5-1.51 design basis actual fuel pin locations. Any non-conservative result would be treated as a bias.

Case 2.3.1.4.3 is compared to the result of the actual design basis results (similar to Case 2.3.1.4.3 but with the bounding insert orientation) to show that the design basis model is conservative.

2.3.1.5 Core Operating Parameters

As previously discussed, CASMO-4 is used to perform depletion calculations to determine the spent fuel isotopic composition. The operating parameters for spent fuel depletion calculations are discussed in this Section. The operating parameters which may have a significant impact on BWR spent fuel isotopic composition are void fraction, control blade history, moderator temperature, fuel temperature, and power density. Other parameters such as axial enrichment distribution and effect of burnable absorbers are discussed in Section 2.3.1.5.3 and Section 2.3.1.5.2, respectively. Sensitivity studies are performed to show the effect of each individual parameter, and to confirm that the selected values are in fact appropriate when combined at their worst case. [redacted]

2.3.1.5.1 Reactor Power Uprate

[redacted] To determine the effect of the power uprate on the reactivity of fuel assemblies in the SFP racks, the following evaluations are performed.

[redacted]

2.3.1.5.2 Integral Reactivity Control Devices

The only type of burnable absorber used for the fuel assemblies covered in this analysis is Gd. The use of Gd does not increase the reactivity of the assembly, compared to an assembly lattice where all rods contain fuel and no Gd. As discussed in Section 2.3.1.1, the Gd in the fuel assembly holds down the fresh fuel assembly reactivity and then, as core depletion occurs, the Gd begins to burnout until it is essentially fully depleted. As the Gd depletes the reactivity of the fuel assembly increases until it reaches a peak. This peak reactivity is the fuel assembly's most reactive condition, which is used for design basis condition. Note that integrated absorbers do not change the amount of water in the assembly, which is a large part of the effect of non-integral absorbers.

2.3.1.5.3 Axial and Planar Enrichment Variations

[redacted]

2.3.1.5.4 Fuel Assembly De-Channeling

The SVEA-96 Optima2 fuel assembly (the most reactive fuel assembly, as will be shown in Section 7) cannot be de-channeled for storage in the SFP because of its specific design. However, GE14 (the most second reactive fuel assembly, as will be shown in Section 7) may be de-channeled. Studies are performed to evaluate the effect of storage of GE14 without the Zr channel at various radial positioning in the storage cells. The following cases are evaluated.

- Case 2.3.1.5.4.1: This is the reference for Case 2.3.1.5.4.2 through Case 2.3.1.5.4.4. The MCNP5-1.51 model used herein is a 2x2 array with the cell centered fuel assembly that includes the Zr channel, as shown in Figure 2.13(a).

- Case 2.3.1.5.4.2: The MCNP5-1.51 is a 2x2 array of GE14 fuel assembly lattice 5 (the most reactive lattice of GE14, as will be shown in Section 7). The Zr channel is removed, as shown in Figure 2.13(b). The fuel assemblies are cell centered.

- Case 2.3.1.5.4.3: The MCNP5-1.51 is the same as that of Case 2.3.1.5.4.2, except the fuel assemblies are eccentric toward the center, as shown in Figure 2.13(c).

- Case 2.3.1.5.4.4: The MCNP5-1.51 is the same as that of Case 2.3.1.5.4.2, except the fuel assemblies are eccentric away from the corner where the insert wings connect, as shown in Figure 2.13(d).

2.3.1.6 [redacted]

[redacted]

2.3.2 Reactivity Effect of Spent Fuel Pool Water Temperature

The Quad Cities Station SFP has a normal pool water temperature operating range below 150 °F. For the nominal condition, the criticality analyses are to be performed at the most reactive temperature and density [2]. Also, there are temperature-dependent cross section effects in MCNP5-1.51 that need to be considered. In general, both density and cross section effects may not have the same reactivity effect for all storage rack scenarios, since configurations with strong neutron absorbers typically show a higher reactivity at lower water temperature, while configurations without such neutron absorbers typically show a higher reactivity at a higher water temperature. For the SFP racks which credit inserts, the most reactive SFP water temperature and density is expected to be at 39.2 °F and 1 g/cc, respectively.

The standard cross section temperature in MCNP5-1.51 is 293.6 K. Cross sections are also available at other temperatures; however, not usually at the desired temperature for SFP criticality analysis. MCNP5-1.51 has the ability to automatically adjust the cross sections to the specified temperature when using the TMP card. Furthermore, MCNP5-1.51 has the ability to make a molecular energy adjustment for select materials (such as water) by using the S(α,β) card. The S(α,β) card is provided for certain fixed temperatures which are not always applicable to SFP criticality analysis. Rather, there are limited temperature options, i.e., 293.6 K and 350 K, etc. Additionally, MCNP5-1.51 does not have the ability to adjust the S(α,β) card for temperatures as it does for the TMP card discussed above. Therefore, additional studies are performed to show the impact of the S(α,β) card at the two available temperatures.

To determine the water temperature and density which result in the maximum reactivity, MCNP5-1.51 calculations are run using the bounding values. Additionally, S(α,β) calculations are performed for both upper and lower bounding S(α,β) values, if needed.

The studies mentioned above are performed for the following cases for the single cell MCNP5-1.51 SFP model (with periodic boundary conditions through the centerline of the surrounding water [2]):

[2] [redacted]

- Case 2.3.2.1 (reference case): Temperature of 39.2 °F (277.15 K) and a density of 1.0 g/cc are used to determine the reactivity at the low end of the temperature range. The S(α,β) card corresponds to a temperature of 68.81 °F (293.6 K).

- Case 2.3.2.2: Temperature of 150 °F (338.71 K) and a corresponding density of 0.98026 g/cc are used to determine the reactivity at the high end of the temperature range. The S(α,β) card corresponds to a temperature of 68.81 °F (293.6 K).

- Case 2.3.2.3: Temperature of 150 °F and a corresponding density of 0.98026 g/cc. The S(α,β) card corresponds to a temperature of 170.33 °F (350 K).

The bounding water temperature and density (the temperature and its corresponding density which result in the maximum reactivity) of the above cases are applied to all further calculations so that the most reactive water temperature and density is considered. Note that the evaluations use the same MCNP5-1.51 models used in the design basis calculation. [redacted]

2.3.3 Fuel Depletion Calculation Uncertainty

To account for the uncertainty of the number densities in the depletion calculations performed in CASMO-4, a 5% depletion uncertainty factor as described in [2] and [6] is used. [redacted]

The depletion uncertainty is applied by multiplying it with the reactivity difference (at 95%/95%) between the MCNP5-1.51 calculation with spent fuel at peak reactivity (includes residual Gd) and a corresponding MCNP5-1.51 calculation with fresh fuel (without Gd_2O_3). Calculations are performed for the single cell model of design basis fuel assembly.

The uncertainty is determined by the following:

$$\text{Uncertainty}_{\text{Isotopics}} = [\ (k_{calc\text{-}2} - k_{calc\text{-}1}) + 2 * \sqrt{(\sigma_{calc\text{-}1}^2 + \sigma_{calc\text{-}2}^2)}\ ] * 0.05$$

with

$k_{calc\text{-}1} = k_{calc}$ with spent fuel
$k_{calc\text{-}2} = k_{calc}$ with fresh fuel
$\sigma_{calc\text{-}1}$ = Standard deviation of $k_{calc\text{-}1}$
$\sigma_{calc\text{-}2}$ = Standard deviation of $k_{calc\text{-}2}$

The result of the MCNP5-1.51 calculation for the fuel depletion calculation uncertainty is statistically combined with other uncertainties to determine k_{eff}.

2.3.4 Fuel and Storage Rack Manufacturing Tolerances

In order to determine the k_{eff} of the SFP at a 95% probability at a 95% confidence level, consideration is given to the effect of the BWR fuel and SFP storage rack manufacturing tolerances on reactivity. The reactivity effects of significant independent tolerance variations are combined statistically [2]. The evaluations use the same MCNP5-1.51 models used in the design basis calculation.

2.3.4.1 Fuel Manufacturing Tolerances

The BWR fuel tolerances for Optima2 Q122 fuel (which is the most reactive fuel design evaluated herein) are presented in Table 5.1(a). Fuel tolerance calculations are performed using the design basis fuel assembly lattice, and therefore only the tolerances applicable to that lattice are applicable. Separate CASMO-4 depletion calculations are performed for each fuel tolerance and the full value of the tolerance is applied for each case in both the depletion and in rack calculations. Pin specific compositions are used. The MCNP5-1.51 tolerance calculation is compared to the MCNP5-1.51 reference case (nominal parameter values) at the 95% probability at a 95% confidence level using the following equation:

$$\text{delta-}k_{calc} = (k_{calc2} - k_{calc1}) \pm 2 * \sqrt{(\sigma_1^2 + \sigma_2^2)}$$

The following fuel tolerances are considered in this analysis:

- Fuel enrichment
- Gd loading
- Fuel pellet density (UO_2 and UO_2+Gd_2O_3 fuel rods)
- Fuel pellet outer diameter (OD)
- Fuel cladding inner diameter (ID)
- Fuel cladding OD
- Fuel pin pitch
- Fuel sub-bundle pitch [3]
- Combination of [4]
    - Water wing canal inner width
    - Channel outer square width
    - Channel corner inner radius
    - Central water canal inner square width
- Combination of [4]
    - channel wall thickness

[3] For fuel sub-bundle pitch uncertainty calculation, the fuel hardware (channel, central water channel and water wings) is fixed. The fuel lattices are moved only.

[4] Conservatively, the various tolerances are considered together. The tolerance limits that result in an increase of the amount of water in the core are considered together in one set of uncertainty calculations, and the tolerance limits that result in a decrease of the amount of water in the core are considered together in another set of uncertainty calculations.

- Water cross wall thickness

The maximum positive reactivity effect of the MCNP5-1.51 calculations for each tolerance is statistically combined with the other tolerance results, and this result is then statistically combined with other uncertainties when determining the k_{eff} value.

2.3.4.2 SFP Storage Rack Manufacturing Tolerances

The SFP rack tolerances are presented in Tables 5.3(a) and 5.3(b). The single cell MCNP5-1.51 model is used to determine the reactivity effect of the tolerance, and the full value of the tolerance is applied for each case. The MCNP5-1.51 tolerance calculation is compared to the MCNP5-1.51 reference case with a 95% probability at a 95% confidence level using the following equation:

$$\text{delta-}k_{calc} = (k_{calc2} - k_{calc1}) \pm 2 * \sqrt{(\sigma_1^2 + \sigma_2^2)}$$

The following SFP rack manufacturing tolerances are considered in this analysis:

- Storage cells:
  - Cell ID and cell pitch
  - Cell wall thickness
- Rack inserts (poison)
  - Width

The maximum positive reactivity effect of the MCNP5-1.51 calculations for each tolerance is statistically combined with the other tolerance results, and this result is then statistically combined with other uncertainties when determining the k_{eff} value.

The evaluations use the same MCNP5-1.51 models used in the design basis calculation. The isotopic compositions of the fuel rods are the same as those of the design basis fuel assembly.

The poison thickness and loading are used at their minimum values; i.e., they are treated as a bias instead of uncertainty, for conservatism and simplification.

2.3.5 Radial Positioning

2.3.5.1 Fuel Assembly Orientation in the Core

The fuel assembly orientation in the core with respect to its control blade does not change and therefore the design basis calculations consider the only possible configuration.

2.3.5.2 Fuel Radial Positioning in the Rack

The BWR fuel that is loaded in the SFP racks may not rest exactly in the center of the storage cell. Evaluations are performed to determine the most limiting fuel radial location. The following eccentric fuel positioning cases are analyzed:

- Case 2.3.5.2.1: This is the reference for Case 2.3.5.2.2 through Case 2.3.5.2.5. The MCNP5-1.51 model used herein is a 2x2 array which is the same as the primary single bundle MCNP5-1.51 model used elsewhere in this analysis. In both models the fuel is centered in the rack cell. See Figure 2.7(a).

- Case 2.3.5.2.2: Every fuel assembly is positioned toward the center, for the 2x2 array, as shown in Figure 2.7(b).

- Case 2.3.5.2.3: Every fuel assembly is positioned toward the corner where the insert wings connect, for the 2x2 array, as shown in Figure 2.7(c).

- Case 2.3.5.2.4: Every fuel assembly is positioned away from the corner where the insert wings connect, for the 2x2 array, as shown in Figure 2.7(d).

- Case 2.3.5.2.5: Every fuel assembly is centered between insert and cell walls, for the 2x2 array, as shown in Figure 2.7(e).

- Case 2.3.5.2.6: This is the reference for Case 2.3.5.2.7 through Case 2.3.5.2.10. The MCNP5-1.51 model used herein is an 8x8 array which is the same as the primary single bundle MCNP5-1.51 model used elsewhere in this analysis. In both models the fuel is centered in the rack cell.

- Case 2.3.5.2.7: Every fuel assembly is positioned toward the center, for the 8x8 array, as shown in Figure 2.8.

- Case 2.3.5.2.8: Every fuel assembly is positioned toward the corner where the insert wings connect, for the 8x8 array.

- Case 2.3.5.2.9: Every fuel assembly is positioned away from the corner where the insert wings connect, for the 8x8 array.

- Case 2.3.5.2.10: Every fuel assembly is centered between insert and cell walls, for the 8x8 array.

- Case 2.3.5.2.11: This is the reference for Case 2.3.5.2.12. The MCNP5-1.51 model used herein is a single rack cell where the fuel is centered.

- Case 2.3.5.2.12: The fuel assembly is centered between insert and cell walls, for the single rack cell.

The maximum positive reactivity effect of the MCNP5-1.51 calculations for the fuel radial positioning is added as the bias and the corresponding 95/95 uncertainty is statistically combined with other uncertainties to determine k_{eff}.

Note that the evaluations use the same MCNP5-1.51 models with periodic boundary conditions used in the design basis calculation, except that the array size is larger. The isotopic compositions of the fuel rods are the same as those of the design basis fuel assembly.

2.3.5.3 Inserts Radial Positioning

Since the insert width and SFR cell inner diameter are comparable, and each insert is installed into the rack cell such that the insert becomes an integral part of the fuel rack, no uncertainty in the positioning for inserts is evaluated. The water gap between rack wall and insert is not assumed, since it may provide a small flux trap effect. Nevertheless, the orientation of fuel assembly with respect to position of insert is considered in Section 2.3.5.4.

2.3.5.4 Fuel Orientation in SFP Rack Cell

As described in Section 5.1, fuel assemblies have various radial fuel enrichments and gadolinium distribution. Also, one corner of each fuel assembly is adjacent to the control blade during the depletion in the core. As a result, the fuel depletion is not uniform (more discussion is provided in Section 2.3.1.1.2) and one fuel assembly corner may be more reactive than other corners and therefore the fuel assembly orientation in the SFP storage cell may have an impact on reactivity.

Five cases are analyzed to assess the fuel assembly orientation variations and to determine the most limiting fuel orientation in SFP rack cell with respect to the insert.

The MCNP5-1.51 model of the reference case is the design basis fuel in the 2x2 array, as shown in Figure 2.9(a). The MCNP5.1.51 models of the other four cases are the same as that of the reference case, except with different orientation of fuel assemblies with respect to the inserts. Figure 2.9(b) through Figure 2.9(e) show the configurations of the fuel assemblies in the SFP cells for the evaluated cases.

Note that the evaluations use the same MCNP5-1.51 models with periodic boundary conditions used in the design basis calculation. The isotopic compositions of the fuel rods are the same as those of the design basis fuel assembly.

2.3.6 [redacted]

[redacted]

2.3.6.1 [redacted]

[redacted]

2.3.6.1.1 [redacted]

[redacted]

[redacted]

2.3.6.1.2 [redacted]

[redacted]

2.3.6.2 [redacted]

[redacted]

[redacted]

2.3.7 Insert Coupon Measurement Uncertainty

There is a measurement uncertainty associated with the B-10 content in the poison test coupons. In this analysis, the minimum B-10 loading and the minimum insert thickness are conservatively used for criticality calculations. Therefore, the coupon measurement uncertainty is not evaluated further in the analysis.

2.3.8 Maximum k_{eff} Calculation for Normal Conditions

The calculation of the maximum k_{eff} of the SFP storage racks fully loaded with design basis fuel assemblies at their maximum reactivity is determined by adding all uncertainties and biases to the calculated reactivity. Note that the insert thickness and its B-10 loading are taken at their worst case values.

k_{eff} is determined by the following equation:

$k_{eff} = k_{calc}$ + uncertainty + bias

where uncertainty includes:

and the bias includes

Note that each uncertainty is statistically combined with other uncertainties, while biases are added together in order to determine k_{eff}.

The approach used in this analysis takes credit for residual Gd.

2.4 *Margin Evaluation*

The criticality analysis is performed using several conservative assumptions which introduce quantifiable margin into the analysis. Four main conservative assumptions are:

- Minimum insert B_4C loading
- Minimum insert thickness
- Minimum amount of B-10 in boron
- Bounding lattice throughout the entire length of fuel assembly.

To evaluate this margin, the following cases are evaluated:

- Case 2.4.1: This is the design basis fuel assembly. This is the reference for Case 2.4.2 and Case 2.4.3.

- Case 2.4.2: This case is the same as Case 2.4.1, except the nominal insert B_4C loading, nominal insert thickness and nominal amount of B-10 in boron are used.

- Case 2.4.3: This case is the same as Case 2.4.1, except the model includes each Optima2 QI22 fuel lattice in the appropriate axial position. However, the top and bottom blankets were conservatively replaced by adjacent fuel lattices. The peak reactivity burnup for each individual Optima2 QI22 lattice under the design basis core operation parameters was determined separately and used in this case (i.e. each lattice is at its individual peak reactivity). Therefore, the model represents a conservative maximum but unrealistic reactivity of the actual Optima2 fuel assembly.

The differences between the reactivity of Cases 2.4.2 and 2.4.3 and the reactivity of reference Case 2.4.1 provide a quantified margin.

Note that the evaluations use the same MCNP5-1.51 models used in the design basis calculation. The isotopic compositions of the fuel rods of Case 2.4.1 and Case 2.4.2 are the same as those of the design basis fuel assembly.

2.5 *Fuel Movement, Inspection and Reconstitution Operations*

[redacted]

2.6 *Accident Condition*

The accidents considered are:

- SFP temperature exceeding the normal range
- Dropped assemblies
- Storage cell distortion
- Missing insert
- Misloaded fuel assembly (a fuel assembly in the wrong location within the storage rack)/ Missing an insert
- Mislocated fuel assembly (a fuel assembly in the wrong location outside the storage rack)
- Miss-installment of an insert on wrong sides of a cell
- Insert mechanical wear
- Rack movement

Those are briefly discussed in the following sections.

Note that the double contingency principle as stated in [2] specifies that "two unlikely independent and concurrent incidents or postulated accidents are beyond the scope of the required analysis." This principle precludes the necessity of considering the simultaneous occurrence of multiple accident conditions. The k_{eff} calculations performed for the accident conditions are done with a 95% probability at a 95% confidence level.

The accident conditions are considered at the 95/95 level using the total corrections from the design basis case. [redacted]

2.6.1 Temperature and Water Density Effects

The SFP water temperature accident conditions for consideration are the increase in SFP water temperature above the maximum SFP operating temperature of 150 °F. The decrease in temperature was already considered for the temperature coefficient determination as discussed in Section 2.3.2. To bound the potential increase in reactivity due to increased SFP temperature, the following case is evaluated:

- Case 2.6.1: This case uses a temperature of 255 °F (397.04 K) and a density of 0.84591 g/cc. The S(α,β) card corresponds to a temperature of 260.33 °F (400 K). In this model, it is assumed that the water modeled includes 10% void. Void is modeled as 10% decrease in density, compared to the density of water at 255 °F.

The evaluation use the same MCNP5-1.51 model used in the design basis calculation.

Note that as discussed in Section 2.3.2, SFP storage racks with strong neutron absorbers, such as inserts, show a higher reactivity at a lower water temperature. The case evaluated above is performed to confirm this statement.

2.6.2 Dropped Assembly – Horizontal

For the case in which a fuel assembly is assumed to be dropped on top of a rack, the fuel assembly will come to rest horizontally on top of the rack with a separation distance more than 12 inches. Also, the length of the inserts (as indicated in Table 5.3(b)) covers this separation distance. Thus, the horizontally dropped assembly is decoupled from the fuel assemblies in the rack. This accident is also bounded by the mislocated case, where the mislocated assembly is closer to the assembly in the racks. Therefore, the horizontally dropped fuel assembly is not evaluated further in the report.

2.6.3 Dropped Assembly – Vertical into a Storage Cell

It is also possible to vertically drop an assembly into a location that might be occupied by another assembly or that might be empty. Such a vertical impact would at most cause a small compression of the stored assembly, if present, or result in a small deformation of the baseplate for an empty cell.

These deformations could potentially increase reactivity. However, the reactivity increase would be small compared to the reactivity increase created by the 'misloaded fuel assembly/missing insert' accident (discussed in Section 2.6.5) that does not include the insert in one rack cell. The vertical drop is therefore bounded by this misload accident and no separate calculation is performed for this drop accident.

2.6.4 Storage Cell Distortion

A storage cell distortion or altered geometry as a result of fuel handling equipment uplift forces is possible. However, the reactivity increase would be small compared to the possible reactivity increase created by the 'misloaded fuel assembly/missing insert'' accident that does not include the insert in one rack cell, as discussed in Section 2.6.5. The storage cell distortion is therefore bounded by the 'misloaded fuel assembly/missing insert' accident and no separate calculation is performed for the storage cell distortion accident.

As a result of significant distortion, the storage cell for whatever reason may not be able to contain the insert and also it will be therefore unacceptable for storage of a fuel assembly. This condition is bounded by the 'misloaded fuel assembly/missing insert' accident. However to show that it is acceptable for normal operation and that the empty storage cell decreases the reactivity of the SFR, the model with an empty storage cell, i.e. without a fuel assembly and insert, in the center of a 8x8 array, is evaluated. Two cases with a cell centered and eccentric position of the fuel assemblies are analyzed.

2.6.5 Misloaded Fuel Assembly/Missing Insert

The fuel storage racks are qualified for storage of fuel assembly with the highest anticipated reactivity; thus it is not possible to misload a fuel assembly if every cell with a fuel assembly has an insert.

However, there are a few cells in the SFP racks which are exempt from fuel storage. Those locations are blocked or have partial interferences. In a hypothetical scenario, it is assumed that a fuel assembly is misloaded into a cell with a missing insert. To evaluate the effect, the following cases are evaluated:

- Case 2.6.5.1: The MCNP5-1.51 model includes an 8x8 array. One cell near the center of the rack does not have the insert. The misloaded fuel assembly is the design basis fuel assembly. This fuel assembly is eccentric toward the walls that are not covered by inserts. Other fuel assemblies are also eccentric toward the misloaded fuel assembly. The periodic boundary conditions are used through the centerline of the surrounding water (BORAFLEX replacement). The temperature of the model is set to the minimum (39.2 ^{o}F) with its corresponding water density and S(α,β) card. These temperature and density are bounding for the SFP racks. See Figure 2.10(a).

- Case 2.6.5.2: The MCNP5-1.51 model is the same as Case 2.6.5.1, except with all fuel assemblies centered in the rack cells. See Figure 2.10(b).

2.6.6 Mislocated Fuel Assembly

The Quad Cities SFP layout was reviewed to determine the possible worst case locations for a mislocated fuel assembly. Three hypothetical locations where a fuel assembly may be mislocated are:

- In the water gap between the racks and the pool wall
- In the corner between two racks
- Between the SFP rack and the inspection platform.

The three cited scenarios are evaluated, as follows.

2.6.6.1 Mislocation of a Fuel Assembly in the Water Gap between the Racks and Pool Wall

A fuel assembly may be mislocated in the water gap between the racks and the pool wall. Due to the neutron leakage to the outside the storage rack area, the effect of this mislocation is bounded by that of 'mislocation of a fuel assembly between the SFP rack and the inspection platform' accident, as discussed in Section 2.6.6.3. No separate calculation is performed for this accident.

2.6.6.2 Mislocation of a Fuel Assembly in the Corner between Two Racks

There are some places in the SFP, but outside of the racks, where the mislocated fuel assembly may be in the corner between two racks (thus the mislocated fuel assembly would be adjacent to the fuel assemblies in racks from two sides). To evaluate the effect of the mislocation of a fuel assembly in the corner between two racks, the following cases are evaluated:

- Case 2.6.6.2.1: The MCNP5-1.51 model is three 8x8 arrays of SFP rack cells. The misplaced fuel assembly is in the corner between two racks. The fuel assemblies in the rack are eccentric toward the mislocated fuel assembly. The misplaced fuel assembly is placed as close to the racks as possible. All fuel assemblies in the model are the design basis fuel assembly. Figures 2.11(a) and 2.11(b) show the MCNP5-1.51 model used for this analysis.

- Case 2.6.6.2.2: The MCNP5-1.51 model is the same as Case 2.6.6.2.1, except with all fuel assemblies are centered. See Figures 2.11(a) and 2.11(c).

- Case 2.6.6.2.3: The MCNP5-1.51 model is the same as Case 2.6.6.2.1, except the temperature of the model is set to the maximum (150 °F).

- Case 2.6.6.2.4: The MCNP5-1.51 model is the same as Case 2.6.6.2.2, except the temperature of the model is set to the maximum (150 °F).

2.6.6.3 Mislocation of a Fuel Assembly between the SFP Rack and the Inspection Platform

As discussed in Section 2.5, the fuel handling/inspection/reconstitution platform may have one fuel assembly in it at a time. There is a possibility that a fuel assembly is mislocated between the

SFP racks and the fuel assembly in the platform. To evaluate the effect of the mislocation of a fuel assembly between the SFP Rack and the Inspection Platform, the following cases are evaluated:

- Case 2.6.6.3.1: The MCNP5-1.51 model is an 8x8 array of SFP rack cells. The misplaced fuel assembly is adjacent to the SFP rack and the inspection platform. The fuel assembly in the platform is lined up with the mislocated fuel assembly. The fuel assemblies in the rack are eccentric toward the mislocated fuel assembly. The misplaced fuel assembly is placed as close to the rack and fuel assembly in the inspection station as possible. All fuel assemblies in the model are design basis fuel assembly. The side of the fuel in the platform which does not have any fuel has at least 12 inches of water. Figure 2.12(a) shows the MCNP5-1.51 model used for this analysis.

- Case 2.6.6.3.2: The MCNP5-1.51 model is the same as Case 2.6.6.3.1, except with all fuel assemblies are centered. See Figure 2.12(b).

- Case 2.6.6.3.3: The MCNP5-1.51 model is the same as Case 2.6.6.3.1, except the temperature of the model is set to the maximum (150 °F).

- Case 2.6.6.3.4: The MCNP5-1.51 model is the same as Case 2.6.6.3.2, except the temperature of the model is set to the maximum (150 °F).

2.6.7 Mis-installment of an Insert on Wrong Side of a Cell

There is a small possibility that an insert is installed on wrong sides of the cell. In this case, there may not be a poison between a fuel assembly placed in that cell and a fuel assembly in an adjacent cell. However, the effect of this mis-installment is bounded by that of 'misloaded fuel assembly/missing insert' accident that does not include the insert in one rack cell, as discussed in Section 2.6.5. No separate calculation is performed for this accident.

2.6.8 Insert Mechanical Wear

Handing accidents and other environmental damage may cause scratches and local wear of inserts. The effect of this accident is bounded by that of 'misloaded fuel assembly/missing insert' accident, as discussed in Section 2.6.5.

2.6.9 Rack Movement

In the event of seismic activity, there is a hypothetical possibility that the storage rack arrays may move and come closer to each other. Since there is no water gap modeled between cells of a storage rack, the reactivity of the rack movement case is bounded by the reactivity of the design basis calculation.

2.7 [redacted]

[redacted]

2.8 *Spent Fuel Rack Interfaces*

The spent fuel pool includes a single type of Region 1 spent fuel racks, which are loaded with the neutron absorbing inserts in every storage cell as well as a uniform fuel assembly loading pattern. Therefore, any possible water gaps and interfaces between the racks are bounded by the infinite array used in the design basis calculations. However, since the neutron absorbing inserts are located in the same corners of rack cells (e.g. south-west), there are two peripheral rows of the cells (correspondingly, north and east periphery of the pool), which are loaded with the fuel assemblies that have one side that is not adjacent to the insert. Furthermore, one fuel assembly in the corner of the spent fuel pool (correspondingly, north-east corner) has two sides that are not adjacent to the insert. Due to the neutron leakage on the periphery of the spent fuel pool the reactivity increase is not expected. Nevertheless, to evaluate the effect of such conditions, the full spent fuel pool model (74x74 array) loaded with the cell centered design basis fuel assemblies and the model where all fuel assemblies are shifted to the fuel assembly in the corner, which is discussed above, were evaluated.

2.9 *Reconstituted Fuel Assemblies*

The SFP contains various reconstituted assemblies which were examined and determined to be relatively old and low reactivity designs. The reconstitution of these fuel assemblies removed fuel rods and replaced them by either fuel rods that are of the same or less initial enrichment and equal or greater Gd loading (with burnup similar to the rod they replaced) or solid stainless steel rods. The reactivity effect of this reconstitution is not sufficient to make the reconstituted fuel assembly more reactive than the bounding lattice. Therefore, reconstituted assemblies are covered by the design basis Optima2 QI22 lattice 146. Future reconstituted assemblies will replace fuel rods with stainless steel rods.

3. ACCEPTANCE CRITERIA

3.1 *Applicable Codes, Standards and Guidance's*

Codes, standard, and regulations or pertinent sections thereof that are applicable to these analyses include the following:

- Code of Federal Regulations, Title 10, Part 50, Appendix A, General Design Criterion 62, "Prevention of Criticality in Fuel Storage and Handling."
- Code of Federal Regulations, Title 10, Part 50.68, "Criticality Accident Requirements."
- USNRC Standard Review Plan, NUREG-0800, Section 9.1.1, Criticality Safety of Fresh and Spent Fuel Storage and Handling, Revision 3 – March 2007.
- L. Kopp, "Guidance on the Regulatory Requirements for Criticality Analysis of Fuel Storage at Light-Water Reactor Power Plants," NRC Memorandum from L. Kopp to T. Collins, August 19, 1998.
- ANSI ANS-8.17-1984, Criticality Safety Criteria for the Handling, Storage and Transportation of LWR Fuel Outside Reactors (withdrawn in 2004).
- USNRC, NUREG/CR-6698, Guide for Validation of Nuclear Criticality Safety Calculational Methodology, January 2001.
- DSS-ISG-2010-01, Revision 0, Staff Guidance Regarding the Nuclear Criticality Safety Analysis for Spent Fuel Pools.

4. ASSUMPTIONS

The analyses apply a number of assumptions, either for conservatism or to simplify the calculation approach. Important aspects of applying those assumptions are as follows:

1. Bounding or sufficiently conservative inputs and assumptions are used essentially throughout the entire analyses, and as necessary studies are presented to show that the selected inputs and parameters are in fact conservative or bounding.
2. Neutron absorption in minor structural members of the fuel assembly is neglected, e.g., spacer grids are replaced by water. It is conservative to neglect the spacer grids because this spent fuel pool contains no soluble boron, the region around the fuel rods is under-moderated, as confirmed by the fuel tolerances calculations that change the fuel to moderator ratio (Section 7.1.7.1); therefore, neglecting the spacer grid places more water within the calculation model. In addition, the inconel springs within the spacer are a stronger neutron absorber than water. The active fuel region repeats periodically in the vertical direction. Therefore, neutron absorption in upper and lower tie plates, fuel plenums, etc. is neglected.
3. The neutron absorber length in the rack is more than the active region of the fuel, but it is modeled to be the same length.
4. The fuel density is assumed to be equal to the pellet density, and is conservatively modeled as a solid right cylinder over the entire active length, neglecting dishing and chamfering. This is acceptable since the amount of fuel modeled is more than the actual amount.
5. For the inserts, only the worst case bounding material specifications are used (minimum B-10 loading and minimum thickness).
6. All models are laterally infinite arrays of the respective configuration, neglecting lateral leakage. The exception is where the model boundaries are water, as specified.
7. All fuel cladding materials are modeled as pure zirconium, while the actual fuel cladding consists of one of several zirconium alloys. This is acceptable since the model neglects the trace elements in the alloy which provide additional neutron absorption.
8. [redacted]
9. The full spent fuel pool model is considered as a 74x74 array of storage cells. The water gaps between the spent fuel racks were conservatively neglected.

5. INPUT DATA

5.1 *Fuel Assembly Specification*

The SFP racks are designed to accommodate the following fuel assembly types used in the Quad Cities Unit 1 and Unit 2, which are presented in a chronologic order along with the initial maximum planar average enrichment (IMPAE):

The specifications for the most reactive fuel assemblies from the fuel product lines discussed above are presented in Table 5.1. The additional specifications for other fuel design variations are presented in Appendix A.

The fuel assembly MCNP model used for the design basis calculations is presented in Figure 5.4. The fuel rod, cladding and channel are explicitly modeled. Axially, the design basis MCNP model considers the bounding lattice along the entire length and uses water reflectors at the top and bottom. The MCNP model for the margin evaluation calculations discussed in Section 2.4 differ from the design basis model in that the active length specifically considers each actual lattice in its actual axial configuration (i.e. all the lattices from the QI22 bundle are modeled in the same MCNP model).

5.2 *Reactor Parameters*

The reactor core parameters are provided in Table 5.2(a). The reactor control blade data are provided in Table 5.2(b). The reactor control parameters used in CASMO-4 screening and design basis calculations are provided in Table 5.2(c).

5.3 *Spent Fuel Pool Parameters*

The spent fuel pool parameters are provided in Table 5.2(a).

5.4 *Storage Rack Specification*

The storage rack specifications that are used in the criticality analysis are summarized in Tables 5.3(a) and 5.3(b). The Quad Cities Unit 1 and Unit 2 SFP are shown in Figures 5.2(a) and 5.2(b), respectively.

[redacted]

[redacted] The MCNP5-1.51 SFP model consists of a single rack cell with periodic boundary conditions through the centerline of the water (BORAFLEX replacement), thus simulating an infinite array of storage cells. The storage rack cell is modeled the same length as the active fuel and all other storage rack materials are neglected. The neutron absorber is modeled with the worst case bounding values (the minimum B-10 loading and the minimum thickness) provided in Table 5.3(b) and Figure 5.3. The cell wall thickness of the boundary is different from that of inner walls. The cell wall thickness of the boundary is thicker than the inner wall thickness. The SFP model uses the inner cell wall thickness only, as given in Table 5.3(a), because it decreases the amount of steel in the model, which acts a neutron absorber.

The MCNP5-1.51 SFP rack cell model is shown in Figure 5.4.

5.4.1 Material Compositions

The MCNP5-1.51 material specification is provided in Table 5.4(a) for non-fuel materials, and in Table 5.4(b) for fuel materials.

6. COMPUTER CODES

The following computer codes were used in this analysis.

- MCNP5-1.51 [1] is a three-dimensional continuous energy Monte Carlo code developed at Los Alamos National Laboratory. This code offers the capability of performing full three dimensional calculations for the loaded storage racks. MCNP5-1.51 was run on the PCs at Holtec.
- CASMO-4 [4] is a two-dimensional multigroup transport theory code developed by Studsvik. CASMO-4 is used to perform the depletion calculation for the pin-specific approach, and for various studies. CASMO-4 was run on the PCs at Holtec.

7. ANALYSIS

7.1 *Design Basis and Uncertainty Evaluations*

7.1.1 [redacted]

[redacted]

7.1.2 Determination of the Design Basis Fuel Assembly Lattice

As discussed in Section 2.3.1.3, MCNP5-1.51 calculations were performed to determine the design basis lattice. The results for the SVEA-96 Optima2 QI22 fuel assembly are presented in Table 7.2(a) . The results for the GE14 lattice type 5 are presented in Table 7.2(b), along with the bounding result of the SVEA-96 Optima2 QI22. As can be seen, the SVEA-96 Optima2 QI22 lattice type 146 is bounding, and thus it is selected as the design basis lattice. The CASMO-4 model of the SVEA-96 Optima2 bundle QI22 lattice 146 used for depletion calculations is shown in Figure 5.1.

7.1.2.1 Fuel Assembly De-Channeling

As discussed in Section 2.3.1.5.4, the reactivity of the second most reactive assembly with no Zr channel at various radial positioning was evaluated. The results are provided in Table 7.2(b) and compared with the reactivity of the design basis lattice (SVEA-96 Optima2 QI22 lattice type 146). As can be seen, the SVEA-96 Optima2 QI22 lattice type 146 is bounding. Therefore, storage of fuel assemblies without channels is acceptable.

7.1.3 Optima2 CASMO-4 Model Simplification Effect

As discussed in Section 2.3.1.4, the effect of CASMO-4 model simplifications on the calculated reactivity of the SVEA-96 Optima2 QI22 lattice 146 was evaluated. The results are provided in Table 7.3. As can be seen, the reactivity of the simplified model is comparable to that of the complete model of SVEA-96 Optima2 QI22 lattice 146 (essentially within the 95/95 uncertainty between the two calculations). Therefore, the results show that the CASMO-4 model simplification

does not have a significant impact on the analysis conclusions regarding the determination of the design basis lattice.

7.1.4 Core Operating Parameters

As discussed in Section 2.3.1.5, the effects of the core operating parameters on the reactivity were evaluated. The results are provided in Table 7.4. The results show that the two dominant core operating parameters are the control blade insertion and void fraction. The other core operating parameters have an insignificant impact. Therefore, the design basis (bounding) core operating parameters are: control blades inserted, 0% void fraction, maximum fuel and moderator temperature and maximum specific power.

7.1.4.1 Reactor Power Uprate

As discussed in Section 2.3.1.5.1, the effect of the MUR on the reactivity was evaluated. The results are provided in Table 7.4. The most important core operating parameters are rodded operation (control blades) and void fraction. Other parameters have relatively negligible effects on reactivity. As can be seen, the calculations with the increased power density show statistically equivalent results, which confirms the negligible effect of the reactor power uprate on reactivity.

7.1.5 Water Temperature and Density Effect

As discussed in Section 2.3.2, the effects of water temperature, and the corresponding water density and temperature adjustments ($S(\alpha,\beta)$) were evaluated for SFP racks. The results of these calculations are presented in Table 7.5.

The results of the SFP temperature and density calculations show that as expected (for poisoned racks) the most reactive water temperature and density for the SFP racks is a temperature of 39.2 °F at a density of 1 g/cc, and these values are used for all calculations in SFP racks.

7.1.6 Depletion Uncertainty

As discussed in Section 2.3.3, the uncertainty of the number densities in the depletion calculations was evaluated. The results of these calculations are presented in Table 7.6(a).

Also, as discussed in Section 2.2.1.1.1, the uncertainty associated with FPs and LFPs was evaluated. The results of these calculations are presented in Table 7.6(b).

These two uncertainties are statistically combined with other uncertainties to determine k_{eff} in Table 7.11 and Table 7.14.

7.1.7 Fuel and Rack Manufacturing Tolerances

7.1.7.1 Fuel Assembly Tolerances

As discussed in Section 2.3.4.1, the effect of the BWR fuel tolerances on reactivity was determined. The results of these calculations are presented in Table 7.7. The maximum positive delta-k value for each tolerance is statistically combined.

The maximum statistical combination of fuel assembly tolerances is used to determine k_{eff} in Table 7.11 and Table 7.14.

7.1.7.2 SFP Rack Tolerances

As discussed in Section 2.3.4.2, the effect of the manufacturing tolerances on reactivity of the SFP racks with inserts was determined. The results of these calculations are presented in Table 7.8. The maximum positive delta-k value for each tolerance is statistically combined.

The maximum statistical combination of the SFP rack tolerances is used to determine k_{eff} in Table 7.11 and Table 7.14.

7.1.8 Radial Positioning

7.1.8.1 Fuel Assembly Radial Positioning in SFP Rack

As discussed in Section 2.3.5.2, twelve fuel assembly radial positioning cases in racks were evaluated. The results of these calculations are presented in Table 7.9(a). For each eccentric position case, the result for similar but cell centered case is considered as a reference. The results show that most cases show a negative reactivity effect, however some delta k_{calc} values are positive. Therefore, a maximum delta k_{calc} value is applied as a bias and the correspondent 95/95 uncertainty is statistically combined with other uncertainties in Table 7.11 and Table 7.14.

7.1.8.2 Fuel Orientation in SFP Rack

As discussed in Section 2.3.5.4, five fuel assembly orientation cases in racks were evaluated. The results of these calculations are presented in Table 7.9(b). The result for the reference case is also included. The results show that all cases are statistically equivalent and the reactivity effect of fuel orientation is negligible. Nevertheless, a maximum positive delta k_{calc} value is applied as a bias and the correspondent 95/95 uncertainty is statistically combined with other uncertainties in Table 7.11 and Table 7.14.

7.1.9 Fuel Rod Geometry Change

7.1.9.1 [redacted]

[redacted] The results are presented in Table 7.10.

The maximum 'k_{calc} - $k_{calc,reference}$' is added as a bias, and the '2 * $\sqrt{(\sigma_{calc}^2 + \sigma_{calc,reference}^2)}$' (95/95 uncertainty) is added as an uncertainty to determine k_{eff} in Table 7.11 and Table 7.14.

7.1.9.2 [redacted]

[redacted]

7.1.10 [redacted]

[redacted]

7.2 *Maximum k_{eff} Calculations for Normal Conditions*

As discussed in Section 2.3.8, the maximum k_{eff} for normal conditions is calculated. The results are tabulated in Table 7.11. The results show that the maximum k_{eff} for the normal conditions in the SFP racks is less than 0.95 at a 95% probability and at a 95% confidence level.

7.3 *Margin Evaluation*

As discussed in Section 2.4, the margin analyses were performed using the nominal values for poison thickness and loading, as well as the actual lattice configuration of the Optima2 QI22 fuel assembly. The results of calculations are provided in Table 7.12(a) and Table 7.12(b). As can be seen and is expected, the reactivity of design basis is larger. The use of a minimum B-10 loading relative to use of a nominal B-10 loading with tolerance uncertainty provide an additional ~1% reactivity margin to the regulatory limit with a 95% probability at a 95% confidence level.

The summary of the margin evaluation is presented in Table 7.12(c). The result shows that quantified margin remains in the analysis to offset potential effects not already considered in the model.

7.4 *Abnormal and Accident Conditions*

As discussed in Section 2.6, the effects of empty storage cell, increased temperature, misloaded fuel assembly/missing insert, and mislocated fuel assembly accidents on reactivity were evaluated. The results are provided in Table 7.13(a) and Table 7.13(b).

As can be seen, the increased water temperature will not result in an increase in reactivity.

Both misloaded fuel assembly/missing insert and mislocated fuel accidents may result in an increase in reactivity. For the SFP racks, the effect on reactivity of the missing insert is the limiting case. Thus, its calculated MCNP5-1.51 k_{calc} is used for maximum k_{eff} calculations for abnormal and accident conditions, discussed in Section 7.5 .

The condition with the empty storage cell without insert in the spent fuel rack shows a lower reactivity than a design basis case, therefore, it is acceptable to have the empty storage cell without insert in the spent fuel pool.

7.5 *Maximum k_{eff} Calculations for Abnormal and Accident Conditions*

As discussed in Section 2.6, the maximum k_{eff} for abnormal and accident conditions is calculated. The results are tabulated in Table 7.14. The results show that the maximum k_{eff} for abnormal and accident conditions in the SFP racks is less than 0.95 at a 95% probability and at a 95% confidence level.

7.6 [redacted]

[redacted]

7.7 *Spent Fuel Rack Interfaces*

As discussed in Sections 2.8, the interface between SFRs and pool walls, i.e. effect on reactivity of the peripheral fuel assemblies, that have a side non-adjacent to the insert, was evaluated. The results are provided in Table 7.17. As can be seen, this condition will not result in an increase of SFR reactivity. This result is expected because the infinite array design basis model is an infinite array of

storage cells with inserts while the full pool model used for these rack interface calculations includes the rack edge along the pool wall where there is no insert along the water gap edge (i.e. no additional cell with an insert). Therefore, this water gap edge allows for neutron leakage and as the calculations show result in statistically equivalent results.

8. CONCLUSION

The criticality analysis for the storage of BWR assemblies in the Quad Cities SFP racks with NETCO-SNAP-IN® inserts has been performed. The results for the normal condition show that k_{eff} is [redacted] with the storage racks fully loaded with fuel of the highest anticipated reactivity, which is SVEA-96 Optima2 QI22 lattice type 146, at a temperature corresponding to the highest reactivity. The results for the accident condition show that k_{eff} is [redacted] with the storage racks fully loaded with fuel of the highest anticipated reactivity, which is SVEA-96 Optima2 [redacted], at a temperature corresponding to the highest reactivity. The maximum calculated reactivity for both normal and accident conditions includes a margin for uncertainty in reactivity calculations with a 95% probability at a 95% confidence level. Reactivity effects of abnormal and accident conditions have been evaluated to assure that under all credible abnormal and accident conditions, the reactivity will not exceed the regulatory limit of 0.95.

9. REFERENCES

[1] "MCNP - A General Monte Carlo N-Particle Transport Code, Version 5," Los Alamos National Laboratory, LA-UR-03-1987, April 24, 2003 (Revised 2/1/2008).

[2] L.I. Kopp, "Guidance on the Regulatory Requirements for Criticality Analysis of Fuel Storage at Light-Water Reactor Power Plants," NRC Memorandum from L. Kopp to T. Collins, August 19, 1998.

[3] "Nuclear Group Computer Code Benchmark Calculations," Holtec Report HI-2104790 Revision 1.

[4] M. Edenius, K. Ekberg, B.H. Forssén, and D. Knott, "CASMO-4 A Fuel Assembly Burnup Program User's Manual," Studsvik/SOA-95/1; and J. Rhodes, K Smith, "CASMO-4 A Fuel Assembly Burnup Program User's Manual," SSP-01/400, Revision 5, Studsvik of America, Inc. and Studsvik Core Analysis AB (proprietary).

[5] D. Knott, "CASMO-4 Benchmark Against Critical Experiments," SOA-94/13, Studsvik of America, Inc., (proprietary); and D. Knott, "CASMO-4 Benchmark Against MCNP," SOA-94/12, Studsvik of America, Inc., (proprietary).

[6] DSS-ISG-2010-01, Staff Guidance Regarding the Nuclear Criticality Safety Analysis for Spent Fuel Pools, Revision 0.

[7] Guide for Validation of Nuclear Criticality Safety Calculational Methodology, NUREG/CR-6698, January 2001.

[8] HI-2002444, Latest Revision, "Final Safety Analysis Report for the HI-STORM 100 Cask System", USNRC Docket 72-1014.

[9] "Sensitivity Studies to Support Criticality Analysis Methodology," HI-2104598 Rev. 1, October 2010.

[10] "Atlas of Neutron Resonances", S.F. Mughabghab, 5th Edition, National Nuclear Data Center, Brookhaven National Laboratory, Upton, USA.

[11] "Spent Nuclear Fuel Burnup Credit Analysis Validation", ORNL Presentation to NRC, September 21, 2010.

[12] An Approach for Validating Actinide and Fission Product Burnup Credit Criticality Safety Analyses—Criticality (k_{eff}) Predictions, NUREG/CR-7109, April 2012.

[13] OECD / NEA Data Bank, Java-based Nuclear Information Software, Janis version 3.3 .

[14] EPRI 1003222, "Poolside Examination Results and Assessment, GE11 BWR Fuel Exposed to 52 to 65 GWd/MTU at the Limerick 1 and 2 Reactors," December 2002.

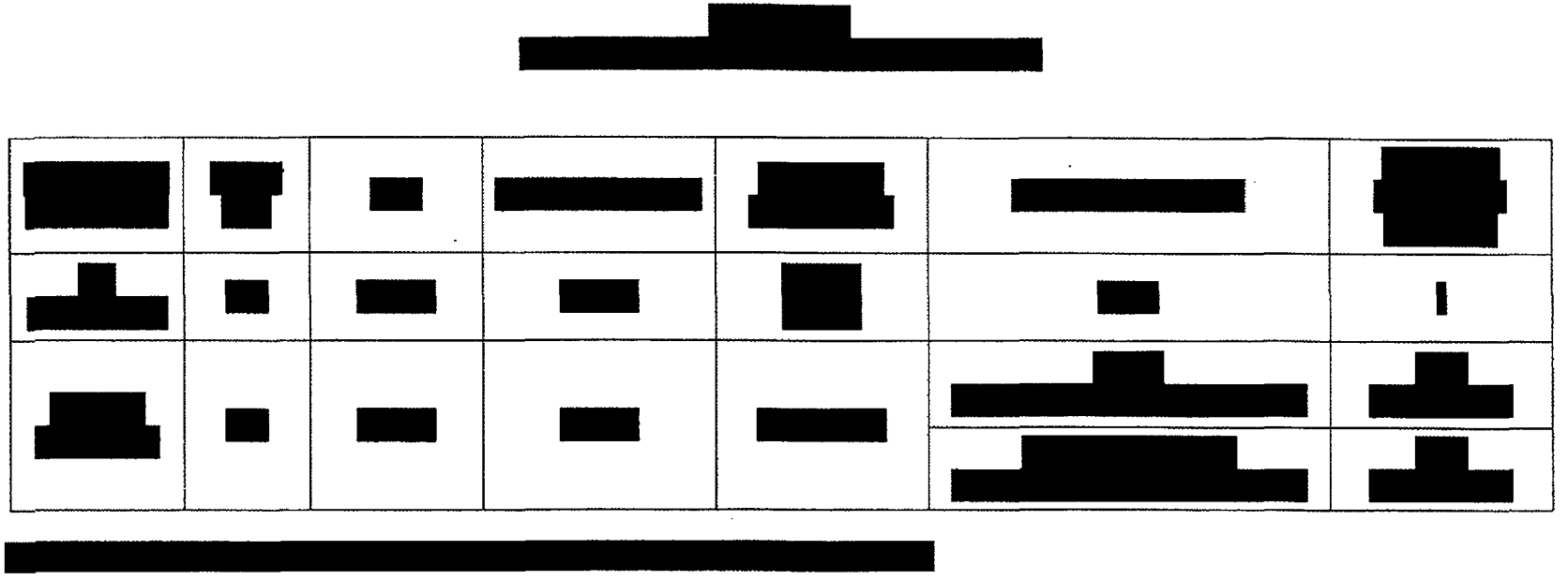

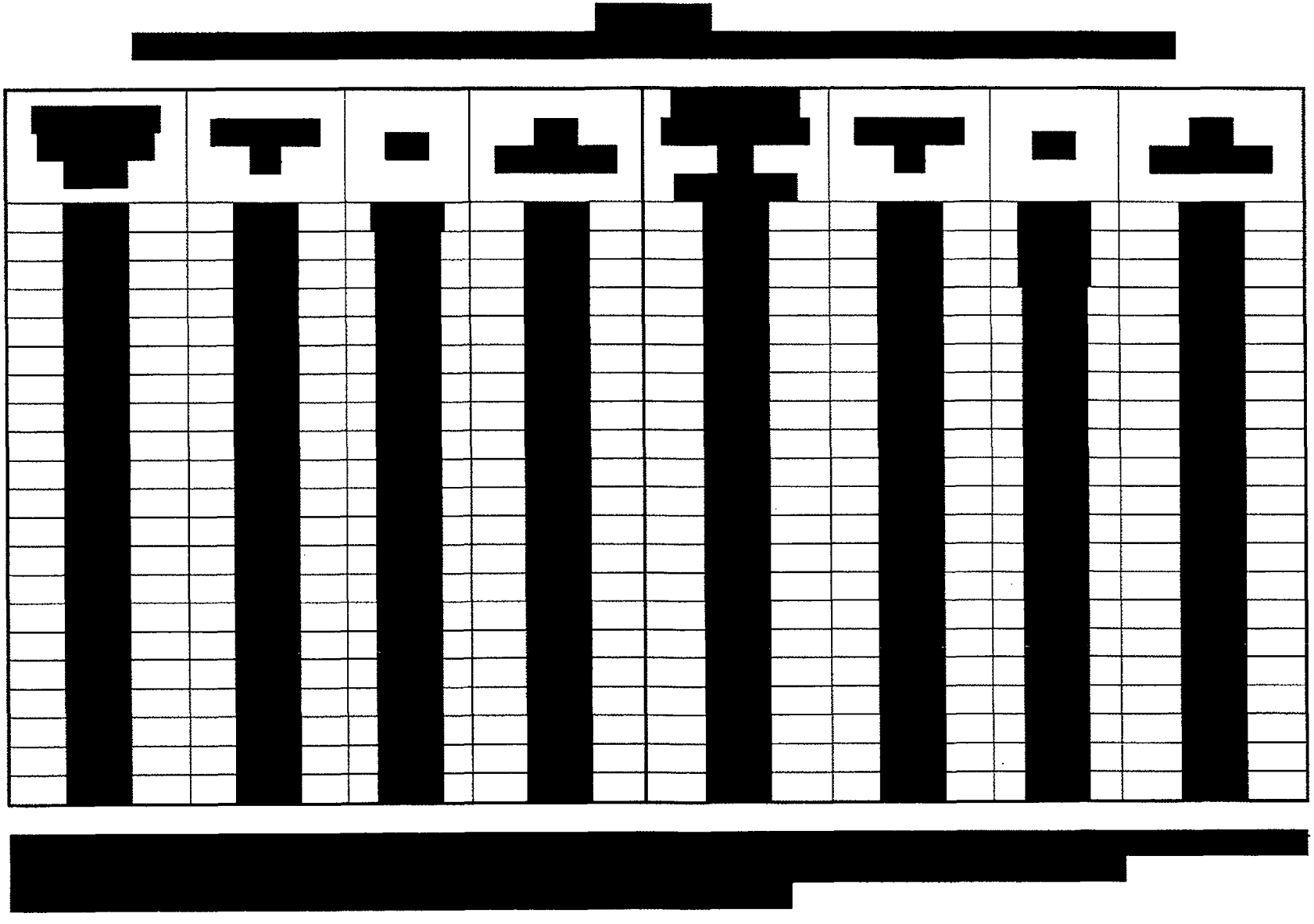

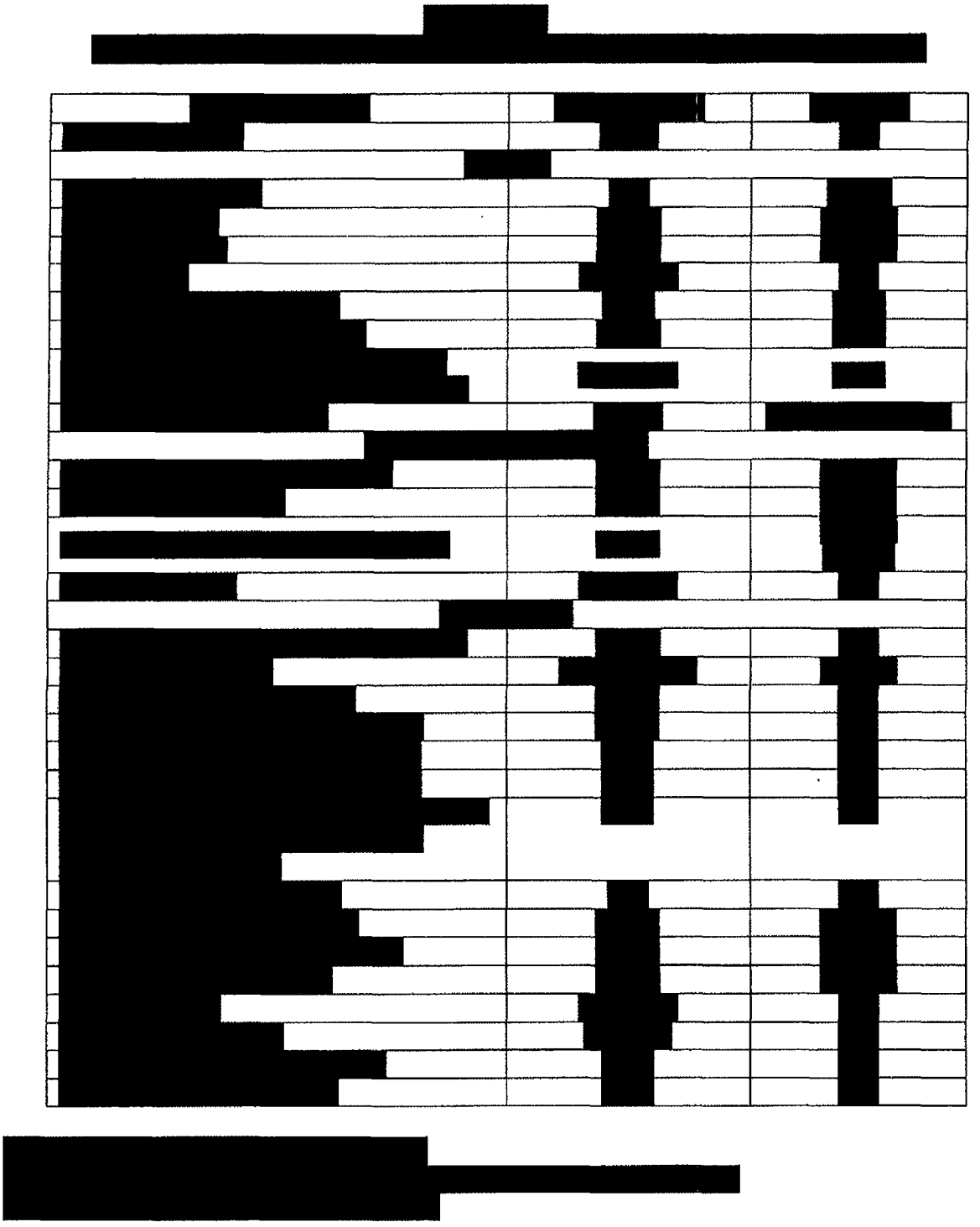

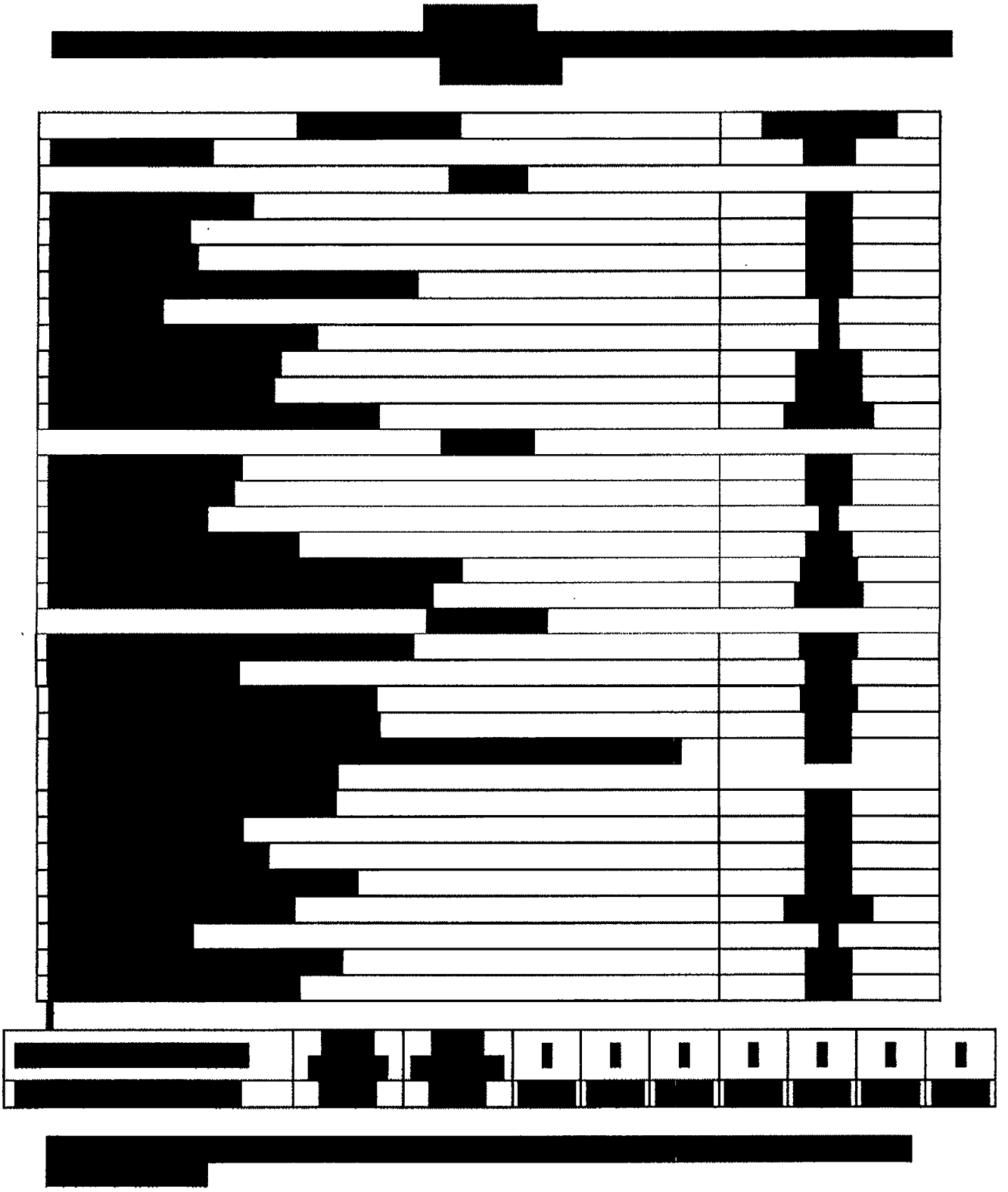

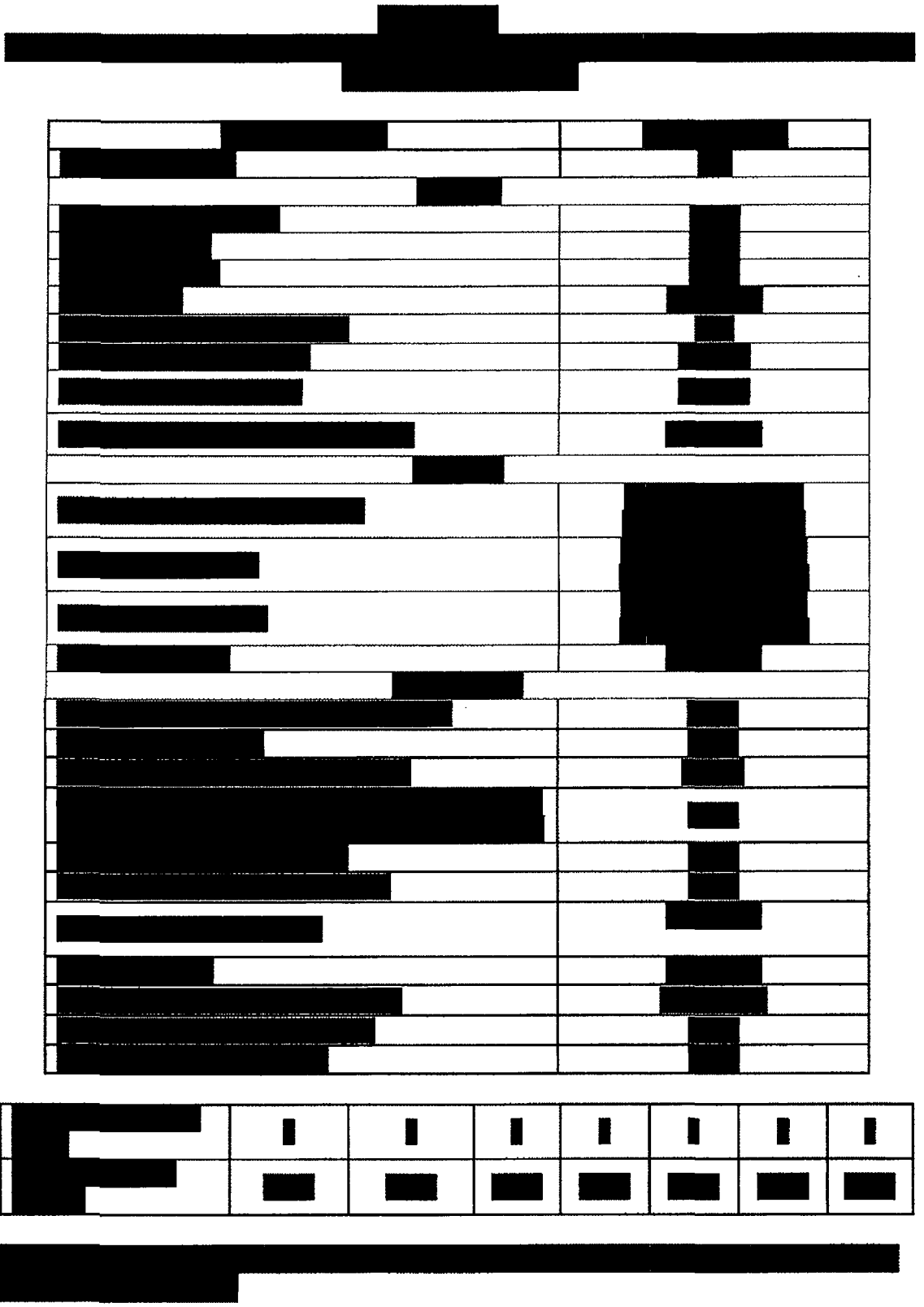

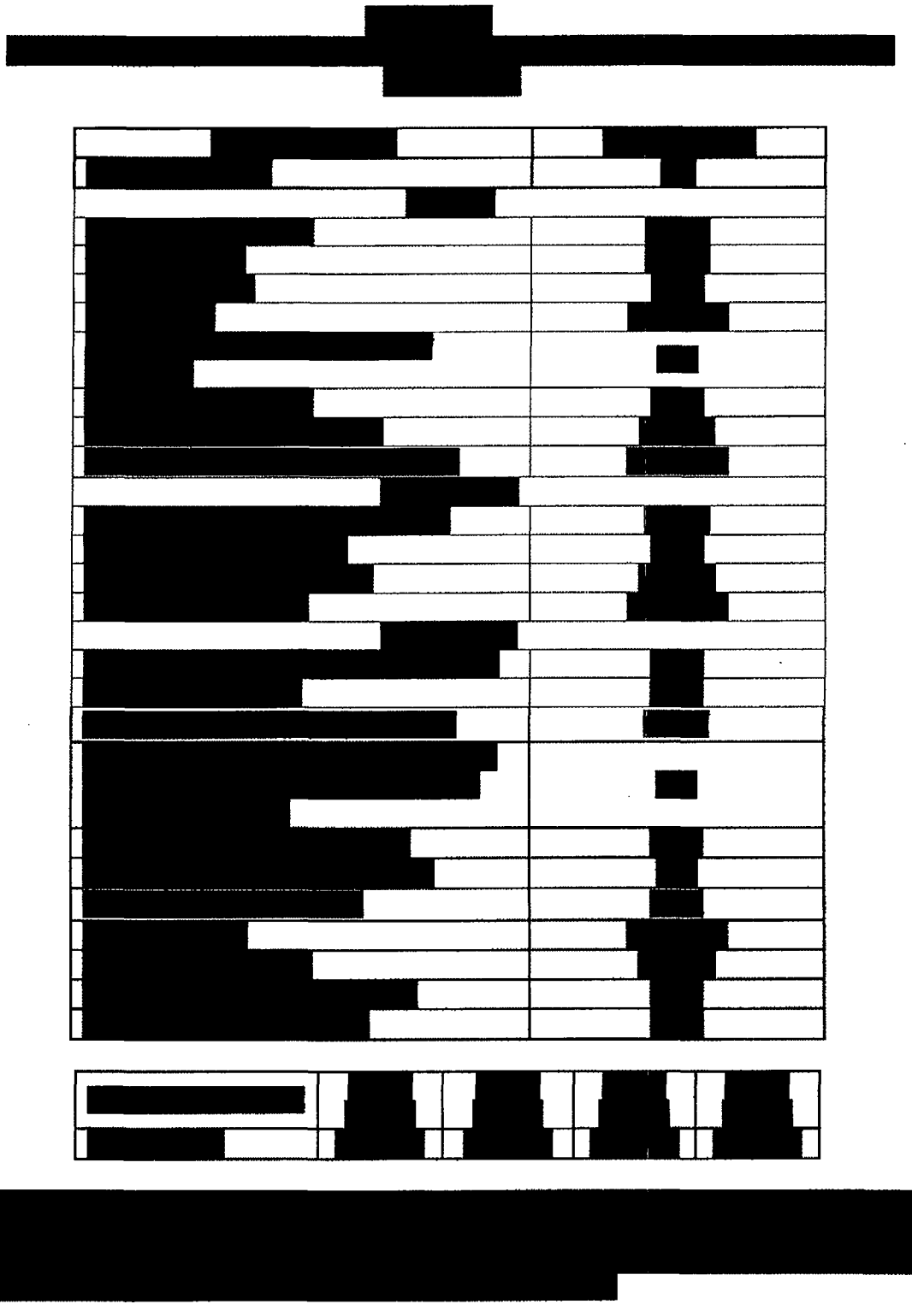

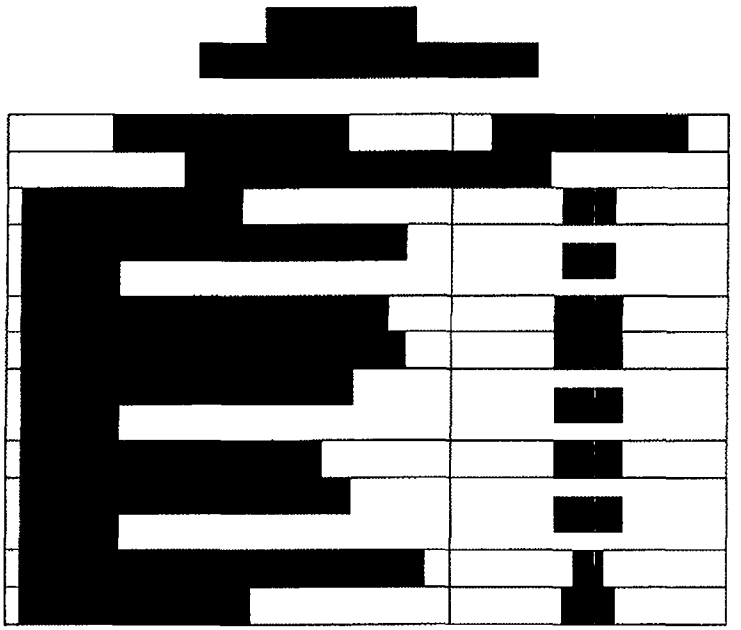

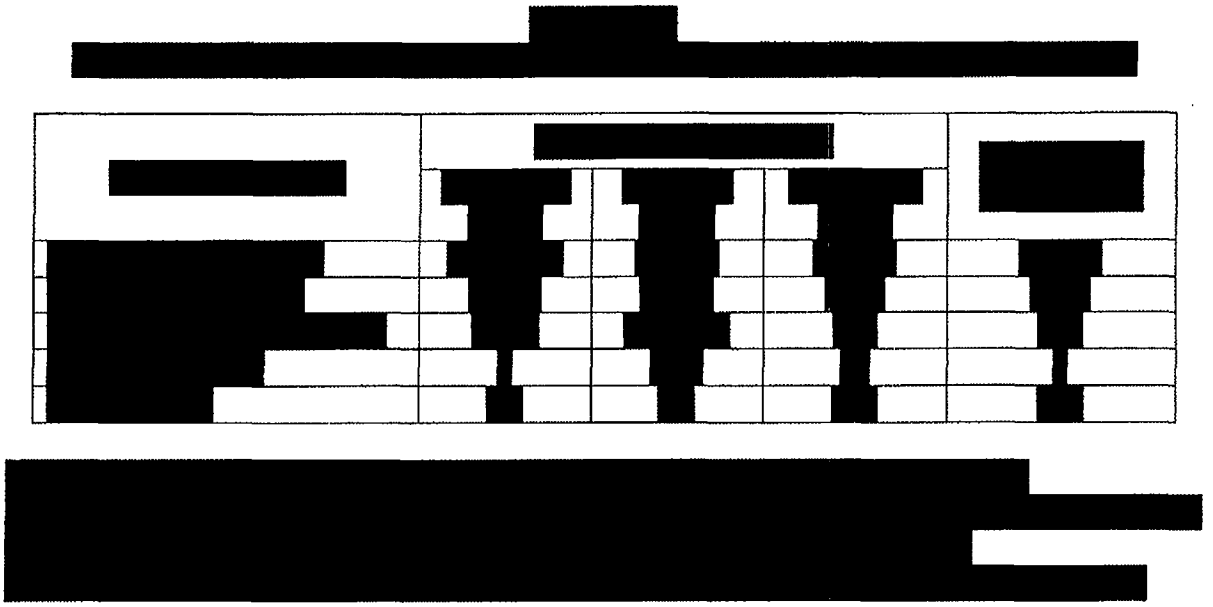

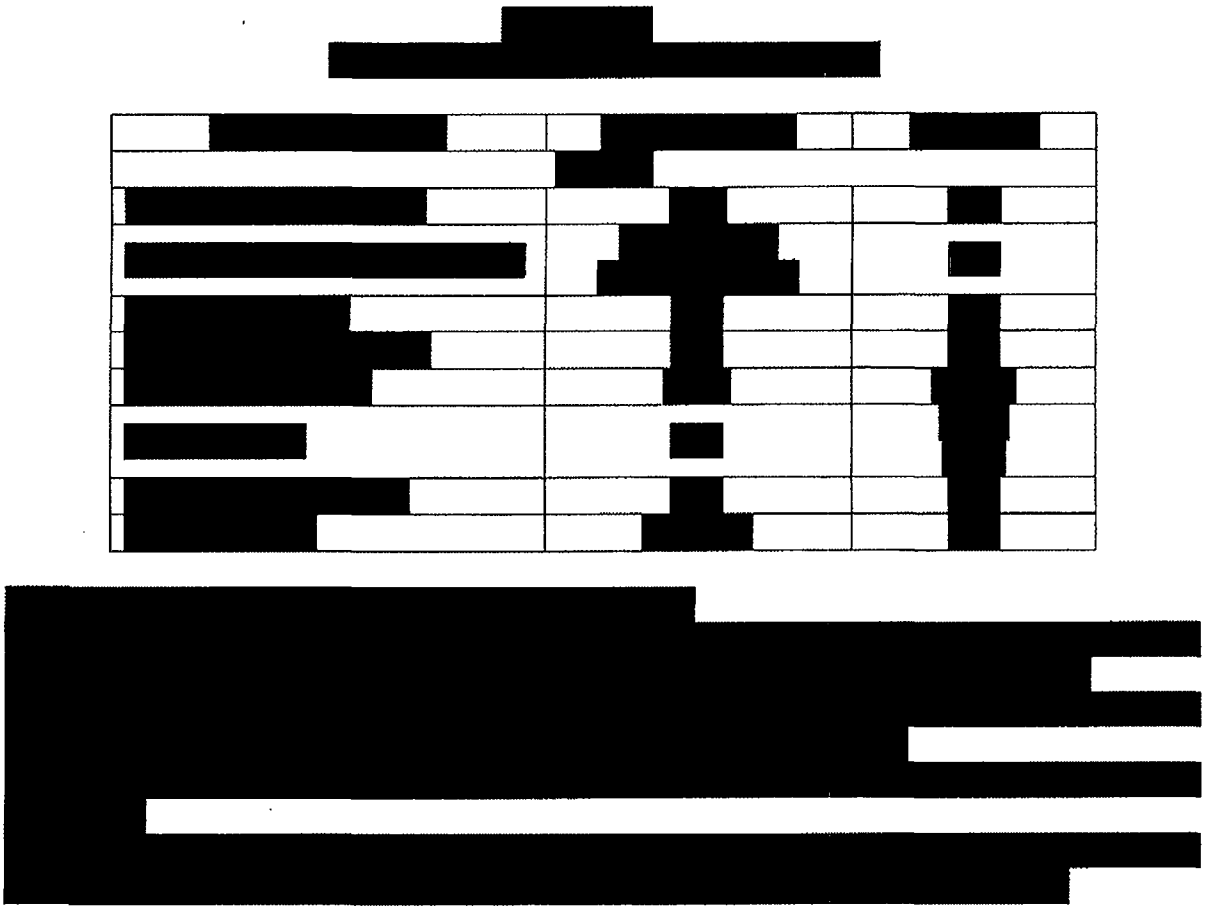

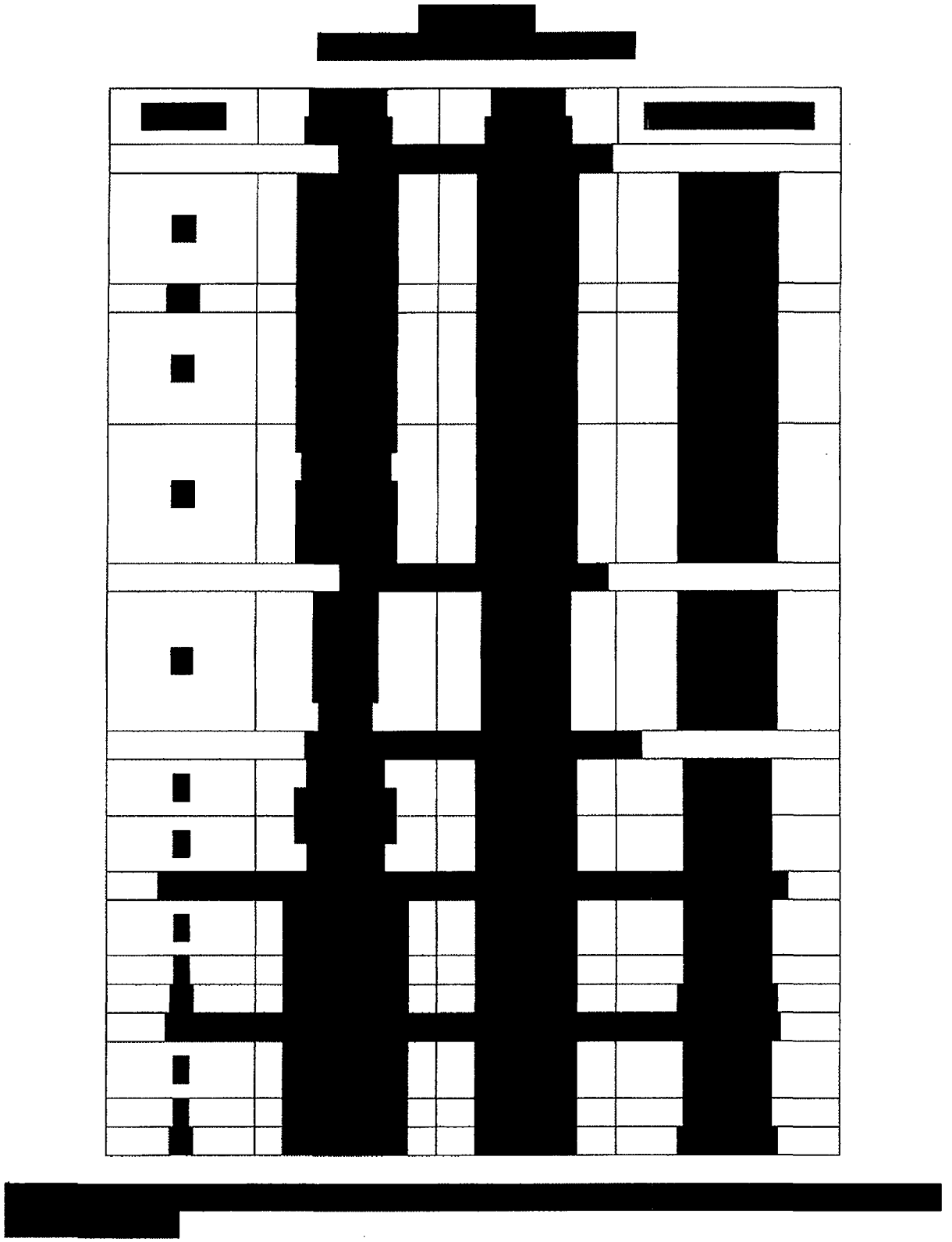

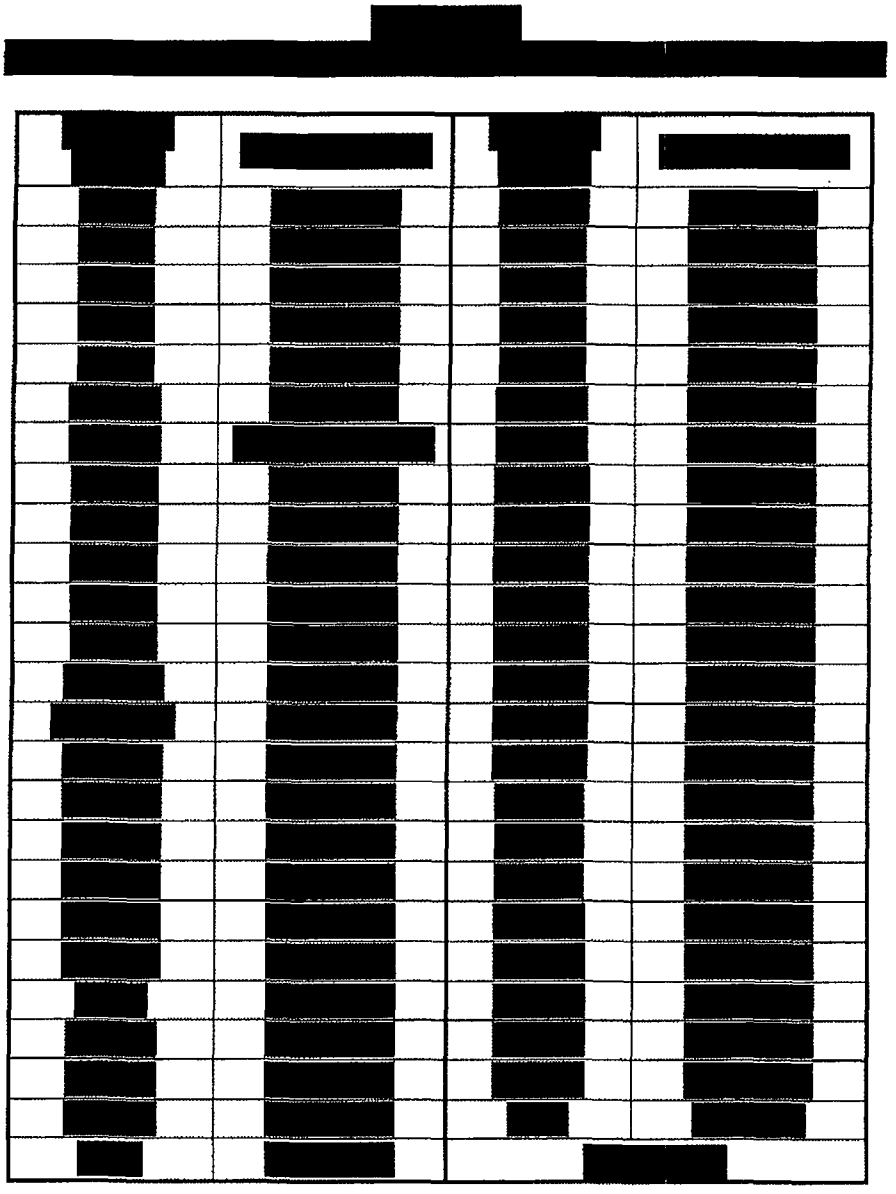

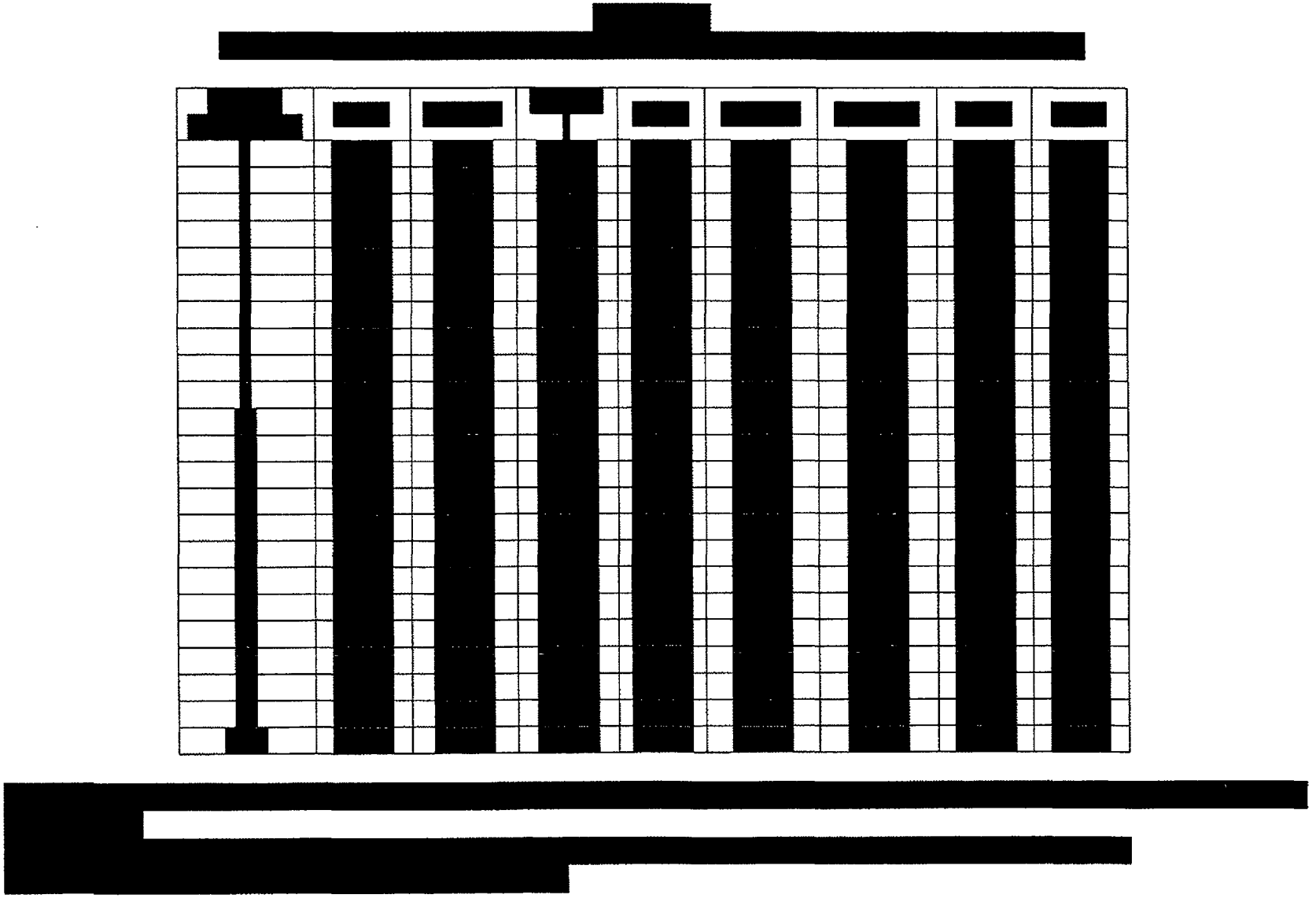

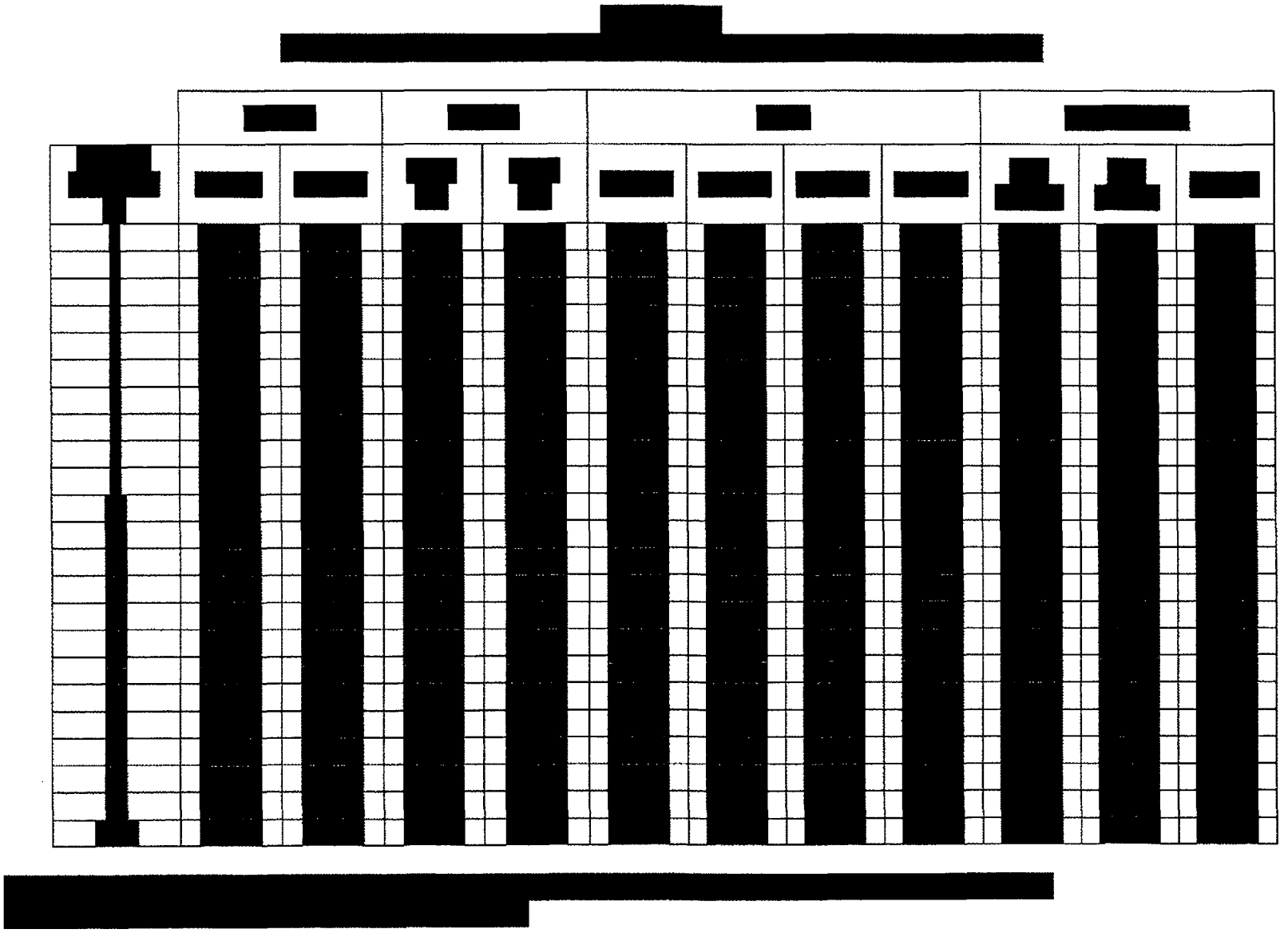

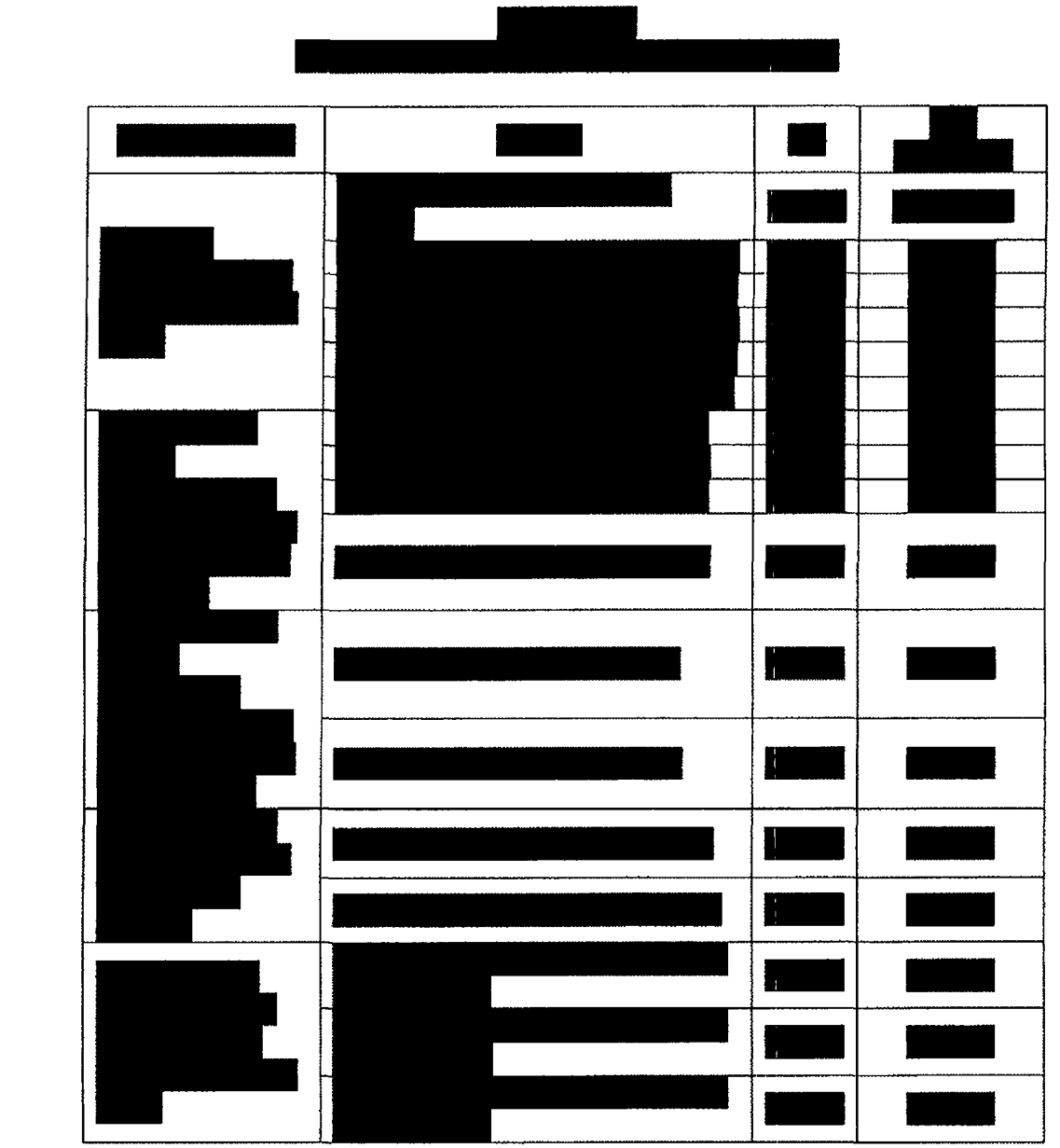

Table 7.2(a)
Results of the MCNP5-1.51 Calculations for SVEA-96 Optima2 QI22 Lattices

Description	Burnup (GWd/mtU)	k_{calc}	sigma	Max k_{calc}	delta k_{calc}	Uncertainty (95/95)
Lattice 146 (reference)	15	[redacted]	[redacted]	[redacted]	**Reference**	**Reference**
	16					
	17					
	18					
	19					
	20					
	21					
Lattice 147 (void)	15			[redacted]	-0.0081	0.0016
	16					
	17					
	18					
	19					
	20					
	21					
Lattice 147 (water) [tt]	15			[redacted]	-0.0097	0.0016
	16					
	17					
	18					
	19					
	20					
	21					
Lattice 148	15			[redacted]	-0.0121	0.0016
	16					
	17					
	18					
	19					
	20					
	21					

[redacted]

Note 2: The maximum calculation uncertainty (sigma) used to determine the 95/95 delta k_{calc} may occur at an exposure which differs from that shown above.

Table 7.2(a) Continued

Description	Burnup (GWd/mtU)	k_{calc}	sigma	Max k_{calc}	delta k_{calc}	Uncert. (95/95)
Lattice 149 (void)	15	[redacted]	[redacted]	[redacted]	-0.0207	0.0016
	16					
	17					
	18					
	19					
	20					
	21					
Lattice 149 (water) ††	15			[redacted]	-0.0189	0.0016
	16					
	17					
	18					
	19					
	20					
	21					
Lattice 150	15			[redacted]	-0.0154	0.0016
	16					
	17					
	18					
	19					
	20					
	21					
Lattice 151	15			[redacted]	-0.0111	0.0016
	16					
	17					
	18					
	19					
	20					
	21					

[redacted]

Note 2: The maximum calculation uncertainty (sigma) used to determine the 95/95 delta k_{calc} may occur at an exposure which differs from that shown above.

Table 7.2(b)
Results of the MCNP5-1.51 Calculations for GE14 Lattice Type 5

Description	Burnup (GWd/mtU)	k_{calc}	sigma	delta k_{calc}	Uncert. (95/95)
SVEA-96 Optima2 QI22 lattice type 146	**15.5**	[redacted]	[redacted]	**Reference**	**Reference**
Single GE14	13	[redacted]	[redacted]	-0.0543	0.0016
Single GE14	13.5	[redacted]	[redacted]	-0.0509	0.0015
Single GE14	14	[redacted]	[redacted]	-0.0491	0.0016
Single GE14	**14.5**	[redacted]	[redacted]	-0.0469	0.0015
Single GE14	15	[redacted]	[redacted]	-0.0473	0.0015
Single GE14	15.5	[redacted]	[redacted]	-0.0479	0.0015
Single GE14	16	[redacted]	[redacted]	-0.0485	0.0015
Single GE14	16.5	[redacted]	[redacted]	-0.0482	0.0015
Single GE14	17	[redacted]	[redacted]	-0.0500	0.0015
2x2 GE14 - with channel (cell centered) (Case 2.3.1.5.4.1)	14.5	[redacted]	[redacted]	Reference	Reference
2x2 GE14 - no channel (Case 2.3.1.5.4.2)	14.5	[redacted]	[redacted]	-0.0044	0.0016
2x2 GE14 - no channel / eccentric center (Case 2.3.1.5.4.3)	14.5	[redacted]	[redacted]	-0.0173	0.0015
2x2 GE14 - no channel / eccentric out (Case 2.3.1.5.4.4)	14.5	[redacted]	[redacted]	-0.0238	0.0015

[redacted]

Note 2: The result of the SVEA-96 Optima2 QI22 lattice type 146 is provided as the reference.
Note 3: The maximum calculation uncertainty (sigma) used to determine the 95/95 delta k_{calc} may occur at an exposure which differs from that shown above.

Table 7.3
Results of the MCNP5-1.51 Calculations for Design Basis and Simplified Model of SVEA-96 Optima2 QI22 Lattice Type 146

Description	Burnup (GWd/mtU)	Code	k_{calc}	sigma
Simplified model of SVEA-96 Optima2 QI22 lattice 146 (Case 2.3.1.4.1)	15.5	CASMO-4	[redacted]	[redacted]
Simplified model of SVEA-96 Optima2 QI22 lattice 146 (Case 2.3.1.4.2)	15.5	MCNP5-1.51	[redacted]	[redacted]
Model of SVEA-96 Optima2 QI22 lattice 146, similar to design basis† (Case 2.3.1.4.3)	15.5	MCNP5-1.51	[redacted]	[redacted]

[redacted]

Note 1: These calculations were performed using the design basis core operating parameters as indicated in Table 5.2(c).

Table 7.4
Results of the MCNP5-1.51 Calculations for Core Operating Parameters

Description	Power Density (W/gU)	Control Blade	Fuel Temp. (K)	Moderator Temp. (°F)	Void Fraction (%)	Burnup (GWd/mtU)	k_{calc}	sigma	delta k_{calc}	Uncert. (95/95)
Design basis (reference)	**23.688**	**Yes**	**1176**	**547**	**0**	**15.5**	[redacted]	[redacted]	[redacted]	[redacted]
Fuel temperature decreasing	23.688	Yes	588	547	0	16	[redacted]	[redacted]	[redacted]	[redacted]
Moderator temperature decreasing	23.688	Yes	1176	528.8	0	15.5	[redacted]	[redacted]	[redacted]	[redacted]
Void fraction increasing	23.688	Yes	1176	547	94	22	[redacted]	[redacted]	[redacted]	[redacted]
Un-rodded operation	23.688	No	1176	547	0	17	[redacted]	[redacted]	[redacted]	[redacted]
[redacted]	24.1617	Yes	1276	547	0	15.5	[redacted]	[redacted]	[redacted]	[redacted]
[redacted]	24.1617	Yes	1376	547	0	15.5	[redacted]	[redacted]	[redacted]	[redacted]
[redacted]	20.1348	Yes	1176	547	0	15.5	[redacted]	[redacted]	[redacted]	[redacted]

Note 1: The burnup calculations for core operating parameters were performed from 14 GWd/mtU to 24 GWd/mtU. For each core operating parameter, only reactivity of the burnup in this range which results in the largest reactivity is reported.
Note 2: The bounding case is bolded.
Note 3: The maximum calculation uncertainty (sigma) used to determine the 95/95 delta k_{calc} may occur at an exposure which differs from that shown above.

Table 7.5
Results of the MCNP5-1.51 Calculations for the Effect of Water Temperature and Density

Description	Burnup (GWd/mtU)	Water Temp. (°F)	Water Density (g/cc)	Temperature Adjustment, S(α,β) (°F)	k_{calc}	sigma	delta k_{calc}	Uncert. (95/95)
Reference: lower bound temperature (Case 2.3.2.1)	15.5	39.2	1	68.81	[redacted]	[redacted]	Reference	Ref.
Upper bound temperature for normal operation, low S(α,β) (Case 2.3.2.2)	15.5	150	0.98026	68.81	[redacted]	[redacted]	-0.0041	0.0015
Upper bound temperature for normal operation, high S(α,β) (Case 2.3.2.3)	15.5	150	0.98026	170.33	[redacted]	[redacted]	-0.0066	0.0015

Note 1: The maximum calculation uncertainty (sigma) used to determine the 95/95 delta k_{calc} may occur at an exposure which differs from that shown above.

Table 7.6(a)
Results of the MCNP5-1.51 Calculations for the Depletion Uncertainty

Description	**k_{calc}**	**sigma**	**Depletion Uncertainty (5%)**
Design basis	[redacted]	[redacted]	Reference
Fresh fuel, no Gd	[redacted]	[redacted]	0.0064

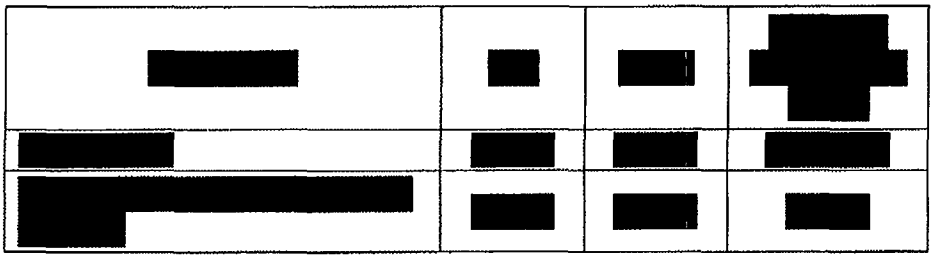

Table 7.7
Results of the MCNP5-1.51 Calculations for Fuel Tolerances

Description	Peak Reactivity Burnup (GWd/mtU)	k_{calc}	sigma	delta k_{calc} (95/95)	Max delta k_{calc} (95/95)
Design basis (reference)	15.5	[redacted]	[redacted]	Reference	Reference
Max fuel enrichment	16	[redacted]	[redacted]	0.0026	0.0026
Min fuel enrichment	15.5	[redacted]	[redacted]	-0.0009	
Max Gd loading	16	[redacted]	[redacted]	-0.0013	0.0038
Min Gd loading	15.5	[redacted]	[redacted]	0.0038	
Max pellet density	16	[redacted]	[redacted]	0.0000	0.0012
Min pellet density	15.5	[redacted]	[redacted]	0.0012	
Max pellet OD	15.5	[redacted]	[redacted]	0.0015	0.0015
Min pellet OD	16	[redacted]	[redacted]	0.0011	
Max clad ID	16	[redacted]	[redacted]	0.0010	0.0010
Min clad ID	16	[redacted]	[redacted]	0.0008	
Max clad OD	15.5	[redacted]	[redacted]	-0.0002	0.0027
Min clad OD	15.5	[redacted]	[redacted]	0.0027	
Max sub-bundle pitch	15	[redacted]	[redacted]	0.0098	0.0098
Min sub-bundle pitch	16.5	[redacted]	[redacted]	-0.0089	
Max pin pitch	15.5	[redacted]	[redacted]	0.0122	0.0122
Min pin pitch	15.5	[redacted]	[redacted]	-0.0086	
Max combined water wing canal inner width, channel outer square width, channel corner inner radius and central water canal inner square width	15	[redacted]	[redacted]	0.0031	0.0031
Min combined water wing canal inner width, channel outer square width, channel corner inner radius and central water canal inner square width	15.5	[redacted]	[redacted]	-0.0011	
Max combination of channel wall thickness and water cross wall thickness	16	[redacted]	[redacted]	0.0008	0.0019
Min combination of channel wall thickness and water cross wall thickness	15.5	[redacted]	[redacted]	0.0019	
Statistical combination of fuel tolerances					0.0171

Note 1: The maximum calculation uncertainty (sigma) used to determine the 95/95 delta k_{calc} may occur at an exposure which differs from that shown above.

Table 7.8
Results of the MCNP5-1.51 Calculations for Rack Tolerances

Description	**Burnup (GWd/mtU)**	**k_{calc}**	**sigma**	**delta k_{calc} (95/95)**	**Max delta k_{calc} (95/95)**
Design basis (reference)	15.5	[redacted]	[redacted]	Reference	Reference
Max cell ID Max cell pitch	15.5	[redacted]	[redacted]	-0.0093	N/A
Max wall thickness	15.5	[redacted]	[redacted]	0.0025	0.0025
Min wall thickness	15.5	[redacted]	[redacted]	0.0008	
Max insert width	15.5	[redacted]	[redacted]	-0.0005	0.0004
Min insert width	15.5	[redacted]	[redacted]	0.0004	
Statistical combination of rack tolerances					0.0026

Table 7.9(a)
Results of the MCNP5-1.51 Calculations for Fuel Radial Positioning in SFP Racks

Description	Burnup (GWd/mtU)	k_{calc}	sigma	delta k_{calc}	Unc. (95/95)
2x2 reference (Case 2.3.5.2.1)	15.5	[redacted]	[redacted]	Reference	Ref.
2x2 eccentric center (Case 2.3.5.2.2)	15.5	[redacted]	[redacted]	-0.0053	0.0015
2x2 eccentric in (Case 2.3.5.2.3)	15.5	[redacted]	[redacted]	-0.0081	0.0013
2x2 eccentric out (Case 2.3.5.2.4)	15.5	[redacted]	[redacted]	-0.0047	0.0014
2x2 insert/cell center (Case 2.3.5.2.5)	15.5	[redacted]	[redacted]	0.0002	0.0013
8x8 reference (Case 2.3.5.2.6)	15.5	[redacted]	[redacted]	Reference	Ref.
8x8 eccentric center (Case 2.3.5.2.7)	15.5	[redacted]	[redacted]	-0.0023	0.0014
8x8 eccentric in (Case 2.3.5.2.8)	15.5	[redacted]	[redacted]	-0.0080	0.0016
8x8 eccentric out (Case 2.3.5.2.9)	15.5	[redacted]	[redacted]	-0.0035	0.0014
8x8 insert/cell center (Case 2.3.5.2.10)	15.5	[redacted]	[redacted]	0.0016	0.0014
1x1 reference (Case 2.3.5.2.11)	15.5	[redacted]	[redacted]	Reference	Ref.
1x1 insert/cell center (Case 2.3.5.2.12)	15.5	[redacted]	[redacted]	0.0000	0.0015

Table 7.9(b)
Results of the MCNP5-1.51 Calculations for Fuel Orientation in SFP Racks

Description	Burnup (GWd/mtU)	k_{calc}	sigma	delta k_{calc}	Unc. (95/95)
Reference (Shown in Figure 2.9(a))	15.5	[redacted]	[redacted]	Reference	Ref.
Rotated fuel assembly (shown in Figure 2.9(b))	15.5	[redacted]	[redacted]	-0.0008	0.0014
Rotated fuel assembly (shown in Figure 2.9(c))	15.5	[redacted]	[redacted]	-0.0007	0.0014
Rotated fuel assembly (shown in Figure 2.9(d))	15.5	[redacted]	[redacted]	-0.0013	0.0013
Rotated fuel assembly (shown in Figure 2.9(e))	15.5	[redacted]	[redacted]	-0.0007	0.0013

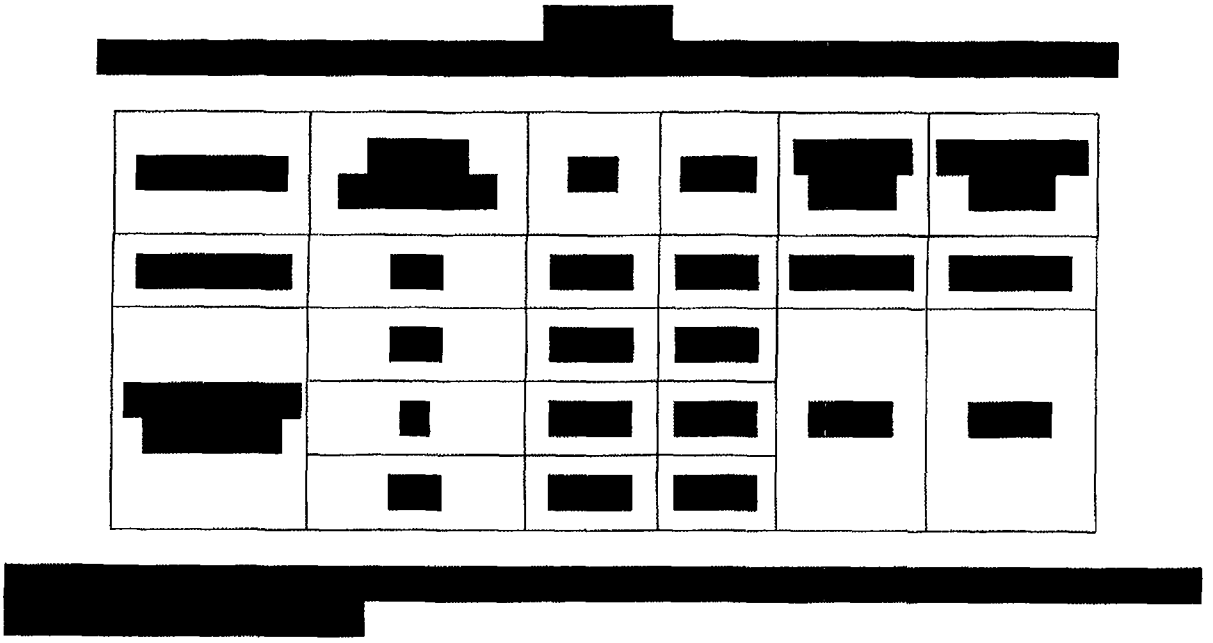

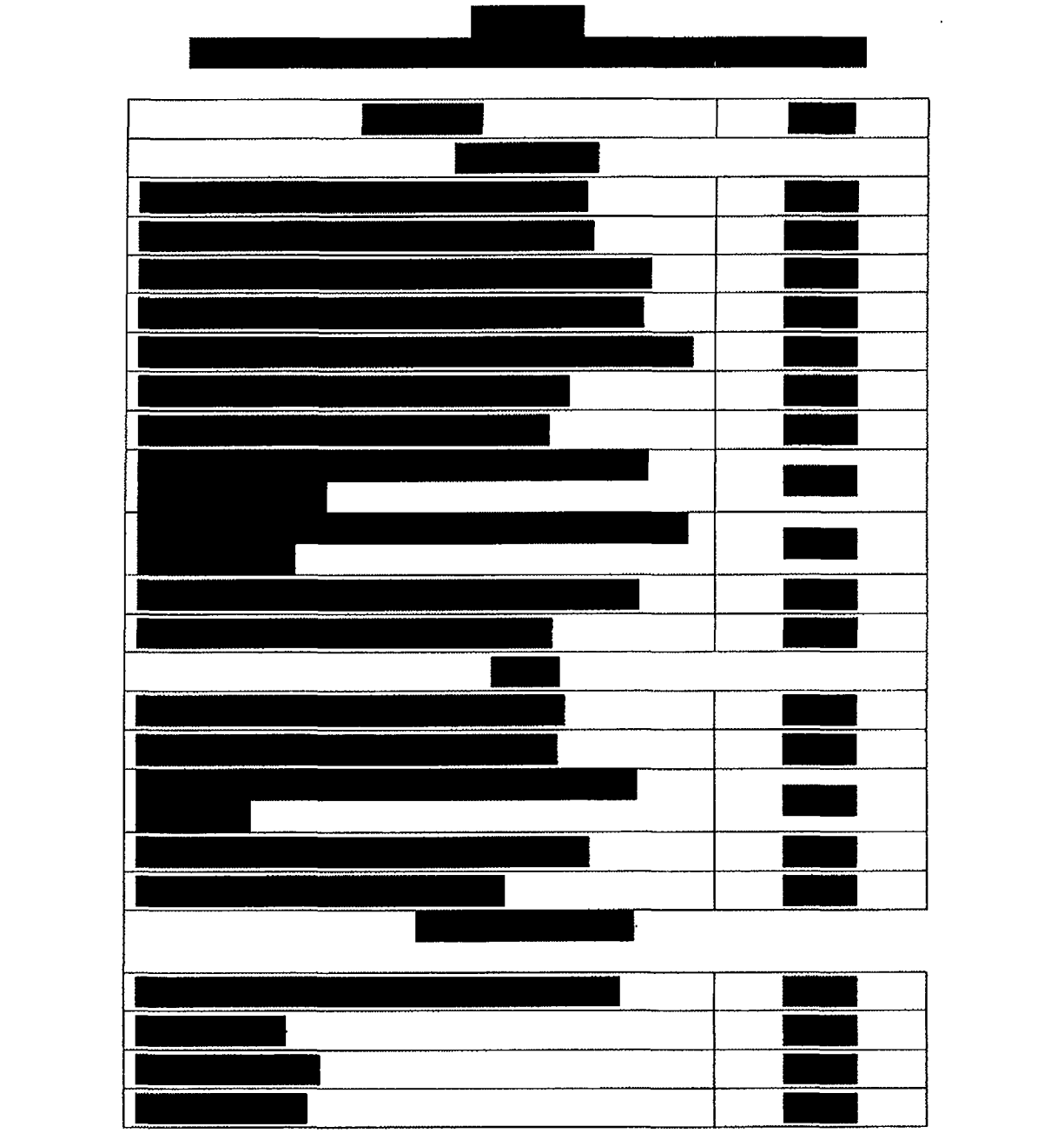

Table 7.12(a)
Margin Evaluation
Results of the MCNP5-1.51 Calculations to Evaluate the Effect of Nominal Values Instead of Using Minimum B_4C Loading and Minimum Insert Thickness on Reactivity

Description	Burnup (GWd/mtU)	B-10 Areal Density (g/cm^2)	k_{calc}	sigma	delta k_{calc}
Reference (design basis) (Case 2.4.1)	15.5	0.0116	[redacted]	[redacted]	Reference
Rack with nominal values for B_4C loading and insert thickness (Case 2.4.2)	15.5	0.0133	[redacted]	[redacted]	-0.0103

Table 7.12(b)
Margin Evaluation
Results of the MCNP5-1.51 Calculations to Evaluate the Effect of the
Actual Optima2 QI22 Fuel Assembly

Description	Burnup (GWd/mtU)	k_{calc}	sigma	Max k_{calc}	delta k_{calc}
Optima2 QI22 Lattice 146 (Design basis) (Case 2.4.1)	**15.5**	[redacted]	[redacted]	Reference	Reference
Optima2 QI22 Lattice 147	15	[redacted]	[redacted]	0.8873	-
	15.5	[redacted]	[redacted]		
	16	[redacted]	[redacted]		
Optima2 QI22 Lattice 148	16	[redacted]	[redacted]	0.8843	-
	16.5	[redacted]	[redacted]		
	17	[redacted]	[redacted]		
Optima2 QI22 Lattice 149	14	[redacted]	[redacted]	0.8825	-
	14.5	[redacted]	[redacted]		
	15	[redacted]	[redacted]		
Optima2 QI22 Lattice 150	14	[redacted]	[redacted]	0.8863	-
	14.5	[redacted]	[redacted]		
	15	[redacted]	[redacted]		
Optima2 QI22 Lattice 151	14	[redacted]	[redacted]	0.8876	-
	14.5	[redacted]	[redacted]		
	15	[redacted]	[redacted]		
Optima2 QI22 Fuel Assembly† (Case 2.4.3)	Peak Reactivity Burnups (bolded)	[redacted]	[redacted]	*0.8925*	*-0.0066*

† The top and bottom natural blankets were conservatively neglected and replaced by adjacent lattice.

Table 7.12(c)
Margin Evaluation
Summary of the Margin Evaluation

Description	Value
Insert Composition Margin, from Table 7.12(a)	-0.0103
Actual Optima2 Fuel Assembly Margin, from Table 7.12(b)	-0.0066
Calculated Margin	-0.0169

[redacted]

[redacted]

Table 7.13(b)
Results of the MCNP5-1.51 Calculations for the Empty Storage Rack Cell without Insert

Description	Burnup (GWd/mtU)	k_{calc}	sigma	delta k_{calc}	Uncertainty (95/95)
Design basis (8x8 array)	15.5	[redacted]	[redacted]	Reference	Reference
Empty storage cell (cell centered)	15.5	[redacted]	[redacted]	-0.0041	0.0016
Empty storage cell (eccentric)	15.5	[redacted]	[redacted]	-0.0081	0.0014

Note 1: The design basis fuel assembly (Optima2 Ql22 Lattice Type 146) is used for these calculations.

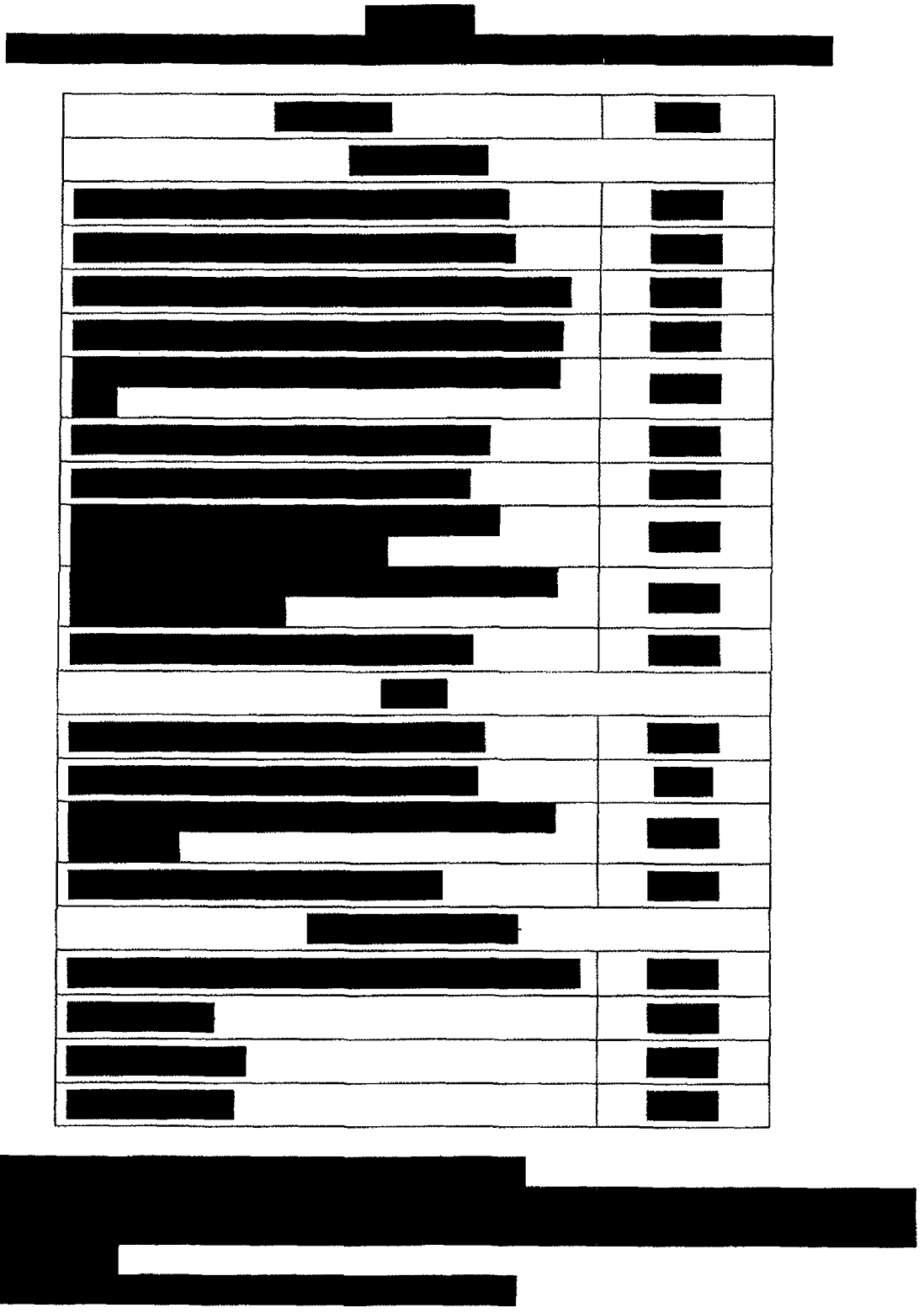

[redacted]

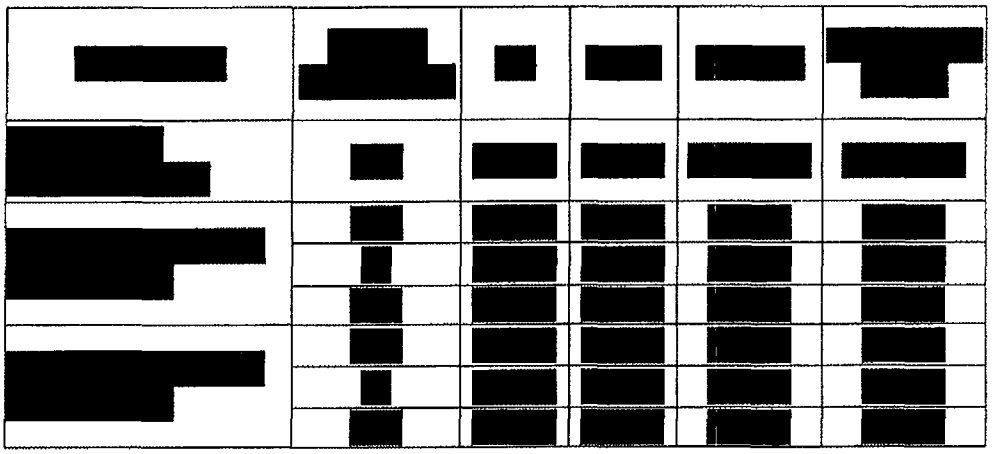

[redacted]

Table 7.16
Results of the MCNP5-1.51 Calculations for Axially Infinite Optima2 QI22 Lattices

Description	Burnup (GWd/mtU)	k_{calc} (reference)	k_{inf} (infinite)	Delta-K	Uncertainty
Optima2 QI22 Lattice 146 (Design basis)	15.5	[redacted]	[redacted]	0.0013	0.0015
Optima2 QI22 Lattice 147	15.5	[redacted]	[redacted]	0.0018	0.0015
Optima2 QI22 Lattice 148	16.5	[redacted]	[redacted]	0.0008	0.0014
Optima2 QI22 Lattice 149	14.5	[redacted]	[redacted]	0.0011	0.0015
Optima2 QI22 Lattice 150	14.5	[redacted]	[redacted]	0.0027	0.0014
Optima2 QI22 Lattice 151	14.5	[redacted]	[redacted]	0.0010	0.0015

Note: The difference between the MCNP models under the "reference" column and the MCNP models under the "infinite" column is described in Section 5.1.

Table 7.17
Results of the MCNP5-1.51 Calculations for SFR Interface

Description	Burnup (GWd/mtU)	k_{calc}	sigma	delta k_{calc}	Uncertainty (95/95)
Design basis	15.5	[redacted]	[redacted]	Reference	Reference
Full SFP (cell centered)	15.5	[redacted]	[redacted]	-0.0008	0.0016
Full SFP (eccentric to SFP corner)	15.5	[redacted]	[redacted]	-0.0053	0.0015

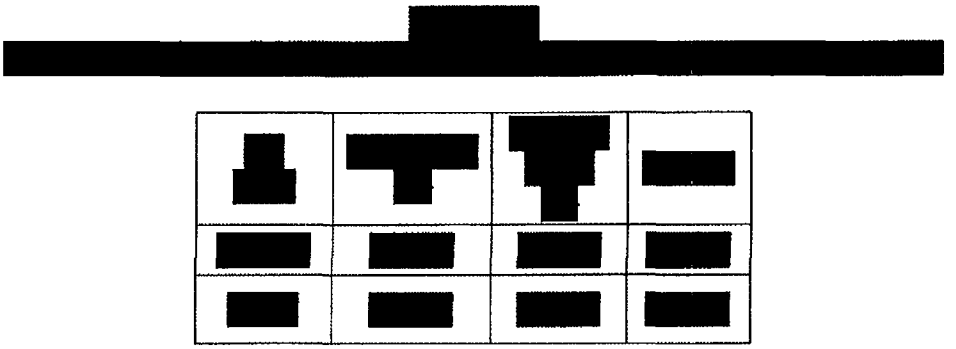

Figure Proprietary

Figure Proprietary

Figure Proprietary

Figure Proprietary

Figure Proprietary

Figure Proprietary

Figure Proprietary

Figure Proprietary

Figure Proprietary

Figure Proprietary

Figure Proprietary

Figure Proprietary

Figure Proprietary

Figure Proprietary

Figure Proprietary

Figure Proprietary

Figure Proprietary

Figure Proprietary

Figure Proprietary

Figure Proprietary

Figure Proprietary

Figure Proprietary

Figure Proprietary

Figure Proprietary

Figure Proprietary

Figure Proprietary

Figure Proprietary

Appendix A

Proprietary

Appendix B

Proprietary

Appendix C

Proprietary

Supplement 1

Additional Calculations to Support the Revised NETCO-SNAP-IN® Rack Insert Design

(11 pages including this page)

S1.1 Introduction

This Supplement documents the criticality safety evaluation for the storage of spent BWR fuel in the Unit 1 and Unit 2 spent fuel pools (SFPs) at Quad Cities Station operated by Exelon. The purpose of this analysis is to justify that the specified changes in the NETCO-SNAP-IN® rack insert design [S1.1] are acceptable and bounded by the current analysis, presented in the main part of the report.

S1.2 Methodology

See Section 2 of the main report and as otherwise discussed below.

S1.3 Acceptance Criteria

See Section 3 of the main report.

S1.4 Assumptions

See Section 4 of the main report and as otherwise discussed below.

S1.5 Input Data

See Section 5 of the main report. The revised dimensions of the NETCO-SNAP-IN® rack insert are presented in Table S1-1 and Figure S1-1.

S1.6 Computer Codes

See Section 6 of the main report.

S1.7 Analysis

The comparison of the revised insert parameters presented in Table S1-1 with the previous insert design in Table 5.3(b) shows that changes are minor and therefore a significant impact on the conclusions made in the main part of the report is not expected. Nevertheless, to verify the negligible or minor impact of the revised insert design on results presented in the main part of the report additional calculations are presented in this Supplement. The additional calculations presented in this Supplement are similar to those in report for the following cases:

- SFP rack tolerances
- Fuel assembly radial positioning in the SFP rack
- Fuel orientation in the SFP rack

These cases are selected because the NETCO-SNAP-IN® rack insert design change may impact the reactivity in the rack. All other calculations from the main report are not affected by the NETCO-SNAP-IN® rack insert design change and the results of the unaffected calculations are

used in this Supplement where applicable. This approach is considered for both normal and accident conditions.

S1.7.1 SFP Rack Tolerances

As discussed in Section S1.7, the effect of the manufacturing tolerances on reactivity of the SFP racks with revised inserts was determined. The results of these calculations are presented in Table S1-2. The maximum positive delta-k value for each tolerance is statistically combined.

The maximum statistical combination of the SFP rack tolerances is used to determine k_{eff} in Table S1-5 and Table S1-6.

S1.7.2 Fuel Assembly Radial Positioning in the SFP Rack

As discussed in Section S1.7, twelve fuel assembly radial positioning cases in the racks were evaluated. The results of these calculations are presented in Table S1-3. For each eccentric position case, the result for similar but cell centered case is considered as a reference. The results show that most cases show a negative reactivity effect, however some delta k_{calc} values are positive. Therefore, a maximum delta k_{calc} value is applied as a bias and the correspondent 95/95 uncertainty is statistically combined with other uncertainties in Table S1-5 and Table S1-6.

S1.7.3 Fuel Orientation in the SFP Rack

As discussed in Section S1.7, five fuel assembly orientation cases in racks were evaluated. The results of these calculations are presented in Table S1-4. The result for the reference case is also included. The results show that all cases are statistically equivalent and the reactivity effect of fuel orientation is negligible. Nevertheless, a maximum positive delta k_{calc} value is applied as a bias and the correspondent 95/95 uncertainty is statistically combined with other uncertainties in Table S1-5 and Table S1-6.

S1.7.4 Maximum k_{eff} Calculations for Normal Conditions

The calculations of the maximum k_{eff} for normal conditions are described in Section 2.3.8 of the main part of the report. The results for the revised NETCO-SNAP-IN® rack insert design and the results from the main part of the report are tabulated in Table S1-5. The results show that the maximum k_{eff} for the normal conditions in the SFP racks is less than 0.95 at a 95% probability and at a 95% confidence level for the revised NETCO-SNAP-IN® rack insert design and are bounded by the results from the main part of the report.

S1.7.5 Maximum k_{eff} Calculations for Abnormal and Accident Conditions

The calculations of the maximum k_{eff} for accident conditions are described in Section 2.6 of the main part of the report. The bounding accident case from the main report is recalculated using the revised NETCO-SNAP-IN® rack insert design. The results for the revised NETCO-SNAP-IN® rack insert design and the results from the main part of the report are tabulated in Table S1-6. The results show that the maximum k_{eff} for abnormal and accident conditions in the SFP racks is less than 0.95 at a 95% probability and at a 95% confidence level for the revised NETCO-SNAP-IN® rack insert design and are bounded by the results from the main part of the report.

S1.8 References

[S1.1] Transmittal of Design Information NF1100434, Revision 1, "Quad Cities SFP Rack Insert Design Information", dated 09/11/2012.

S1.9 Conclusions

The criticality analysis for the storage of BWR assemblies in the Quad Cities SFP racks with revised NETCO-SNAP-IN® inserts has been performed. The results show that k_{eff} is [redacted] with the storage racks fully loaded with fuel of the highest anticipated reactivity, which is SVEA-96 Optima2 [redacted], at a temperature corresponding to the highest reactivity. The maximum calculated reactivity includes a margin for uncertainty in reactivity calculations with a 95% probability at a 95% confidence level. Reactivity effects of abnormal and accident conditions have been evaluated to assure that under all credible abnormal and accident conditions, the reactivity will not exceed the regulatory limit of 0.95.

The results show that the specified changes in the insert design are acceptable and bounded by the current analysis, presented in the main part of the report. [redacted] Therefore, any insert width dimension between the value used in the main report including the specified manufacturing tolerances and the value evaluated in this Supplement is acceptable.

Table S1-1
Fuel Rack Insert Revised Dimensions [S1.1]

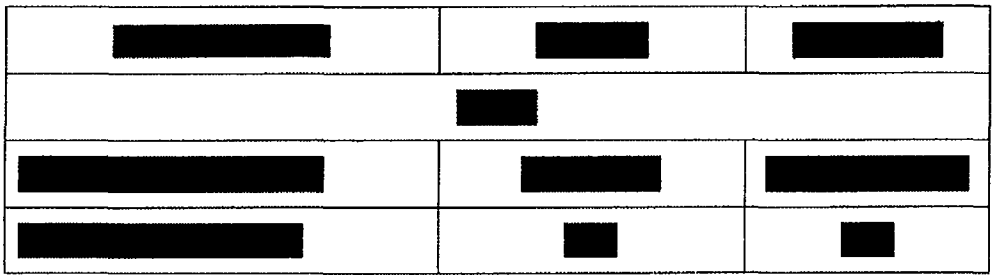

† For the details of the insert dimensions, see Figure S1-1.
†† See Table 5.3(b)

Table S1-2
Results of the MCNP5 Calculations for Revised Rack Tolerances

Description	Burnup (GWd/mtU)	Filename	k_{calc}	sigma	delta k_{calc} (95/95)	Revised Max delta k_{calc} (95/95)	Reference Max delta k_{calc} † (95/95)
Design basis (reference)	15.5	op146-rt201155r	[redacted]	[redacted]	Reference	Reference	Reference
Max cell ID Max cell pitch	15.5	op146-rt202155r	[redacted]	[redacted]	-0.0091	0.0000	0.0000
Max wall thickness	15.5	op146-rt203155r	[redacted]	[redacted]	0.0017	0.0017	0.0025
Min wall thickness	15.5	op146-rt204155r	[redacted]	[redacted]	0.0011		
Max insert width	15.5	op146-rt206155r	[redacted]	[redacted]	0.0016	0.0030	0.0004
Min insert width	15.5	op146-rt207155r	[redacted]	[redacted]	0.0030		
Statistical combination of rack tolerances						0.0035	0.0026

† See Table 7.8
Note 1: The CASMO depletion calculation filenames are op146-dbc(-ac).

Table S1-3
Results of the MCNP5-1.51 Calculations for Revised Fuel Radial Positioning in SFP Racks

Description	Burnup (GWd/mtU)	Filename	k_{calc}	sigma	Revised delta k_{calc}	Revised Unc. (95/95)	Reference delta k_{calc} †	Reference Unc. † (95/95)
2x2 reference (Case 2.3.5.2.1)	15.5	2x2dbrot0155r	[redacted]	[redacted]	Ref.	Ref.	Ref.	Ref.
2x2 eccentric center (Case 2.3.5.2.2)	15.5	2x2ecnt155r	[redacted]	[redacted]	-0.0028	0.0015	-0.0053	0.0015
2x2 eccentric in (Case 2.3.5.2.3)	15.5	2x2ein155r	[redacted]	[redacted]	-0.0054	0.0015	-0.0081	0.0013
2x2 eccentric out (Case 2.3.5.2.4)	15.5	2x2eout155r	[redacted]	[redacted]	-0.0014	0.0015	-0.0047	0.0014
2x2 insert/cell center (Case 2.3.5.2.5)	15.5	2x2icnt155r	[redacted]	[redacted]	0.0001	0.0016	0.0002	0.0013
8x8 reference (Case 2.3.5.2.6)	15.5	8x8dbc155r	[redacted]	[redacted]	Ref.	Ref.	Ref.	Ref.
8x8 eccentric center (Case 2.3.5.2.7)	15.5	8x8ecnt155r	[redacted]	[redacted]	-0.0032	0.0015	-0.0023	0.0014
8x8 eccentric in (Case 2.3.5.2.8)	15.5	8x8ein155r	[redacted]	[redacted]	-0.0071	0.0015	-0.0080	0.0016
8x8 eccentric out (Case 2.3.5.2.9)	15.5	8x8eout155r	[redacted]	[redacted]	-0.0035	0.0016	-0.0035	0.0014
8x8 insert/cell center (Case 2.3.5.2.10)	15.5	8x8icnt155r	[redacted]	[redacted]	0.0009	0.0014	0.0016	0.0014
1x1 reference (Case 2.3.5.2.11)	15.5	op146-dbc155r	[redacted]	[redacted]	Ref.	Ref.	Ref.	Ref.
1x1 insert/cell center (Case 2.3.5.2.12)	15.5	1x1icnt155r	[redacted]	[redacted]	0.0004	0.0015	0.0000	0.0015

† See Table 7.9(a)
Note 1: The CASMO depletion calculation filenames are op146-dbc(-ac).

Table S1-4
Results of the MCNP5-1.51 Calculations for Revised Fuel Orientation in SFP Racks

Description	Burnup (GWd/mtU)	Filename	k_{calc}	sigma	Revised delta k_{calc}	Revised Unc. (95/95)	Reference delta k_{calc} †	Reference Unc.† (95/95)
Reference (Shown in Figure 2.9(a))	15.5	2x2dbrot0155r	[redacted]	[redacted]	Ref.	Ref.	Ref.	Ref.
Rotated fuel assembly (shown in Figure 2.9(b))	15.5	2x2dbrot1155r	[redacted]	[redacted]	0.0004	0.0014	-0.0008	0.0014
Rotated fuel assembly (shown in Figure 2.9(c))	15.5	2x2dbrot2155r	[redacted]	[redacted]	0.0011	0.0015	-0.0007	0.0014
Rotated fuel assembly (shown in Figure 2.9(d))	15.5	2x2dbrot3155r	[redacted]	[redacted]	0.0016	0.0014	-0.0013	0.0013
Rotated fuel assembly (shown in Figure 2.9(e))	15.5	2x2dbrot4155r	[redacted]	[redacted]	0.0024	0.0016	-0.0007	0.0013

† See Table 7.9(b)
Note 1: The CASMO depletion calculation filenames are op146-dbc(-ac).

[redacted]

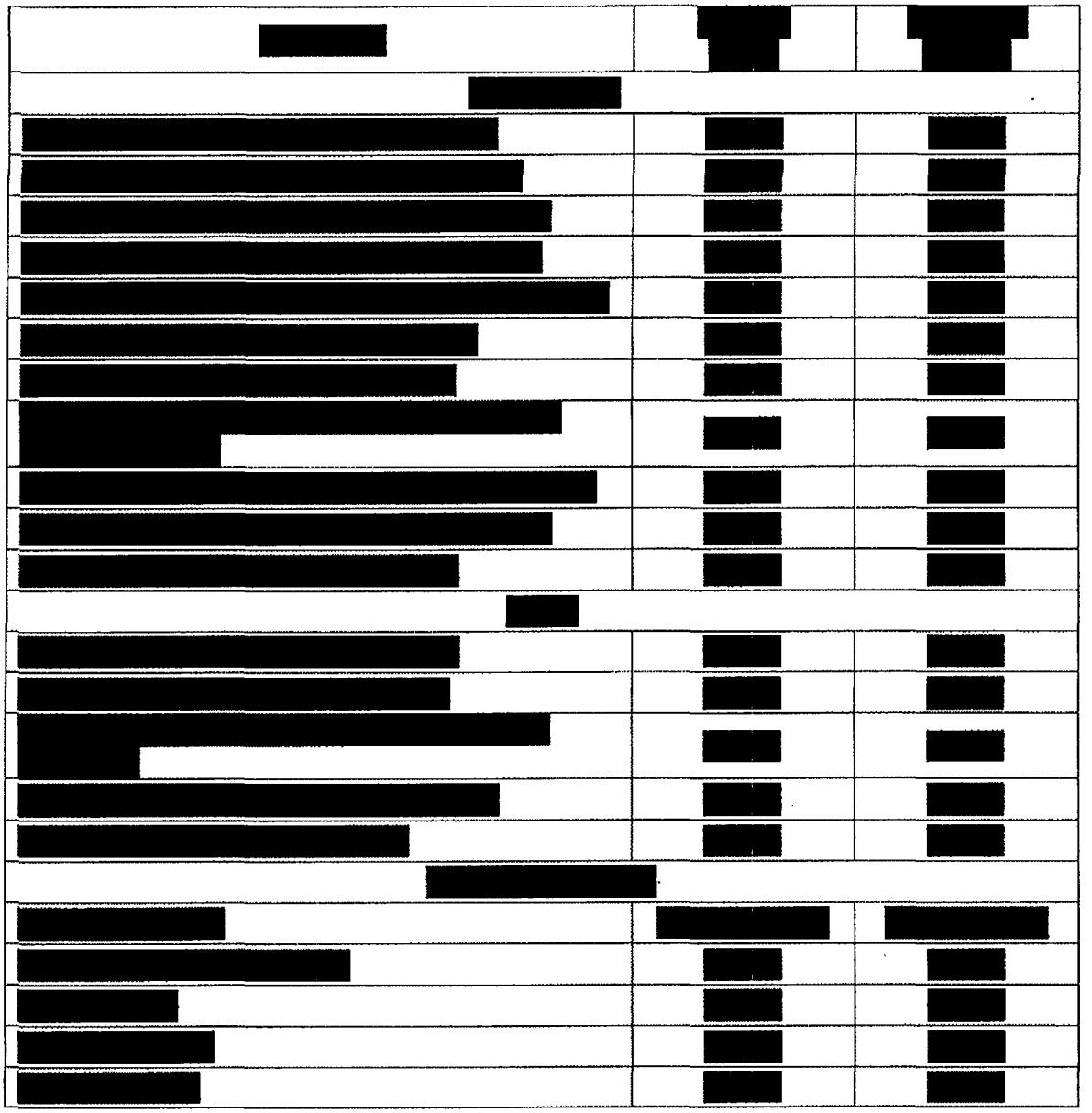

[redacted]

[redacted]

Figure Proprietary